Return Dynamics with Lévy Jumps: Evidence from Stock and Option Prices

HAITAO LI,[1] MATIN T. WELLS,[2] AND CINDY L. YU[3]

ABSTRACT

We examine the performances of Lévy jump models and affine jump-diffusion models in capturing the joint dynamics of stock and option prices. We discuss the change of measure for infinite-activity Lévy jumps and develop efficient Markov chain Monte Carlo methods for estimating model parameters and latent volatility and jump variables using stock and option prices. Using daily returns and option prices of the S&P 500 index, we show that models with infinite-activity Lévy jumps in returns significantly outperform affine jump-diffusion models with compound Poisson jumps in returns and volatility in capturing both the physical and the risk-neutral dynamics of the S&P 500 index.

---

[1]Li is from the Stephen M. Ross School of Business, University of Michigan, Ann Arbor, MI 48109; E-mail: htli@umich.edu; phone: (734)-764-6409. [2]Wells is from the Department of Biological Statistics and Computational Biology and the Department of Social Statistics, Cornell University, Ithaca, NY 14853; E-mail: mtw1@cornell.edu; phone: (607)-255-4388; he gratefully acknowledges the support of NSF Grant DMS 02-04252. [3]Yu is from the Department of Statistics, Iowa State University, Ames, IA 50011; E-mail: cindyyu@iastate.edu; phone: (515)-294-3319. We would like to thank Torben Andersen and Luca Benzoni for their help in the early stage of this study. We thank Yacine Aït-Sahalia (the editor), Antje Berndt, Peter Carr, Bjorn Eraker, Bob Jarrow, Nour Meddahi, Ray Renken, Sidney Resnick, Ernst Schaumburg, Neil Shephard, George Tauchen, Liuren Wu, an anonymous referee, and seminar participants at Cornell University, the 2004 CIREQ/CIRANO financial econometrics conference, the 2004 International Chinese Statistical Association Applied Statistics Symposium, and the 2004 Institute of Mathematical Statistics Annual Meeting/6th Bernoulli World Congress for helpful comments. We are responsible for any remaining errors.

Return Dynamics with Lévy Jumps: Evidence from Stock and Option Prices

ABSTRACT

We examine the performances of Lévy jump models and affine jump-diffusion models in capturing the joint dynamics of stock and option prices. We discuss the change of measure for infinite-activity Lévy jumps and develop efficient Markov chain Monte Carlo methods for estimating model parameters and latent volatility and jump variables using stock and option prices. Using daily returns and option prices of the S&P 500 index, we show that models with infinite-activity Lévy jumps in returns significantly outperform affine jump-diffusion models with compound Poisson jumps in returns and volatility in capturing both the physical and the risk-neutral dynamics of the S&P 500 index.

Modeling the dynamics of stock returns is a key issue in modern asset pricing. A realistic model of return dynamics is essential for option pricing, portfolio analysis, and risk management. One of the most popular continuous-time models for return dynamics in the current literature is the affine jump-diffusion (hereafter AJD) models of Duffie, Pan, and Singleton (2000) (hereafter DPS). In AJD models, stock returns are driven by affine diffusions and compound Poisson processes. AJD models capture important stylized behaviors of index returns and are highly tractable. They allow closed-form pricing formulae for a wide range of equity and fixed-income derivatives.

Despite the successes of AJD models, Brownian motion and compound Poisson process (the two main building blocks of AJD models) are only two special cases of Lévy processes, which are continuous-time stochastic processes with stationary and independent increments. Lévy processes are much more flexible than Brownian motion and compound Poisson process for modeling purposes. For example, Lévy processes allow non-normal increments (compared to normal increments of Brownian motion) and much richer jump structures than compound Poisson process. Moreover, Carr and Wu (2004) show that Lévy processes are as tractable as AJD models for pricing purposes: Closed-form pricing formulae are available for a wide range of derivative securities under Lévy processes.

These appealing features of Lévy processes have spurred a fast-growing literature that models return dynamics using Lévy processes in recent years.[1] This new development, however, has raised some challenging theoretical and empirical issues in the current literature. While existing studies of Lévy processes have mainly focused on either the physical or the risk-neutral return dynamics, a key remaining question is whether Lévy processes have significant empirical advantages over AJD models in modeling the joint return dynamics.[2] This is an important question because the ultimate

[1]See Wu (2006) for an excellent review of the current literature on Lévy processes. See Aït-Sahalia (2004) and Aït-Sahalia and Jacod (2004) on some fundamental issues on statistical inferences of Lévy processes.

[2]Madan, Carr, and Chang (1998), Carr, Geman, Madan, and Yor (2002), Huang and Wu (2003), and Carr and Wu

test of the success of a model should be its ability to capture both the physical and the risk-neutral dynamics of asset returns. In addition, the most sophisticated AJD models in the literature can capture many important stylized behaviors of index returns. One such model is the double-jump model of Eraker, Johannes, and Polson (2003) (hereafter EJP), which includes not only stochastic volatility and leverage effect, but also compound Poisson jumps in both returns and volatility. There are no direct comparisons between Lévy jump models and the double-jump model of EJP (2003) in capturing the joint return dynamics in the current literature.[3]

In this paper, we compare the performances of some widely used Lévy jump models with that of the most sophisticated AJD models in capturing the joint dynamics of spot and option prices of the S&P 500 index. In particular, we consider models with stochastic volatility and jumps in returns that follow variance gamma (VG) or log stable (LS) processes, two most commonly used Lévy processes in the current literature. We also consider AJD models with stochastic volatility and compound Poisson jumps in returns or correlated compound Poisson jumps in both returns and volatility. The latter is the preferred model of EJP (2003).

Our approach has several advantages over most existing studies on Lévy processes. First, our analysis focuses on the joint dynamics of spot and options prices. In contrast, most existing studies on Lévy processes have mainly focused on either the physical or the risk-neutral dynamics. Second, by using both spot and option prices, we could obtain more accurate estimates of model parameters and latent volatility and jump variables, because both sets of prices contain important information about the same return dynamics. Finally, the joint analysis allows us to estimate market prices of risks that govern the change of measure process. This is impossible to do in most previous studies

(2003) have studied various Lévy processes, such as variance gamma (VG) and log stable (LS) processes, for option pricing. On the other hand, Li, Wells, and Yu (2006) provide a Bayesian analysis of return models with stochastic volatility and Lévy jumps using S&P 500 index returns.

[3]Existing studies of Lévy processes using option prices, such as Huang and Wu (2003), do not compare the performances of Lévy jump models with that of the double-jump model.

because spot (option) prices allow identification of only the physical (risk-neutral) parameters.

We face several challenges in our joint analysis of Lévy jump models. First, while the change of measure for Brownian motion and compound Poisson process is well understood, the change of measure for infinite-activity Lévy jumps is more complicated and less studied in the literature. Second, the estimation of Lévy processes is generally quite difficult. For example, for stable distribution, except for some special cases, the probability density generally does not have a closed form and higher moments of returns do not even exist. As a result, it is difficult to use likelihood- or moment-based methods for estimation. Finally, the inclusion of option prices significantly increases the computational complexity because certain parameters enter into the option pricing formulae nonlinearly and the computation of option prices involves numerical integrations.

Our paper overcomes these difficulties and contributes to the fast-growing literature on Lévy processes in several dimensions. First, based on an important result of Sato (1999), we provide a detailed analysis on the change of measure for VG and LS processes. In existing AJD models, jumps under both the physical and the risk-neutral measures are restricted to follow the same compound Poisson processes. For a fair comparison between AJD and Lévy jump models, we restrict jumps in our Lévy models to follow the same Lévy processes under both measures.

Second, we develop and implement efficient Markov chain Monte Carlo (MCMC) methods for estimating model parameters, latent volatility and jump variables of Lévy jump models using spot and option prices. The MCMC methods allow us to filter out latent volatility and jump variables, which are important for understanding the contributions of these factors to model performance. The MCMC methods developed here are extensions of that of Li, Wells, and Yu (2006) (hereafter LWY), who mainly focus on estimating Lévy jump models using spot prices. Due to the nonlinear option pricing formulae involved, we rely on more sophisticated updating procedures for many model parameters and latent variables.

Finally, we apply the MCMC methods to estimate the AJD and Lévy jump models using daily returns of the S&P 500 index and daily prices of a short-term ATM SPX option from January 4, 1993 to December 31, 1993. We show that our Lévy jump models significantly outperform the preferred AJD model of EJP (2003) in capturing the joint dynamics of the spot and option prices of the S&P 500 index. For the physical dynamics, the infinite-activity Lévy jumps capture many small movements in index returns that are too big for Brownian motion to model and too small for compound Poisson process to capture. For the risk-neutral dynamics, the Lévy jump models have significantly smaller in-sample and out-of-sample option pricing errors than the preferred AJD model. We also confirm the result of Eraker (2004) that jumps in volatility do not significantly improve the modeling of option prices, although they improve the modeling of the physical dynamics.

There are only a few other studies that estimate Lévy processes using spot and option prices jointly. Wu (2004) introduces the so-called dampened power law to capture the tail behaviors of index returns under the physical and the risk-neutral measures. Bakshi and Wu (2005) estimate Lévy jump models using the spot and option prices of the Nasdaq 100 index during the Internet "bubble" period. Our study differs from and complements these papers in terms of our research objective, theoretical approach, and estimation method.

The main focus of our paper is to address a basic and yet fundamental issue in the current continuous-time finance literature: Can commonly used Lévy jump models outperform the most sophisticated AJD models in capturing the joint dynamics of spot and option prices? The empirical advantages of Lévy jump models over AJD models documented here will help to remove any doubts on the empirical relevance of Lévy processes and will help to further advance the literature on Lévy processes. On the other hand, while Wu (2004) and Bakshi and Wu (2005) consider more sophisticated Lévy models, they do not compare the performances of their models with that of AJD models and thus do not address the basic question studied in this paper.

Consistent with the main objective of our study, we also adopt a different approach to the change of measure for Lévy processes from that of Wu (2004) and Bakshi and Wu (2005). We require that jumps follow the same Lévy processes under the physical and the risk-neutral measures in order to have a fair comparison with AJD models in which jumps under both measures follow compound Poisson processes. Given this restriction, we obtain the Radon-Nikodym derivatives for VG and LS processes based on Sato's (1999) theorem. In contrast, Wu (2004) and Bakshi and Wu (2005) fix the form of the Radon-Nikodym derivative, which is defined by the so-called Esscher transform. Under this transform, jumps generally follow different Lévy processes under the two measures. The two approaches to the change of measure impose different restrictions on model structures and are appropriate for different applications.

The estimation method used in our paper is also different from that of Wu (2004) and Bakshi and Wu (2005), which is likelihood based. The MCMC approach we adopt is particularly suitable to deal with the large number of latent volatility and jump variables and allows us to study the impacts of priors and parameter uncertainties in applications such as hedging, portfolio selection, and VaR calculation.

The rest of the paper is organized as follows. In Section 1, we introduce the AJD and Lévy jump models and discuss the change of measure and option pricing under these models. In Section 2, we develop MCMC methods for estimating model parameters and latent variables of Lévy jump models using spot and option prices. Section 3 contains empirical results using daily S&P 500 index returns and prices of SPX options. Section 4 concludes the paper. Appendix A provides mathematical proofs and Appendix B provides detailed discussions of the MCMC methods.

1. AJD and Lévy Jump Models for Return Dynamics

In this section, we introduce some of the most sophisticated AJD models and some commonly used Lévy jump models for return dynamics. We also discuss the change of measure (between the physical and the risk-neutral measures) and option pricing under these models. This section provides the theoretical foundation for the empirical analysis in the later part of the paper.

1.1 AJD Models for Return Dynamics

Suppose the uncertainty of the economy is described by a probability space $(\Omega, \mathcal{F}, \mathbb{P})$ and a filtration $\{\mathcal{F}_t\}$. We refer to $\mathbb{P}$ as the physical probability measure which represents the probability measure of the real world in which we reside. Let S_t be the price of a stock and Y_t be the continuously compounded return on the stock, i.e., $Y_t = \log S_t$. We assume that the dynamics of Y_t are characterized by the following model:

$$\begin{aligned} dY_t &= \mu dt + \sqrt{v_t} dW_t^{(1)}(\mathbb{P}) + dJ_t^y(\mathbb{P}), \quad (1) \\ dv_t &= \kappa(\theta - v_t)\, dt + \sigma_v \sqrt{v_t}\left(\rho dW_t^{(1)}(\mathbb{P}) + \sqrt{1-\rho^2} dW_t^{(2)}(\mathbb{P})\right) + dJ_t^v(\mathbb{P}), \quad (2) \end{aligned}$$

where μ measures the expected rate of return, v_t measures the instantaneous volatility of return, $W_t^{(1)}(\mathbb{P})$ and $W_t^{(2)}(\mathbb{P})$ are independent standard Brownian motions under $\mathbb{P}$, and $J_t^y(\mathbb{P})$ and $J_t^v(\mathbb{P})$ represent jumps in returns and volatility under $\mathbb{P}$, respectively.

In the above model, the instantaneous volatility of returns is stochastic and follows the square-root process of Heston (1993): θ represents the long-run mean of v_t, κ is the speed of mean reversion, σ_v is the so-called volatility of volatility, and ρ measures the correlation between volatility and returns. Many studies have documented a strong negative correlation between volatility and returns, the so-called "leverage" effect, and the correlation coefficient ρ helps to capture this phenomenon.

The above model is sometimes referred to as the double-jump model because of the jumps in both returns and volatility. As shown in EJP (2003), the negative jumps in returns, $J_t^y(\mathbb{P})$, help to capture the major crashes observed in the U.S. market; and the jumps in volatility, $J_t^v(\mathbb{P})$, help to model rapid increase in volatility that cannot be easily captured by the square-root process.

In models with jumps only in returns, it is often assumed that the jump component follows a compound Poisson process with a constant jump intensity and jump sizes that follow a normal distribution:

$$J_t^y(\mathbb{P}) = \sum_{n=1}^{N_t} \xi_n^y,$$

where $N_t \sim Poisson(\lambda t)$ and $\xi_n^y \sim N(\mu_y, \sigma_y^2)$. We refer to this model as the Merton Jump (hereafter MJ) model because it was first introduced in Merton (1976). Among models with jumps in both returns and volatility, the correlated Merton Jump (hereafter CMJ) model is the preferred model in EJP (2003) and Eraker (2004):

$$\begin{pmatrix} J_t^y(\mathbb{P}) \\ J_t^v(\mathbb{P}) \end{pmatrix} = \sum_{n=1}^{N_t} \begin{pmatrix} \xi_n^y \\ \xi_n^v \end{pmatrix},$$

where $N_t \sim Poisson(\lambda t)$, $\xi_n^v \sim \exp(\mu_v)$, and $\xi_n^y | \xi_n^v \sim N(\mu_y + \rho_J \xi_n^v, \sigma_y^2)$.

The model in (1)-(2) nests most AJD models for return dynamics under the physical measure in the existing literature. For example, without jumps in returns and volatility, the above model reduces to the stochastic volatility model of Heston (1993). With MJ jumps only in returns, we have the stochastic volatility and MJ jump model of Bates (1996), Bakshi, Cao, and Chen (1997), Andersen, Benzoni, and Lund (2002), and Pan (2002) among others.

We consider two AJD models in our empirical analysis. The first model, denoted as SVMJ, has stochastic volatility and MJ jumps in returns. The second model, denoted as SVCMJ, has stochastic volatility and correlated MJ jumps in returns and volatility and is the preferred model of EJP (2003).

1.2 Lévy Jump Models for Return Dynamics

The two basic building blocks for AJD models, Brownian motion and compound Poisson process, are special cases of Lévy processes, which are continuous-time stochastic processes with stationary and independent increments. Formally, if X_t is a scalar Lévy process with respect to the filtration $\{\mathcal{F}_t\}$, then X_t is adapted to $\mathcal{F}_t$, the sample paths of X_t are right-continuous with left limits, and $X_s - X_t$ is independent of $\mathcal{F}_t$ and distributed as X_{s-t} for $0 \leq t < s$. Lévy processes are much more flexible than Brownian motion and compound Poisson process because they allow discontinuous sample paths, non-normal increments, and more flexible jump structures that have (possibly) infinite arrival rates.

Although the probability densities of Lévy processes are generally not known in closed form, their characteristic functions $\phi_{X_t}(u)$ can be explicitly specified as follows,

$$\phi_{X_t}(u) = E\left[e^{iuX_t}\right] = e^{-t\psi_x(u)},\ t \geq 0,$$

where $\psi_x(u)$ is called the characteristic exponent and satisfies the following Lévy-Khintchine formula (see Bertoin, 1996, p. 12)

$$\psi_x(u) \equiv -i\bar{\mu}u + \frac{\bar{\sigma}^2 u^2}{2} + \int_{\mathbb{R}_0} \left(1 - e^{iux} + iux1_{|x|<1}\right)\pi(dx),$$

$u \in \mathbb{R}$, $\bar{\mu} \in \mathbb{R}$, $\bar{\sigma} \in \mathbb{R}^+$, and π is a measure on $\mathbb{R}_0 = \mathbb{R}\setminus\{0\}$ ($\mathbb{R}$ less zero) with

$$\int_{\mathbb{R}_0} \min\left(1, x^2\right)\pi(dx) < \infty.$$

The Lévy-Khintchine formula suggests that a Lévy process consists of three independent components: a linear deterministic drift part, a Brownian part, and a pure jump part. The triplet $\left(\bar{\mu}, \bar{\sigma}^2, \pi(\cdot)\right)$, often called the characteristics of the Lévy process, completely describe the probabilistic behavior of the process. The Lévy measure $\pi(dx)$ dictates the jump behavior of the process. It has the interpretation that $\pi(E)$, for any subset $E \subset \mathbb{R}$, is the rate at which the process takes jumps of size $x \in E$. In other words, $\pi(E)$ measures the number of jumps whose jump sizes falling in E per unit of time.

Depending on its Lévy measure $\pi(\cdot)$, a pure jump Lévy process can exhibit rich jump behaviors. For finite-activity jump processes, which have a finite number of jumps within any finite time interval, π needs to be integrable, that is,

$$\int_{\mathbb{R}_0} \pi(dx) = \lambda < \infty. \tag{3}$$

The classical example of a finite-activity jump process is the MJ model, in which the integral in (3) defines the Poisson arrival intensity λ. Conditional on one jump occurring, the MJ model assumes that the jump magnitude is normally distributed with mean μ_y and variance σ_y^2. The Lévy measure of the MJ model is given by

$$\pi_{MJ}(dx) = \lambda \frac{1}{\sqrt{2\pi\sigma_y^2}} \exp\left(-\frac{(x-\mu_y)^2}{2\sigma_y^2}\right) dx.$$

Obviously, one can choose any distribution, $F(x)$, for the jump size under the compound Poisson framework and obtain the Lévy measure $\pi(dx) = \lambda dF(x)$.

Unlike finite-activity jump processes, an infinite-activity jump process allows an (possibly) infinite number of jumps within any finite time interval. The integral of the Lévy measure in (3) is no longer finite. Within the infinite-activity category, the sample path of the jump process can exhibit either finite or infinite variation, meaning that the aggregate absolute distance traveled by the process is finite or infinite, respectively, over any finite time interval.

In our empirical analysis, we choose the relatively parsimonious variance-gamma (hereafter VG) model of Madan, Carr, and Chang (1998) as a representative of the infinite-activity but finite variation jump model. The VG process is obtained by subordinating an arithmetic Brownian motion with drift γ and variance σ by an independent gamma process with unit mean rate and variance rate ν, G_t^ν. That is,

$$X_{VG}(t|\sigma,\gamma,\nu) = \gamma G_t^\nu + \sigma W(G_t^\nu),$$

where $W(t)$ is a standard Brownian motion and is independent of G_t^ν. The Lévy measure of the VG process is given by

$$\pi_{VG}(dx) = \begin{cases} \frac{1}{\nu}\frac{\exp(-Mx)}{x}dx & x > 0 \\ \frac{1}{\nu}\frac{\exp(-G|x|)}{|x|}dx & x < 0 \end{cases},$$

where $M = \left(\sqrt{\frac{1}{4}\gamma^2\nu^2 + \frac{1}{2}\sigma^2\nu} + \frac{1}{2}\gamma\nu\right)^{-1}$ and $G = \left(\sqrt{\frac{1}{4}\gamma^2\nu^2 + \frac{1}{2}\sigma^2\nu} - \frac{1}{2}\gamma\nu\right)^{-1}$. If $\gamma = 0$, then the jump structure is symmetric around zero, and $M = G$. Note that as the jump size approaches zero, the arrival rate approaches infinity. Thus, an infinite-activity model incorporates (possibly) infinitely many small jumps. The Lévy measure of an infinite-activity jump process is singular at a zero jump size.

Another example of infinite-activity jump model is the Lévy α-stable process. In this process, jump sizes follow an α-stable distribution denoted as $S_\alpha(\beta, \delta, \gamma)$, with a tail index $\alpha \in (0, 2]$, a skew parameter $\beta \in [-1, 1]$, a scale parameter $\delta \geq 0$, and a location parameter $\gamma \in \mathbb{R}$. The parameter α determines the shape of the distribution, while β determines the skewness of the distribution. Stable densities are supported on either $\mathbb{R}$ or $\mathbb{R}^+$. The latter situation occurs only when $\alpha < 1$ and $\beta = \pm 1$. The characteristic function of an α-stable distribution S is given by

$$E\left[e^{iuS}\right] = \begin{cases} \exp\left(-\delta^\alpha |u|^\alpha \left[1 - i\beta \left(\tan \frac{\pi\alpha}{2}\right)(\text{sign } u)\right] + i\gamma u\right) & \alpha \neq 1 \\ \exp\left(-\delta |u| \left[1 + i\beta \frac{2}{\pi} (\text{sign } u) \ln |u|\right] + i\gamma u\right) & \alpha = 1. \end{cases}$$

For a standardized α-stable distribution, denoted as $S_\alpha(\beta, 1, 0)$, $\delta = 1$ and $\gamma = 0$.

All α-stable processes are built upon a fundamental process called α-stable motion. A process X_t is an α-stable motion if (i) $X_0 = 0$ a.s., (ii) X_t has independent increments, and (iii) the increment $X_t - X_s$ $(t > s)$ follows an α-stable distribution $S_\alpha\left(\beta, (t-s)^{\frac{1}{\alpha}}, 0\right)$. The role that α-stable motion plays for α-stable processes is similar to that of Brownian motion for diffusion processes. Among α-stable processes, we choose the finite moment log-stable (hereafter LS) process of Carr and Wu (2003) in our analysis. We obtain this process by multiplying an α-stable motion by a constant σ. Following Carr and Wu (2003), we set $\beta = -1$ to achieve finite moments for index levels under the risk-neutral measure (and thus finite option prices), and negative skewness in the return density, a feature that cannot be captured by either a Brownian motion or a symmetric Lévy α-stable motion. We also restrict $\alpha \in (1, 2)$ so that the process has the support of the whole real line. The α-stable process defined in this way is a Lévy process with infinite activity and infinite variation and has a Lévy measure

$$\pi_{LS}(dx) = \begin{cases} c_1 \frac{1}{x^{1+\alpha}} dx & x > 0 \\ c_2 \frac{1}{|x|^{1+\alpha}} dx & x < 0 \end{cases},$$

where $c_1 = \frac{\sigma^{\alpha}(1+\beta)}{2}$ and $c_2 = \frac{\sigma^{\alpha}(1-\beta)}{2}$. In the LS model, c_1 becomes zero so that only negative jumps are allowed in the Lévy measure. However, it is important to point out that in addition to the pure jump part characterized by the Lévy measure $\pi_{LS}(dx)$, the LS process also has a deterministic drift part that compensates the negative jumps so that the whole process is a martingale. For infinite-variation jumps, the compensation is so much that the admissible domain of LS actually covers the whole real line, although there are only negative jumps. As a result, the LS process has an α-stable distribution with infinite p-th moment for $p > \alpha$.

Therefore, we consider the following Lévy jump models for return dynamics in our empirical analysis,

$$dY_t = \mu dt + \sqrt{v_t} dW_t^{(1)}(\mathbb{P}) + dJ_t^y(\mathbb{P}), \tag{4}$$

$$dv_t = \kappa(\theta - v_t)\, dt + \sigma_v \sqrt{v_t}\left(\rho dW_t^{(1)}(\mathbb{P}) + \sqrt{1-\rho^2} dW_t^{(2)}(\mathbb{P})\right), \tag{5}$$

where $J_t^y(\mathbb{P})$ follows either the VG or LS processes: $J_t^y(\mathbb{P}) = X_{VG}(t|\sigma, \gamma, \nu)$ or $J_t^y(\mathbb{P}) = X_{LS}(t|\alpha, \sigma)$. We refer to the above model with VG or LS jumps in returns as SVVG and SVLS, respectively. These two models allow us to compare the performances of infinite-activity jumps in returns with that of compound Poisson jumps in both returns and volatility.

1.3 Change of Measure and Option Pricing for AJD and Lévy Jump Models

While equations (1)-(2) and (4)-(5) describe the AJD and Lévy jump models respectively under the physical measure $\mathbb{P}$, for the purpose of option pricing, we also need return dynamics under the risk-neutral measure $\mathbb{Q}$. Thus we need to consider the change of measure between $\mathbb{P}$ and $\mathbb{Q}$ for these models.

The change of measure for Brownian motion is well understood in the literature. Following the standard practice of Pan (2002), we assume that the market prices of risks of Brownian shocks to returns and volatility are

$$\gamma_t^{(1)} = \eta^s \sqrt{v_t}, \tag{6}$$

$$\gamma_t^{(2)} = -\frac{1}{\sqrt{1-\rho^2}}\left(\rho\eta^s + \frac{\eta^v}{\sigma_v}\right)\sqrt{v_t}, \tag{7}$$

respectively. Thus, the change of measure for the two Brownian motions is

$$\begin{aligned} dW_t^{(1)}(\mathbb{Q}) &= dW_t^{(1)}(\mathbb{P}) + \gamma_t^{(1)} dt, \\ dW_t^{(2)}(\mathbb{Q}) &= dW_t^{(2)}(\mathbb{P}) + \gamma_t^{(2)} dt, \end{aligned}$$

where $dW_t^{(1)}(\mathbb{Q})$ and $dW_t^{(2)}(\mathbb{Q})$ are independent standard Brownian motions under $\mathbb{Q}$.

While the change of measure for Brownian motion only involves changing the drift term, the change of measure for Lévy processes is much more complicated. The important result of Sato (1999) provides the theoretical foundation for the change of measure of Lévy processes considered in this paper.

Theorem 1. (Sato (1999)). Let $\left(X_t^{\mathbb{P}}, \mathbb{P}\right)$ and $\left(X_t^{\mathbb{Q}}, \mathbb{Q}\right)$ be two Lévy processes on $\mathbb{R}$ with corresponding characteristic triplets $\left(\bar{\mu}_{\mathbb{P}}, \bar{\sigma}_{\mathbb{P}}^2, \pi_{\mathbb{P}}(dx)\right)$ and $\left(\bar{\mu}_{\mathbb{Q}}, \bar{\sigma}_{\mathbb{Q}}^2, \pi_{\mathbb{Q}}(dx)\right)$, and $\phi(x) = \log\left(\frac{\pi_{\mathbb{Q}}(x)}{\pi_{\mathbb{P}}(x)}\right)$. Then $\mathbb{P}$ and $\mathbb{Q}$ are equivalent for all t if and only if the following conditions are satisfied: (i) $\bar{\sigma}_{\mathbb{P}} = \bar{\sigma}_{\mathbb{Q}}$; (ii) The Lévy measures are equivalent with $\int_{-\infty}^{\infty}\left(e^{\phi(x)/2} - 1\right)^2 \pi_{\mathbb{P}}(dx) < \infty$; and (iii) If $\bar{\sigma}_{\mathbb{P}} = 0$, then we must in addition have $\bar{\mu}_{\mathbb{Q}} - \bar{\mu}_{\mathbb{P}} = \int_{-1}^{1} x\left(\pi_{\mathbb{Q}}(x) - \pi_{\mathbb{P}}(x)\right)dx$. And the Radon-Nikodym derivative equals e^{U_t}, where U_t is a Lévy process with characteristic triplet $\left(\bar{\mu}_u, \bar{\sigma}_u^2, \pi_u(dx)\right)$: (i) $\bar{\sigma}_u^2 = 0$; (ii) $\bar{\mu}_u = -\int_{-\infty}^{\infty}\left(e^y - 1 - y_{|y|\le 1}\right)\left(\pi_{\mathbb{P}}\phi^{-1}\right)dy$; and (iii) $\pi_u = \pi_{\mathbb{P}}\phi^{-1}$.

Proof. See Sato (1999).

The above theorem provides the necessary and sufficient conditions for two probability measures of Lévy processes to be equivalent. The three conditions are imposed on the drift, Brownian, and jump parts of a Lévy process, respectively. The first condition requires that the change of measure does not affect the volatility of the Brownian part of a Lévy process, which is similar to the change of measure for Brownian motions. The second condition requires the Hellinger distance between the two Lévy measures to be finite. That is, for the two probability measures to be equivalent, the jump structures of the two Lévy processes cannot be too different from each other. The third condition imposes restriction between the drift terms and the Lévy measures of the two Lévy processes.

Sato's (1999) theorem is very general, and to apply it in empirical analysis, some restrictions on model structures have to be imposed. One approach that has been adopted by Wu (2004) and Bakshi and Wu (2005) is based on the Esscher transform, which explicitly specifies the form of the Radon-Nikodym derivative between $\mathbb{P}$ and $\mathbb{Q}$. Under this approach, if we have a Lévy jump under one measure, we can easily get its representation under the other measure. Because the Radon-Nikodym derivative is fixed, the Lévy jumps under the two measures may not follow the same Lévy processes. This approach allows greater flexibility for modeling purposes, because the Esscher transform allows different Lévy jumps under the physical and the risk-neutral measures.

However, under AJD models, jumps under both $\mathbb{P}$ and $\mathbb{Q}$ follow the same compound Poisson processes with different parameters. To be consistent with the main objective of our study, we choose a different approach to the change of measure from that of Wu (2004) and Bakshi and Wu (2005). Specifically, to have a fair comparison with AJD models, we restrict Lévy jumps under $\mathbb{P}$ and $\mathbb{Q}$ to follow the same Lévy process. That is, if the Lévy jump under $\mathbb{P}$ is VG (LS), then the Lévy jump under $\mathbb{Q}$ has to be VG (LS) as well, although with possible different parameters. Under this restriction, the Radon-Nikodym derivative between $\mathbb{P}$ and $\mathbb{Q}$ generally will be different from that of Wu (2004) and Bakshi and Wu (2005). Based on the general result of Sato (1999) and our specific model restriction, we obtain the following results on the change of measure for the four jump processes considered in our paper.

Proposition 1. The parameters of the following four jump processes under measures $\mathbb{P}$ and $\mathbb{Q}$ must satisfy the following restrictions:

- All parameters of MJ, $(\lambda, \mu_y, \sigma_y)$, can change freely between $\mathbb{P}$ and $\mathbb{Q}$;
- All parameters of CMJ, $(\lambda, \mu_y, \sigma_y, \rho_J, \mu_v)$, can change freely between $\mathbb{P}$ and $\mathbb{Q}$;

- Among the parameters of VG, (ν, γ, σ), γ and σ can change freely between $\mathbb{P}$ and $\mathbb{Q}$, while ν has to be the same under $\mathbb{P}$ and $\mathbb{Q}$;

- None of the parameters of a Lévy α-stable process, $(\alpha, \beta, \sigma, \gamma)$, can change between $\mathbb{P}$ and $\mathbb{Q}$.

Proof. See Appendix A.

The above results impose restrictions on the physical and the risk-neutral parameters of the four jump processes. For MJ and CMJ, all parameters can take different values under the physical and the risk-neutral measures. Previous studies, such as Pan (2002) and Eraker (2004), show that allowing all the parameters to change between measures makes econometric identification difficult. As a result, they only allow the mean jump size μ_y to be different between $\mathbb{P}$ and $\mathbb{Q}$. To compare our results with existing studies, we follow the same approach. As a result, the parameters of MJ and CMJ under both measures are $\left(\lambda, \sigma_y, \mu_y, \mu_y^{\mathbb{Q}}\right)$ and $\left(\lambda, \sigma_y, \sigma_v, \rho_J, \mu_y, \mu_y^{\mathbb{Q}}\right)$, respectively. The parameters of VG and LS under both measures are $\left(\nu, \gamma, \sigma, \gamma^{\mathbb{Q}}, \sigma^{\mathbb{Q}}\right)$ and (α, σ), respectively.

If the Lévy measures of the four jump processes under $\mathbb{P}$ and $\mathbb{Q}$ satisfy the restrictions in Proposition 1, then the Radon-Nikodym derivatives of these processes are given as e^{U_t}, where U_t is defined as in the second part of Sato's (1999) theorem. Combining this with the change of measure for the two Brownian motions, we obtain the Radon-Nikodym derivatives for the AJD and Lévy jump models:

$$\frac{d\mathbb{Q}}{d\mathbb{P}}|_t = \exp\left\{-\int_0^t \gamma_s^{(1)} dW_s^{(1)}(\mathbb{P}) - \int_0^t \gamma_s^{(2)} dW_s^{(2)}(\mathbb{P}) - \frac{1}{2}\left(\int_0^t \gamma_s^{(1)2} ds + \int_0^t \gamma_s^{(2)2} ds\right)\right\} \exp U_t.$$

This naturally leads to the risk-neutral return dynamics of all four models we consider

$$dY_t = \left[r_t - \frac{1}{2}v_t + \psi_J^{\mathbb{Q}}(-i)\right] dt + \sqrt{v_t} dW_t^{(1)}(\mathbb{Q}) + dJ_t^y(\mathbb{Q}), \tag{9}$$

$$dv_t = \left[\kappa(\theta - v_t) + \eta^v v_t\right] dt + \sigma_v \sqrt{v_t}\left(\rho dW_t^{(1)}(\mathbb{Q}) + \sqrt{1-\rho^2} dW_t^{(2)}(\mathbb{Q})\right) + dJ_t^v(\mathbb{Q}), \tag{10}$$

where $J_t^v(\mathbb{Q}) = 0$ for SVMJ, SVVG, and SVLS. The drift term of the return process under $\mathbb{Q}$ has three components: the risk-free interest rate r_t, the Ito adjustment for log price $-\frac{1}{2}v_t$, and the jump compensator in returns $\psi_J^{\mathbb{Q}}(-i)$ under $\mathbb{Q}$.[4] Consequently the drift term of the return process under $\mathbb{P}$ equals $\mu = r_t - \frac{1}{2}v_t + \psi_J^{\mathbb{Q}}(-i) + \eta^s v_t$.

Option prices are determined by the risk-neutral dynamics of stock returns. Carr and Wu (2004) show that Lévy processes are as tractable as AJD models for the purpose of option pricing: The risk-neutral dynamics in (9)-(10) lead to closed-form solution to the characteristic function of the log stock price under $\mathbb{Q}$. That is, when interest rate is constant,

$$\begin{aligned}
\phi_t(u) &= E_0^{\mathbb{Q}}\left[e^{iuY_t}\right] \\
&= E_0^{\mathbb{Q}}\left[e^{iuY_0+iu(r+\psi_J(-i))t+iu\left(\int_0^t \sqrt{v_t}dW_s^{(1)}(\mathbb{Q})-\frac{1}{2}\int_0^t v_s ds\right)+iuJ_t^y}\right] \\
&= e^{iuY_0+iu(r+\psi_J(-i))t}E_0^{\mathbb{Q}}\left[e^{iuJ_t^y}\right]E_0^{\mathbb{Q}}\left[e^{iu\left(\int_0^t \sqrt{v_t}dW_s^{(1)}(\mathbb{Q})-\frac{1}{2}\int_0^t v_s ds\right)}\right] \\
&= e^{iuY_0+iu(r+\psi_J(-i))t}e^{-t\psi_J(u)}e^{-b(t)v_0-c(t)},
\end{aligned}$$

where

$$\begin{aligned}
b(t) &= \frac{\left(iu+u^2\right)\left(1-e^{-\delta t}\right)}{\left(\delta+\kappa^M\right)+\left(\delta-\kappa^M\right)e^{-\delta t}}, \\
c(t) &= \frac{\kappa\theta}{\sigma_v^2}\left[2\ln\frac{2\delta-\left(\delta-\kappa^M\right)\left(1-e^{-\delta t}\right)}{2\delta}+\left(\delta-\kappa^M\right)t\right],
\end{aligned}$$

$\kappa^M = \kappa - \eta^v - iu\sigma_v\rho$, $\delta = \sqrt{\left(\kappa^M\right)^2 + \left(iu+u^2\right)\sigma_v^2}$, and $Y_0 = \log(S_0)$.

The closed-form expression of the characteristic function of the log stock price naturally leads to closed-form expression of the Fourier transform of option prices. Consequently, option price can be solved using the Fourier inversion formula. The time-0 price of a European call option with time-to-maturity of τ and strike price of K equals

$$\begin{aligned}
F(Y_0, v_0, \tau, K) &= E_0^{\mathbb{Q}}\left[e^{-r\tau}\left(S_\tau - K\right)^+\right] \\
&= \frac{e^{-r\tau}}{\pi}\times\mathrm{Re}\left(\int_0^\infty e^{-ix\log(K)}\frac{\phi_\tau(x-i)}{-x^2+ix}dx\right).
\end{aligned}$$

[4] The explicit expressions of $\psi_J(\cdot)$ of the four jump processes are given in Appendix A.

In addition to the contractual terms of the option, the option price also depends on the current levels of the stock price (Y_0) and the instantaneous stochastic volatility (v_0).

2. MCMC Estimation of Lévy Jump Models Using Spot and Option Prices

In this section, we discuss Bayesian MCMC estimation of Lévy jump models using spot and option prices. We first summarize the specifications of all models considered in our empirical studies. Then we discuss the econometric methods used for model estimation and comparison.

2.1 Summary of Model Specifications

In our joint estimation of Lévy jump models, we use daily returns on the S&P 500 index and daily prices of a short-term ATM SPX option. Let $C(t, \tau, K)$ be the market price at t of the option with time-to-maturity τ and strike price K, and $F(t, \tau, K, Y_t, v_t; \mathbf{\Theta})$ be the theoretical price of the same option in a given model where the log stock price equals Y_t, the instantaneous volatility equals v_t, and the vector of model parameters is denoted as $\mathbf{\Theta}$. We assume that the market price of the option equals its theoretical price plus some random noises:

$$C(t, \tau, K) = F(t, \tau, K, Y_t, v_t; \mathbf{\Theta}) + \varpi_t^c,$$

where ϖ_t^c is the option pricing error. Similar to Eraker (2004), we allow first-order autocorrelation in option pricing errors,

$$\varpi_t^c \sim N\left(\rho_c \varpi_{t-1}^c, \sigma_c^2\right).$$

This specification intends to capture the phenomenon that if option pricing error is high on one day, it is likely to be high on the next day.

We consider first-order Euler discretization of the continuous-time models at daily frequency. Simulation studies in EJP (2003) and LWY (2006) show that the bias introduced by daily discretization is very small. Therefore, the joint dynamics of the daily spot and the option prices under the four models we consider are summarized by the following system of equations:

$$\left\{ \begin{array}{c} C_{t+1} - F_{t+1} = \rho_c (C_t - F_t) + \sigma_c \epsilon_t^c \\ \\ Y_{t+1} = Y_t + \mu\Delta + \sqrt{v_t \Delta}\epsilon_{t+1}^y + J_{t+1}^y, \\ \\ v_{t+1} = v_t + \kappa(\theta - v_t)\Delta + \sigma_v \sqrt{v_t \Delta}\epsilon_{t+1}^v + J_{t+1}^v, \end{array} \right. \tag{11}$$

where $\Delta = \frac{1}{252}$, $\mu = r_t - \frac{1}{2} v_t + \psi_J(-i) + \eta^s v_t$, ϵ_t^c, ϵ_{t+1}^y, and $\epsilon_{t+1}^v \sim N(0,1)$, $corr(\epsilon_{t+1}^y, \epsilon_{t+1}^v) = \rho$, and ϵ_t^c is independent of ϵ_{t+1}^y and ϵ_{t+1}^v.

Specializing (11) to each of the four models, we have the following exact specifications of each model.

- **SVMJ.** In this model, $J_{t+1}^y = \xi_{t+1}^y N_{t+1}^y$, $P(N_{t+1}^y = 1) = \lambda\Delta$, $\xi_{t+1}^y \sim N(\mu_y, \sigma_y^2)$, and $J_{t+1}^v = 0$ for all t. We have observations $(Y_t, C_t)_{t=0}^T$; latent volatility variables $(v_t)_{t=0}^T$, jump times $(N_t^y)_{t=1}^T$, and jump sizes $(\xi_t^y)_{t=1}^T$; and parameters $\mathbf{\Theta} = \{(\kappa, \theta, \sigma_v, \rho, \mu_y, \sigma_y, \lambda), (\mu_y^{\mathbb{Q}}), (\eta^s, \eta^v), (\rho_c, \sigma_c)\}$, where the first group of parameters is either common to both measures or unique to the physical measure, the second one is unique to the risk-neutral measure, the third one represents the market prices of return and volatility risks, and the last one represents option pricing errors.

- **SVCMJ.** In this model, $J_{t+1}^y = \xi_{t+1}^y N_{t+1}$, $J_{t+1}^v = \xi_{t+1}^v N_{t+1}$, $P(N_{t+1} = 1) = \lambda\Delta$, $\xi_{t+1}^v \sim \exp(\mu_v)$, and $\xi_{t+1}^y | \xi_{t+1}^v \sim N\left(\mu_y + \rho_J \xi_{t+1}^v, \sigma_y^2\right)$. We have observations $(Y_t, C_t)_{t=0}^T$; latent volatility variables $(v_t)_{t=0}^T$, jump times $(N_t)_{t=1}^T$, and jump sizes $(\xi_t^v)_{t=1}^T$ and $(\xi_t^y)_{t=1}^T$; and parameters $\mathbf{\Theta} = \{(\kappa, \theta, \sigma_v, \rho, \mu_y, \sigma_y, \lambda, \rho_J, \mu_v), (\mu_y^{\mathbb{Q}}), (\eta^s, \eta^v), (\rho_c, \sigma_c)\}$, where the first group of parameters is either common to both measures or unique to the physical measure, the second one is unique to the risk-neutral measure, the third one represents the market prices of return and volatility risks, and the last one represents option pricing errors.

- **SVVG.** In this model, $J_{t+1}^v = 0$ for all t, and J_{t+1}^y follows a VG process whose discretized version is

$$J_{t+1}^y = \gamma G_{t+1} + \sigma \sqrt{G_{t+1}} \epsilon_{t+1}^J,$$

where $\epsilon^J_{t+1} \sim N(0,1)$ and $G_{t+1} \sim \Gamma(\frac{\Delta}{\nu}, \nu)$. ϵ^J_{t+1} and G_{t+1} are independent of each other and are independent of ϵ^y_{t+1} and ϵ^v_{t+1}. The parametrization of the Gamma distribution, $\Gamma(\alpha, \beta)$, used in this paper has density form $\frac{1}{\beta^\alpha \Gamma(\alpha)} x^{\alpha-1} e^{x/\beta}$. We have observations $(Y_t, C_t)^T_{t=0}$; latent volatility variables $(v_t)^T_{t=0}$, jump times/sizes $(J^y_t)^T_{t=1}$, and time-change variables $(G_t)^T_{t=1}$; and parameters $\mathbf{\Theta} = \{(\kappa, \theta, \sigma_v, \rho, \nu, \gamma, \sigma), (\gamma^{\mathbb{Q}}, \sigma^{\mathbb{Q}}), (\eta^s, \eta^v), (\rho_c, \sigma_c)\}$, where the first group of parameters is either common to both measures or unique to the physical measure, the second one is unique to the risk-neutral measure, the third one represents the market prices of return and volatility risks, and the last one represents option pricing errors.

- **SVLS.** In this model, $J^v_{t+1} = 0$ for all t. The jump size J^y_{t+1}, independent of ϵ^y_{t+1} and ϵ^v_{t+1}, follows a stable distribution with shape parameter α, skewness parameter -1, zero drift, and scale parameter $\sigma\Delta^{\frac{1}{\alpha}}$. That is, $J^y_{t+1} \sim S_\alpha(-1, \sigma\Delta^{\frac{1}{\alpha}}, 0)$. We have observations $(Y_t, C_t)^T_{t=1}$; latent volatility variables $(v_t)^T_{t=0}$, and jump times/sizes $(J^y_t)^T_{t=1}$; and parameters $\mathbf{\Theta} = \{(\kappa, \theta, \sigma_v, \rho, \alpha, \sigma), (\eta^s, \eta^v), (\rho_c, \sigma_c)\}$, where the first group of parameters is either common to both measures or unique to the physical measure, the second one represents the market prices of return and volatility risks, and the last one represents option pricing errors.

2.2 MCMC Methods

Estimation of Lévy processes is generally very difficult for several reasons. First, the probability densities for most Lévy processes are not known in closed form, and for certain Lévy processes higher moments of asset returns do not even exist. Second, the high dimensionality of latent variables, such as stochastic volatility, jump sizes and jump times, significantly complicates the estimation. Computationally it is very demanding to integrate out the large number of latent variables when implementing either likelihood or moment-based approaches. The inclusion of option prices significantly increases the computational complexity because certain parameters enter into the option pricing formulae nonlinearly, and the computation of option prices involves numerical integrations.

LWY (2006) have developed efficient Bayesian MCMC methods for estimating Lévy processes using only the spot price.[5] We extend their methods to estimate the physical and risk-neutral dynamics of Lévy processes jointly using spot and option prices. The main difference here is that we need to rely on more sophisticated updating procedures for many model parameters and latent variables due to the nonlinear option pricing formula involved.

Since MCMC analysis of SVMJ and SVCMJ has been considered in previous studies, such as EJP (2003) and Eraker (2004), we focus our discussions of MCMC methods on SVVG and SVLS. We mainly discuss how to derive the joint posterior distributions of model parameters and latent variables for the two models and briefly explain how to obtain posterior samples for individual parameters and latent variables by simulating from the complicated joint posterior distributions. More detailed discussions of our MCMC methods are provided in Appendix B.

We first consider SVVG. To simplify notation, we denote the index returns as $\mathbf{Y} = \{Y_t\}_{t=0}^{T}$, the option prices as $\mathbf{C} = \{C_t\}_{t=0}^{T}$, the volatility variables as $\mathbf{V} = \{v_t\}_{t=0}^{T}$, the jump times/sizes as $\mathbf{J} = \{J_t^y\}_{t=1}^{T}$, and the time-change variables as $\mathbf{G} = \{G_t\}_{t=1}^{T}$. The joint posterior distribution of parameters and latent variables, $p(\mathbf{\Theta}, \mathbf{V}, \mathbf{J}, \mathbf{G}|\mathbf{Y}, \mathbf{C})$, can be decomposed into products of individual conditionals

$$\begin{aligned} p(\mathbf{\Theta}, \mathbf{V}, \mathbf{J}, \mathbf{G}|\mathbf{Y}, \mathbf{C}) &\propto p(\mathbf{Y}, \mathbf{C}, \mathbf{V}, \mathbf{J}, \mathbf{G}, \mathbf{\Theta}) \\ &= p(\mathbf{C}|\mathbf{Y}, \mathbf{V}, \mathbf{\Theta})\, p(\mathbf{Y}, \mathbf{V}|\mathbf{J}) p(\mathbf{J}|\mathbf{G}, \mathbf{\Theta}) p(\mathbf{G}|\mathbf{\Theta}) p(\mathbf{\Theta}). \end{aligned}$$

Given the assumed option price dynamics, we have

$$p(\mathbf{C}|\mathbf{Y}, \mathbf{V}, \mathbf{\Theta}) = \prod_{t=0}^{T-1} \frac{1}{\sqrt{2\pi}\sigma_c} \exp\left\{ -\frac{[(C_{t+1} - F_{t+1}) - \rho_c (C_t - F_t)]^2}{2\sigma_c^2} \right\}.$$

[5] Earlier studies, such as Jacquier, Polson, and Rossi (1994), Kim, Shephard, and Chib (1998), and Chib, Nardari, and Shephard (2003), apply MCMC methods to estimate discrete-time stochastic volatility models. Other studies that apply MCMC methods to continuous-time models for stock price or interest rate include Jones (1998, 2003a, b), Eraker (2001, 2004), and Elerian, Chib, and Shephard (2001).

Conditioning on v_t and J^y_{t+1}, $Y_{t+1}-Y_t$ and $v_{t+1}-v_t$ follow a bivariate normal distribution

$$\begin{pmatrix} Y_{t+1}-Y_t \\ v_{t+1}-v_t \end{pmatrix} |v_t, J^y_{t+1} \sim N\left(\begin{pmatrix} \mu\Delta + J^y_{t+1} \\ \kappa(\theta - v_t)\Delta \end{pmatrix}, v_t\Delta \begin{pmatrix} 1 & \rho\sigma_v \\ \rho\sigma_v & \sigma_v^2 \end{pmatrix}\right),$$

$$J^y_{t+1}|G_{t+1}, \mathbf{\Theta} \sim N(\gamma G_{t+1}, \sigma^2 G_{t+1}) \text{ and } G_{t+1}|\mathbf{\Theta} \sim \Gamma(\frac{\Delta}{\nu}, \nu).$$

Therefore, the joint posterior distribution of parameters and latent variables is given as

$$p(\mathbf{\Theta}, \mathbf{V}, \mathbf{J}, \mathbf{G}|\mathbf{Y}, \mathbf{C}) \propto \prod_{t=0}^{T-1} \frac{1}{\sqrt{2\pi}\sigma_c} \exp\left\{-\frac{[(C_{t+1}-F_{t+1}) - \rho_c(C_t - F_t)]^2}{2\sigma_c^2}\right\}$$

$$\times \prod_{t=0}^{T-1} \frac{1}{\sigma_v v_t \Delta\sqrt{1-\rho^2}} \exp\left\{-\frac{1}{2(1-\rho^2)}\left(\left(\epsilon^y_{t+1}\right)^2 - 2\rho\epsilon^y_{t+1}\epsilon^v_{t+1} + \left(\epsilon^v_{t+1}\right)^2\right)\right\}$$

$$\times \prod_{t=0}^{T-1} \frac{1}{\sigma\sqrt{G_{t+1}}} \exp\left\{-\frac{(J_{t+1}-\gamma G_{t+1})^2}{2\sigma^2 G_{t+1}}\right\} \times \prod_{t=0}^{T-1} \frac{1}{\nu^{\frac{\Delta}{\nu}}\Gamma(\frac{\Delta}{\nu})} G_{t+1}^{\frac{\Delta}{\nu}-1} \exp\{-\frac{G_{t+1}}{\nu}\} \times p(\mathbf{\Theta}),$$

where $\epsilon^y_{t+1} = \left(Y_{t+1} - Y_t - \mu\Delta - J^y_{t+1}\right)/\sqrt{v_t\Delta}$ and $\epsilon^v_{t+1} = (v_{t+1} - v_t - \kappa(\theta - v_t)\Delta)/\left(\sigma_v\sqrt{v_t\Delta}\right)$.

In SVLS, conditioning on v_t and S_{t+1}, $Y_{t+1}-Y_t$ and $v_{t+1}-v_t$ follow a bivariate normal distribution

$$\begin{pmatrix} Y_{t+1}-Y_t \\ v_{t+1}-v_t \end{pmatrix} |v_t, S_{t+1} \sim N\left(\begin{pmatrix} \mu\Delta + S_{t+1} \\ \kappa(\theta - v_t)\Delta \end{pmatrix}, v_t\Delta \begin{pmatrix} 1 & \rho\sigma_v \\ \rho\sigma_v & \sigma_v^2 \end{pmatrix}\right),$$

$$S_{t+1} \sim S_\alpha(-1, \sigma\Delta^{\frac{1}{\alpha}}, 0).$$

In SVLS, we model jumps using stable process which can exhibit skewness and heavier tails than normal distributions. Unfortunately, the probability density of S_{t+1}, $p(S_{t+1}|\mathbf{\Theta})$, is unknown. This makes it difficult to explicitly write down the joint likelihood function of $(Y_{t+1}, v_{t+1}, S_{t+1})$, because $p(Y_{t+1}, v_{t+1}, S_{t+1}|\mathbf{\Theta}) = p(Y_{t+1}, v_{t+1}|S_{t+1}, \mathbf{\Theta})\, p(S_{t+1}|\mathbf{\Theta})$. Consequently, it is difficult to obtain the joint posterior distribution for SVLS.

Buckle (1995) provides a representation of a stable variable which makes it possible to estimate parameters of stable distributions using MCMC. The basic observation of Buckle (1995) is that although the density of a stable variable is generally unknown, the joint density of the stable variable and a well-chosen auxiliary variable is explicitly known. This joint density in turn leads to known joint posterior density of the stable variable and the auxiliary variable, which can be used in our MCMC algorithm.

For the LS process we consider, we set $\alpha \in (1,2]$, $\beta = -1$, $\gamma = 0$ and $\delta = \sigma\Delta^{\frac{1}{\alpha}}$. We denote the index returns as $\mathbf{Y} = \{Y_t\}_{t=0}^T$, the option prices as $\mathbf{C} = \{C_t\}_{t=0}^T$, the volatility variables as $\mathbf{V} = \{v_t\}_{t=0}^T$, the jump times/sizes as $\mathbf{S} = \{S_t\}_{t=1}^T$, and the auxiliary variables as $\mathbf{U} = \{U_t\}_{t=1}^T$. Based on Buckle's (1995) result, we obtain the joint posterior distribution of $\mathbf{V}$, $\mathbf{S}$, $\mathbf{U}$ and $\mathbf{\Theta}$ as

$$
\begin{aligned}
p\left(\mathbf{\Theta}, \mathbf{V}, \mathbf{S}, \mathbf{U} | \mathbf{Y}, \mathbf{C}\right) &\propto p(\mathbf{Y}, \mathbf{C}, \mathbf{V}, \mathbf{S}, \mathbf{U}, \mathbf{\Theta}) \\
&= p\left(\mathbf{C} | \mathbf{Y}, \mathbf{V}, \mathbf{\Theta}\right) p(\mathbf{Y}, \mathbf{V} | \mathbf{S}) p(\mathbf{S}, \mathbf{U} | \mathbf{\Theta}) p(\mathbf{\Theta})
\end{aligned}
$$

$$
\propto \prod_{t=0}^{T-1} \frac{1}{\sqrt{2\pi}\sigma_c} \exp\left\{ -\frac{\left[(C_{t+1} - F_{t+1}) - \rho_c \left(C_t - F_t\right)\right]^2}{2\sigma_c^2} \right\}
$$

$$
\times \prod_{t=0}^{T-1} \frac{1}{\sigma_v v_t \Delta \sqrt{1-\rho^2}} \exp\left\{ -\frac{1}{2(1-\rho^2)} \left(\left(\epsilon_{t+1}^y\right)^2 - 2\rho \epsilon_{t+1}^y \epsilon_{t+1}^v + \left(\epsilon_{t+1}^v\right)^2 \right) \right\}
$$

$$
\times \left(\frac{\alpha}{|\alpha - 1| \Delta^{\frac{1}{\alpha}} \sigma}\right)^T \times \exp\left\{ -\sum_{t=0}^{T-1} \left| \frac{S_{t+1}}{\sigma \Delta^{\frac{1}{\Delta}} t_\alpha(U_{t+1})} \right|^{\frac{\alpha}{\alpha-1}} \right\} \times \prod_{t=0}^{T-1} \left\{ \left| \frac{S_{t+1}}{\sigma \Delta^{\frac{1}{\alpha}} t_\alpha(U_{t+1})} \right|^{\frac{\alpha}{\alpha-1}} \frac{1}{\left| \frac{S_{t+1}}{\sigma \Delta^{\frac{1}{\alpha}}} \right|} \right\}
$$

$$
\times \prod_{t=0}^{T-1} \left[\mathbf{1}_{S_{t+1} \in (-\infty, 0) \cap U_{t+1} \in (-\frac{1}{2}, l_\alpha)} + \mathbf{1}_{S_{t+1} \in (0, \infty) \cap U_{t+1} \in (l_\alpha, \frac{1}{2})} \right] \times p(\mathbf{\Theta})
$$

where $\epsilon_{t+1}^y = \left(Y_{t+1} - Y_t - \mu\Delta - S_{t+1}\right) / \sqrt{v_t \Delta}$, $\epsilon_{t+1}^v = \left(v_{t+1} - v_t - \kappa(\theta - v_t)\Delta\right) / \left(\sigma_v \sqrt{v_t \Delta}\right)$, $l_\alpha = \frac{\alpha - 2}{2\alpha}$, and $t_\alpha(U_{t+1}) = \left(\frac{sin[\pi\alpha U_{t+1} + \frac{(2-\alpha)\pi}{2}]}{cos[\pi U_{t+1}]}\right)\left(\frac{cos[\pi U_{t+1}]}{cos[\pi(\alpha-1)U_{t+1} + \frac{(2-\alpha)\pi}{2}]}\right)^{(\alpha-1)/\alpha}$. We obtain joint posterior samples of $\mathbf{\Theta}, \mathbf{V}$, $\mathbf{S}$, and $\mathbf{U}$ by simulating from the above joint posterior density. We then marginalize $\mathbf{U}$ out to obtain the samples for $\mathbf{\Theta}, \mathbf{V}$, and $\mathbf{S}$. That is, we simply throw away the observations of $\mathbf{U}$ and retain the observations of $\mathbf{\Theta}, \mathbf{V}$, and $\mathbf{S}$.

In general, it is difficult to simulate directly from the above high-dimensional posterior distributions. Instead, we derive the complete conditional distributions for each individual parameter and latent variable and obtain posterior samples by simulating from these individual complete conditionals iteratively following standard MCMC procedure. For example, for SVVG, we obtain the posterior distribution $p\left(\Theta_i | \mathbf{\Theta}_{-i}, \mathbf{J}, \mathbf{G}, \mathbf{V}, \mathbf{Y}, \mathbf{C}\right)$ for $i = 1, ..., k$, where Θ_i is the i-th element of $\mathbf{\Theta}$

and $\mathbf{\Theta}_{-i} = (\theta_1, ..., \theta_{i-1}, \theta_{i+1}, ..., \theta_k)$, the posterior distribution for jump times $p\left(J_t^y|\mathbf{\Theta}, \mathbf{G}, \mathbf{V}, \mathbf{Y}, \mathbf{C}\right)$, jump sizes $p\left(G_t|\mathbf{\Theta}, \mathbf{J}, \mathbf{V}, \mathbf{Y}, \mathbf{C}\right)$, and latent volatility variables $p\left(v_t|v_{t+1}, v_{t-1}, \mathbf{\Theta}, \mathbf{J}, \mathbf{G}, \mathbf{Y}, \mathbf{C}\right)$, for all t. In estimation, we draw posterior samples from the above complete conditional distributions and use the means of the posterior samples as parameter estimates and the standard deviations of the posterior samples as standard errors of the parameter estimates. Appendix B provides the priors, the posterior distributions, and the updating procedures for model parameters and latent variables for all four models.

2.3 Model Diagnostics and Comparisons

The posterior estimates of model parameters and latent state variables allow us to examine the performances of all four models in capturing the joint dynamics of spot and option prices.

One way to gauge the performances of each model in capturing the spot price is to test whether the standardized model residuals of both returns and volatility follow an $N(0,1)$ distribution as in EJP (2003) and LWY (2006). For example, for SVLS, if the model is correctly specified, then

$$\frac{Y_{t+1} - Y_t - \mu\Delta - S_{t+1}}{\sqrt{v_t \Delta}} = \epsilon_{t+1}^y \sim N(0,1),$$

and

$$\frac{v_{t+1} - v_t - \kappa(\theta - v_t)\Delta}{\sigma_v \sqrt{v_t \Delta}} = \epsilon_{t+1}^v \sim N(0,1).$$

Deviations of ϵ_{t+1}^y and ϵ_{t+1}^v from $N(0,1)$ can reveal rich information on potential sources of model misspecifications.

To compare the performances of different models in capturing the risk-neutral dynamics, we test whether one model has significantly smaller option pricing errors than another. For this purpose, we adopt an approach developed by Diebold and Mariano (1995) (hereafter DM) in time series forecasting literature. Consider two models whose associated daily option pricing errors are $\{\varepsilon_1(t)\}_{t=1}^T$ and $\{\varepsilon_2(t)\}_{t=1}^T$, respectively. The null hypothesis that the two models have the same pricing errors is $E[\varepsilon_1(t)] = E[\varepsilon_2(t)]$, or $E[d(t)] = 0$, where $d(t) = \varepsilon_1(t) - \varepsilon_2(t)$. DM (1995) show that if $\{d(t)\}_{t=1}^T$

is covariance stationary and short memory, then

$$\sqrt{T}\left(\overline{d}-\mu_d\right)\sim N\left(0,2\pi f_d\left(0\right)\right),$$

where $\overline{d}=\frac{1}{T}\sum_{t=1}^{T}\left[\varepsilon_1\left(t\right)-\varepsilon_2\left(t\right)\right]$, $f_d\left(0\right)=\frac{1}{2\pi}\sum_{q=-\infty}^{\infty}\gamma_d\left(q\right)$ and $\gamma_d\left(q\right)=E\left[\left(d_t-\mu_d\right)\left(d_{t-q}-\mu_d\right)\right].$ In large samples, $\overline{d}$ is approximately normally distributed with mean μ_d and variance $2\pi f_d\left(0\right)/T$. Thus, under the null hypothesis of equal pricing errors, the following DM statistic

$$DM=\frac{\overline{d}}{\sqrt{2\pi\widehat{f}_d\left(0\right)/T}}$$

is distributed asymptotically as $N\left(0,1\right)$, where $\widehat{f}_d\left(0\right)$ is a consistent estimator of $f_d\left(0\right)$.[6] To compare the overall performances of the two models, we use the DM statistic to measure whether one model has significantly smaller option pricing errors than another. We also use the DM statistic to measure whether one model has smaller pricing errors than another for options in a specific moneyness and maturity group.

3. Empirical Results

In this section, we provide empirical analysis of the four models (SVMJ, SVCMJ, SVVG, and SVLS) using the spot and option prices of the S&P 500 index. We first introduce the data used in our analysis. We then examine the performances of the four models based on their (i) estimates of model parameters and latent volatility/jump variables; (ii) empirical fits of the spot price; and (iii) in-sample and out-of-sample option pricing errors.

3.1 The Data

We use the same data as that in Aït-Sahalia and Lo (1998), which include daily spot and option prices of the S&P 500 index between January 4, 1993 and December 31, 1993. Aït-Sahalia and Lo (1998) take the midpoint of the bid and ask prices of each option as observed market price and

[6] We estimate the variance of the test statistic using the Bartlett estimate of Newey and West (1987) with a lag order of 50.

eliminate observations with time-to-maturity less than one day, implied volatility greater than 70 percent, and price less than $\frac{1}{8}$. To deal with potential nonsynchronous trading and unobservable dividend yield, they back out the futures price of the underlying index at the time the option prices are observed. They obtain prices of calls and puts that have the same time-to-maturity and strike price and are closest to the money. Using put-call parity, they solve for the futures price at that certain maturity, which then can be used to back out the implied dividend yield via the cost-of-carry relation.[7]

Our estimation uses daily returns of the S&P 500 index and daily prices of a short-term ATM SPX option that we choose for each day.[8] We require that the option has a time-to-maturity between 20 and 50 days and is closest to the money, i.e., its strike to spot price ratio is closest to one.[9] On a few days without such options, we use an option whose time-to-maturity is closet to 20 days. Table 1 provides summary statistics on the data used directly in our estimation. During 1993, the mean and standard deviation of annualized continuously compounded daily returns of the index are 7.36% and 8.94%, respectively. Index returns exhibit slight negative skewness and high kurtosis. The mean and median time-to-maturities of the short-term options are 34 and 35 days, respectively, while the shortest and longest time-to-maturities are 16 and 50 days, respectively. The price of the options has a mean of \$7.14 and a range between \$3.44 and \$10.72. The implied volatility has a mean of 9.2% and a range between 6.7% and 12.23%. The ratio between the strike and the spot price of the short-term option is very close to 1. Aït-Sahalia and Lo (1998) note that the short-term interest rates exhibit little variation during 1993, ranging from 2.85 percent to 3.21 percent. As a result, we assume constant interest rate in our estimation and use the prevailing interest rate each day in our

[7]See Aït-Sahalia and Lo (1998) for more detailed descriptions of the dataset.

[8]Short-term ATM options are among the most liquid options and should have the most efficient prices in the market.

[9]Since the time-to-maturity of an option changes daily, we have to use different options on different days in our estimation.

pricing formula.

Figure 1 provides time series plots of the level and log change of the S&P 500 index, and the implied volatility of the short-term SPX options. The level of the index has increased steadily during 1993, with occasional relatively large negative returns, although none is as large as that of several major stock market crashes in other periods. The implied volatility fluctuates between 5% and 15% during 1993 with strong mean reversion.

3.2 Estimates of Model Parameters and Latent Volatility/Jump Variables

Table 2 reports posterior estimates of (i) model parameters under both the physical and the risk-neutral measures; (ii) market prices of risks for the two Brownian shocks (η^v and η^s); and (iii) parameters describing option pricing errors (ρ_c and σ_c). Figures 2 and 3 provide time series plots of the filtered volatility and jump variables for the four models, respectively. The estimates of model parameters and latent variables reveal both similarities and differences among the four models.

Consistent with existing studies, all four models exhibit strong negative correlations between volatility and returns: The estimates of ρ for the four models range from -0.56 to -0.82. The four models share similar estimates of the long-run mean (θ) of the volatility processes.[10] The estimates of the market prices of return and volatility risks are very similar across the four models and are similar to those in previous studies. For example, the estimates of η^s (η^v) in the four models are between 3.5 and 4.4 (2.9 and 4.8), while the estimate of η^s (η^v) in Pan (2002) equals 3.6 (3.1). The four models also share similar estimates of parameters describing option pricing errors (ρ_c and σ_c). In particular, the estimates of ρ_c in the four models are about 0.90, confirming that there is indeed strong autocorrelation in option pricing errors.

The four models also differ from each other in important ways. For example, the volatility process of SVVG has the strongest mean-reversion (κ) and the highest volatility of volatility (σ_v) among the

[10]Due to jumps in volatility in SVCMJ, the long-run mean of volatility in this model should include the impact of jumps.

four models.[11] The filtered volatility variables of the four models in Figure 2 confirm this fact and show that the other three models have much smoother volatility factors. Interestingly, the filtered volatility variables of SVVG mimic the behavior of the implied volatilities of the short-term SPX options (shown in Figure 1) much more closely than that of the other three models.

AJD and Lévy jump models exhibit dramatically different jump behaviors. The estimated jump intensities (λ) for SVMJ and SVCMJ suggest that on average there are about one to two jumps per year. While the mean jump sizes under $\mathbb{P}$ $\left(\mu_y^{\mathbb{P}}\right)$ in the two models are close to zero, the mean jump sizes under $\mathbb{Q}$ $\left(\mu_y^{\mathbb{Q}}\right)$ are much more negative. The filtered jump sizes and times of the two models in Figure 3 also show that there are a few large jumps in returns (and volatility) in SVMJ (SVCMJ). On the other hand, Figure 3 shows that in addition to several large jumps, SVVG and SVLS also exhibit many frequent small jumps in returns. Hence, the infinite-activity Lévy jumps have the advantage of capturing both the infrequent large jumps as well as the frequent small jumps in returns. The risk-neutral jump distribution of VG is less positively skewed than its physical jump distribution, suggesting that jumps are less positive under $\mathbb{Q}$ than under $\mathbb{P}$. This fact suggests that LS is likely to underperform VG in modeling the joint dynamics of index returns because its parameters are restricted to be the same under both measures. The estimated jump risk premium in index returns is given by $\psi_J^{\mathbb{Q}}(-i) - \psi_J^{\mathbb{P}}(-i)$ for each model. The jump risk premiums for SVMJ and SVCMJ are 0.29% and 0.12%, respectively. The jump risk premium for SVVG is much higher at 2.28%, and by definition the jump risk premium for SVLS is zero.

3.3 Performances in Modeling the Spot Price

In this section, we examine the performances of the four models in capturing the physical dynamics of the S&P 500 index. Based on estimated model parameters and latent volatility/jump

[11] The estimates of κ in this paper differ from that in LWY (2006) in magnitude mainly because we use a different scale on observables in our estimation. While LWY (2006) consider index returns in percentages, we express index returns in decimal points.

variables, we calculate the standardized residuals for both returns and volatility, ϵ_{t+1}^{y} and ϵ_{t+1}^{v}. If a given model is correctly specified, then the distributions of both residuals should be close to $N(0,1)$.

Figure 4 (5) plots kernel density estimators of ϵ_{t+1}^{y} (ϵ_{t+1}^{v}) of each of the four models and the density function of $N(0,1)$. For both SVMJ and SVCMJ, ϵ_{t+1}^{y} and ϵ_{t+1}^{v} exhibit clear deviations from standard normal: There is a high peak at the center of the distributions of both residuals, suggesting that the two models fail to capture the many small movements in both returns and volatility. On the other hand, the distributions of ϵ_{t+1}^{y} and ϵ_{t+1}^{v} of the two Lévy jump models are much closer to standard normal. The residuals of SVVG are closer to standard normal than that of SVLS. The fact that none of the parameters of LS can change between $\mathbb{P}$ and $\mathbb{Q}$ limits its ability in capturing the joint dynamics of index returns.

In addition to graphical illustrations, we also formally test whether ϵ_{t+1}^{y} and ϵ_{t+1}^{v} follow $N(0,1)$ using the Kolmogorov-Smirnov (KS hereafter) test. For each set of the residuals, the KS test compares the empirical cumulative distribution function (CDF) with the CDF of $N(0,1)$ and rejects the null hypothesis if the maximum distance between the two CDFs is too big. The KS tests in Table 3 reject the null hypothesis that ϵ_{t+1}^{y} and ϵ_{t+1}^{v} of SVMJ and SVCMJ follow a standard normal distribution. The p-values are between 3-4% for most cases, except that the p-value equals 5.37% for ϵ_{t+1}^{v} of SVCMJ. This suggests that including MJ jumps in volatility improves the modeling of the volatility process. Consistent with Figures 4 and 5, the KS test fails to reject the null hypothesis that ϵ_{t+1}^{y} and ϵ_{t+1}^{v} of the two Lévy models follow a standard normal distribution (p-values range from 25% to 38% for the two residuals under both models).

The above findings are consistent with the theoretical results of Aït-Sahalia (2004), and the simulation and empirical evidence in LWY (2006). Aït-Sahalia (2004) shows that although infinite-activity Lévy jumps can generate an infinite number of small jumps within any finite time interval, the frequency at which such jumps can occur is still a magnitude smaller than the frequency of movements in a Brownian motion. The size of such jumps also tend to be a magnitude larger than that of a Brownian motion. Through numerical simulations, LWY (2006) show that Aït-Sahalia's results, although derived for pure Lévy jumps, also hold for models with stochastic volatility and Lévy jumps. Using daily returns of the S&P 500 index between January 1980 and December 2000, LWY (2006) show that infinite-activity Lévy jumps can capture the many small jumps in index returns that are too big for Brownian motion to model and too small for compound Poisson process to capture.

3.4 Performances in Modeling Option Prices

There is no guarantee that a model that captures the physical dynamics better also can fit option prices better. For example, Eraker (2004) shows that while the double-jump model of EJP (2003) captures index returns better than SVMJ, it does not have significantly smaller option pricing errors. In this section, we address the basic question whether the Lévy jump models we consider can capture the joint dynamics of the S&P 500 index returns better than the AJD models.

Panel A of Table 4 reports the time series mean of daily absolute and percentage pricing errors of the short-term ATM SPX options used in model estimation for the four models.[12] We find similar pricing errors for SVMJ and SVCMJ: The mean absolute pricing errors of the two models are about 44 cents (the mean option price is \$7.14); and the mean percentage pricing errors of the two models are about 6.3%, which is bigger than the percentage bid-ask spread of the option. On the other hand, the mean absolute pricing errors of SVVG and SVLS are about 16 and 24 cents, respectively, and the mean percentage pricing errors are about 2.4 and 3.6%, respectively. Consistent with the results of Eraker (2004), the DM statistics in Panel B of Table 4 show that the pricing errors of SVMJ and SVCMJ are not significantly different from each other. In contrast, SVVG and SVLS have significantly smaller absolute and percentage pricing errors than SVMJ and SVCMJ, and SVVG has

[12] Absolute pricing error of an option is the absolute value of the difference between model and market prices of the option, and percentage pricing error of an option is the absolute pricing error divided by the market price of the option.

significantly smaller pricing errors than SVLS. The time series plots of the daily absolute (percentage) pricing errors of the four models in Figure 6 (7) show that SVVG and SVLS have smaller absolute (percentage) pricing errors than SVMJ and SVCMJ during most of the sample period. In particular, SVVG has almost uniformly smaller in-sample option pricing errors than the AJD models. SVLS has somewhat worse performances than SVVG and has relatively large percentage pricing errors during the last few days of March 1993. Panel C of Table 4 shows that the KS test fails to reject the null hypothesis at the 5% level that the option pricing errors ϵ_t^c follow $N(0,1)$ for all models, confirming our econometric specification of option pricing errors.

In addition to the short-term ATM SPX options used in estimation, we also examine the performances of the four models in pricing 12,725 other options in the dataset.[13] Because these options have not been used in model estimation, they provide evidence on the out-of-sample performances of the four models in option pricing. We divide all options into six moneyness groups, from deep in-the-money (ITM) to deep out-of-the-money (OTM) options, and five maturity groups, with time-to-maturities from less than one month to longer than six months. The majority of these options are ITM options with time-to-maturities between one to six months, and we do not observe many short-term deep OTM options. Based on the estimated model parameters and latent volatility variables, we calculate the theoretical price of each of these options under each model. Then based on options that are available on each day, we obtain daily arithmetic weighted average of absolute and percentage pricing errors for (i) all options; (ii) options within each of the moneyness groups (options across all maturities that belong to a certain moneyness group) or each of the maturity groups (options across all moneyness that belong to a certain maturity group); and (iii) options within each individual moneyness/maturity group.

We first examine the overall performances of the four models by focusing on the average pricing

[13] We eliminate options with prices that are less than one dollar.

errors of the 12,725 out-of-sample options. The time series mean of daily weighted average of the absolute and percentage pricing errors of all options are reported in the last four rows of the last column in Panels A and B of Table 5, respectively. We see clearly that SVCMJ has smaller absolute and percentage pricing errors than SVMJ, and SVVG and SVLS have smaller absolute and percentage pricing errors than SVMJ and SVCMJ. While SVLS has the smallest absolute pricing errors, SVVG has the smallest percentage pricing errors. The DM statistics for pair-wise comparisons of the four models based on the absolute and percentage pricing errors of all options are reported in the last six rows of the last column in Panels C and D of Table 5, respectively. While SVCMJ has significantly smaller absolute pricing errors than SVMJ, the percentage pricing errors of the two options are not significantly different from each other. In contrast, SVVG has significantly smaller absolute and percentage pricing errors than both SVMJ and SVCMJ. SVLS has somewhat worse performances than SVVG. For example, SVVG has significantly smaller percentage pricing errors than SVLS, and SVLS has percentage pricing errors that are not significantly smaller than that of SVCMJ. Figure 8 (9) provides time series plots of daily weighted average of the absolute (percentage) pricing errors of all options for the four models during our sample period. Consistent with the DM statistics, we find that SVVG and SVLS have smaller absolute pricing errors than SVMJ and SVCMJ during most of the sample period. While SVVG has smaller percentage pricing errors than SVMJ and SVCMJ during most of the sample period, SVLS does not have a clear dominance over SVCMJ in terms of percentage pricing errors.

Next we examine the performances of the four models in pricing options grouped by time-to-maturity. The time series mean of daily weighted average of the absolute and percentage pricing errors of options in each of the five maturity groups are reported in the last column in Panels A and B of Table 5, respectively. The DM statistics for pair-wise comparisons of the four models based on the absolute and percentage pricing errors of options in the five maturity groups are reported in the last column in Panels C and D of Table 5, respectively. We find similar patterns in model performances for options in each maturity group as that for all options. For example, we find that SVVG has significantly smaller absolute and percentage pricing errors than SVMJ and SVCMJ for most maturity groups. While SVLS has significantly smaller absolute pricing errors than SVMJ and SVCMJ for all maturity groups, it has significantly smaller percentage pricing errors than SVMJ and SVCMJ only for options with shortest time-to-maturities. SVVG has smaller percentage pricing errors, although not all significant, than SVLS for all maturity groups. Interestingly, we find that SVCMJ does not have significantly smaller absolute and percentage pricing errors than SVMJ for all five maturity groups.

Finally, we examine the performances of the four models in pricing options grouped by moneyness. The time series mean of daily weighted average of the absolute and percentage pricing errors of options in each of the six moneyness groups are reported in the last four rows in Panels A and B of Table 5, respectively. The DM statistics for pair-wise comparisons of the four models based on the absolute and percentage pricing errors of options in the six moneyness groups are reported in the last six rows in Panels C and D of Table 5, respectively. We find that SVCMJ has significantly smaller absolute (percentage) pricing errors than SVMJ only for ITM (deep ITM) options. In contrast, SVVG and SVLS have significantly smaller absolute and percentage pricing errors than SVMJ and SVCMJ for most ITM and slightly OTM ($1.0 < K/S < 1.03$) options. While SVVG has smaller absolute and percentage pricing errors than SVMJ and SVCMJ for all deep OTM options ($K/S > 1.03$), the differences are statistically significant only for absolute but not for percentage pricing errors. SVVG tends to have larger (smaller) pricing errors than SVLS for ITM (OTM) options. We obtain similar findings for moneyness groups with different time-to-maturities, although the advantages of the Lévy jump models over the AJD models become less significant for options with longer time-to-maturities.

The analysis in this section clearly demonstrates the advantages of the Lévy jump models over the AJD models in modeling the joint dynamics of the spot and option prices of the S&P 500 index. The infinite-activity Lévy jumps capture the many small movements in index returns that cannot be captured by the AJD models. The Lévy jump models also have significantly smaller in-sample and out-of-sample option pricing errors than the AJD models, although LS is less flexible than VG due to more stringent restrictions on its jump parameters. We emphasize that the superior performances of the Lévy jump models are obtained under the restriction that jumps under the physical and the risk-neutral measures must follow the same Lévy process. If we allow jumps to follow different Lévy processes under the two measures, Lévy jump models are likely to have even better performances in capturing the joint dynamics of index returns. Therefore, our analysis points out the great potentials of Lévy processes for continuous-time finance modeling and strongly suggests that we can enrich existing AJD models by incorporating infinite-activity Lévy jumps.

4. Conclusion

In this paper, we address a basic and yet fundamental question in the current continuous-time finance literature: Whether newly proposed Lévy jump models can outperform the most sophisticated AJD models in capturing the joint dynamics of stock and option prices. We provide detailed analysis on the change of measure for infinite-activity Lévy jumps and develop efficient Markov chain Monte Carlo methods for estimating Lévy jump models using spot and option prices. We show that models with infinite-activity Lévy jumps in returns significantly outperform AJD models with Merton jumps in both returns and volatility in capturing the joint dynamics of the spot and options prices of the S&P 500 index. Our analysis strongly suggests that incorporating infinite-activity Lévy jumps into existing AJD models can substantially increase the flexibility of AJD models without sacrificing their tractability.

REFERENCES

Aït-Sahalia, Y., 2004, Disentangling diffusion from jumps, *Journal of Financial Economics* 74, 487-528.

Aït-Sahalia, Y. and J. Jacod, 2004, Fisher's information for discretely sampled Lévy processes, *Annals of Statistics* forthcoming.

Aït-Sahalia, Y. and A. Lo, 1998, Nonparametric estimation of state-price densities implicit in financial asset prices, *Journal of Finance* 53, 499-547.

Anderson, T., L. Benzoni, and J. Lund, 2002, An empirical investigation of continuous-time equity return models, *Journal of Finance* 57, 1239-1284.

Bakshi, G., C. Cao, and Z. Chen, 1997, Empirical performance of alternative option pricing models, *Journal of Finance* 52, 2003-2049.

Bakshi, G. and L. Wu, 2005, Investor irrationality and the Nasdaq bubble, Working paper, Baruch College and University of Maryland.

Bates, D., 1996, Jumps and stochastic volatility: Exchange rate processes implicit in Deutschemark options, *Review of Financial Studies* 9, 69-107.

Barndorff-Nielsen, O. and N. Shephard, 2004, Impact of jumps on returns and realized variances: econometric analysis of time-deformed Lévy processes, Working paper, Nuffield College, University of Oxford.

Buckle, D.J., 1995, Bayesian inference for stable distributions, *Journal of the American Statistical Association* 90, 605-613.

Carr, P. and L. Wu, 2003, The finite moment log stable process and option pricing, *Journal of Finance* 58, 753-777.

Carr, P. and L. Wu, 2004, Time-changed Lévy processes and option pricing, *Journal of Financial Economics* 71, 113-141.

Carr, P., H. Geman, D. Madan, and M. Yor, 2002, The fine structure of asset returns: An empirical investigation, *Journal of Business* 75, 305-332.

Chambers, J., C. Mallows, and B. Stuck, 1976, A method for simulating stable random variables, *Journal of the American Statistical Association* 71, 340-344.

Chib, S., F. Nardari, and N. Shephard, 2002, Markov chain Monte Carlo methods for stochastic volatility models, *Journal of Econometrics* 108, 281-316.

Chib, S. and E. Greenberg, 1995, Understanding the Metropolis-Hastings algorithm, *The American Statistician* 49, 327-335.

Damien, P., J. Wakefield, and S. Walker, 1999, Gibbs sampling for Bayesian non-conjugate and hierarchical models by using auxiliary variables, *Journal of Royal Statistical Society* 61, 331-344.

Devroye, L., 1986, *Nonuniform Random Variate Generation*, New York: Springer-Verlag.

Diebold, F. and R. Mariano, 1995, Comparing predictive accuracy, *Journal of Business and Economic Statistics* 13, 253-265.

Duffie, D., J. Pan, and K. Singleton, 2000, Transform Analysis and Asset Pricing for Affine Jump-Diffusions, *Econometrica* 68, 1343-1376.

Elerian, O., S. Chib, and N. Shephard, 2001, Likelihood inference for discretely observed nonlinear diffusions, *Econometrica* 69, 959-994.

Eraker, B., 2001, MCMC Analysis of diffusion models with applications to finance, *Journal of Business and Economic Statistics* 19, 177-191.

Eraker, B., 2004, Do stock prices and volatility jump? Reconciling evidence from spot and option prices, *Journal of Finance* 59, 1367-1403

Eraker, B., M. Johannes, and N. Polson, 2003, The impact of jumps in equity index volatility and returns, *Journal of Finance* 58, 1269-1300.

Fielitz, B., and J. Rozell, 1983, Stable distributions and mixtures of distributions hypotheses for common stock returns, *Journal of the American Statistical Association* 78, 28-36.

Gilk, W. R., 1992, Derivative-Free Adaptive Rejection Sampling for Gibbs Sampling, *Bayesian Statistics 4*, Oxford University Press.

Hastings, W.K., 1970, Monte Carlo sampling methods using Markov chain and their applications, *Biometrika* 57, 97-109.

Heston, S., 1993, A closed-form solution for options with stochastic volatility with applications to bond and currency options, *Review of Financial Studies* 6, 327-343.

Huang, J. and L. Wu, 2003, Specification analysis of option pricing models based on time-changed Lévy processes, *Journal of Finance* 59, 1405-1439.

Jacquier, E., N. Polson, and P. Rossi, 1994, Bayesian analysis of stochastic volatility models, *Journal of Business and Economic Statistics* 12, 371-389.

Johannes, M. and N. Polson, 2003, MCMC methods for continuous-time financial econometrics, *Handbook of Financial Econometrics* forthcoming.

Jones, C.S., 2003a, The dynamics of stochastic volatility: Evidence from underlying and options markets, *Journal of Econometrics* 116, 181-224.

Jones, C.S., 2003b, Nonlinear mean reversion in the short-term interest rates, *Review of Financial Studies* 16, 793-843.

Kass, R. and A. Raftery, 1994, Bayes factors, *Journal of the American Statistical Association* 90, 773-795.

Kim, S., N. Shephard, and S. Chib, 1998, Stochastic volatility: Likelihood inference and comparison with ARCH models, *Review of Economic Studies 65*, 361-393.

Lévy, P., 1924, Theorie des erreurs. La loide Gauss et less lois exceptionells, *Bull. Soc. Math* 52, 49-85.

Li, H., M. Wells, and C. Yu, 2006, A Bayesian analysis of return dynamics with Lévy jumps, *Review of Financial Studies* forthcoming.

Madan, D., P. Carr, and E. Chang, 1998, The variance gamma process and option pricing, *European Finance Review* 2, 79-105.

Merton, R., 1976, Option pricing when the underlying stock returns are discontinuous, *Journal of Financial Economics* 3, 125-144.

Murihead, R., 1982, *Aspects of Multivariate Statistical Theory*, New York: Wiley.

Newey, W. and K. West, 1987, A simple, positive semi-definite, heteroskedasticity and autocorrelation consistent covariance matrix, *Econometrica* 55, 703-708.

Pan, J., 2002, The jump-risk premia implicit in options: Evidence from an integrated time-series study, *Journal of Financial Economics* 63, 3-50.

Robert, C. and G. Casella, 1999, *Monte Carlo Statistical Methods*, New York: Springer.

Ripley, B.D., 1987, *Stochastic Simulation*, New York: John Wiley.

Sato, K., 1999, *Lévy Processes and Infinitely Divisible Distributions*, Cambridge University Press: Cambridge, UK.

Wu, L., 2004, Dampened power law: Reconciling the tail behavior of financial security returns, *Journal of Business* forthcoming.

Wu, L., 2006, Modeling financial security returns using Lévy processes, Working paper, Baruch College.

APPENDIX A. Change of Measure for Lévy Jump Processes

In this section, we provide the proof of Proposition 1, which imposes restrictions on the parameters of the four jump processes (MJ, CMJ, VG, and LS) under the physical measure $\mathbb{P}$ and the risk-neutral measure $\mathbb{Q}$. We need the following preliminary results for the proof of Proposition 1.

A.1 Characteristic component, Lévy measure and drift for MJ, CMJ, VG, and LS

We first provide analytical expressions of the characteristic component, Lévy measure and drift for MJ, CMJ, VG, and LS, which will be used in later analysis. To emphasize the generality of these results, we omit dependence of model parameters on probability measures.

MJ:

$$\psi_J(u) = \lambda(1 - e^{iu\mu_y - \frac{1}{2}\sigma_y^2 u^2}),\ \pi(x) = \frac{\lambda}{\sqrt{2\pi}\sigma_y} e^{-\frac{(x-\mu_y)^2}{2\sigma_y^2}},\ \bar{\mu} = \int_{|x|\le 1} x\pi(dx).$$

CMJ:

$$\psi_J(u) = \lambda(1 - \frac{e^{iu_1\mu_y - \frac{1}{2}\sigma_y^2 u_1^2}}{1 - iu_1\mu_v\rho_J - iu_2\mu_v}),\ \pi(x) = \frac{\lambda}{\mu_v\sqrt{2\pi}\sigma_y} e^{-\frac{x_2}{\mu_v} - \frac{(x_1-\mu_y-\rho_J x_2)^2}{2\sigma_y^2}},\ \bar{\mu} = \int_{|x|\le 1} x\pi(dx).$$

VG:

$$\psi_J(u) = \frac{\log(1 - iu\gamma\nu + \frac{\sigma^2\nu u^2}{2})}{\nu}, \pi(x) = \begin{cases} \frac{1}{\nu}\frac{\exp(-Mx)}{x} & x > 0 \\ \frac{1}{\nu}\frac{\exp(-G|x|)}{|x|} & x < 0 \end{cases},\ \bar{\mu} = \int_{|x|\le 1} x\pi(dx),$$

where $M = \left(\sqrt{\frac{1}{4}\gamma^2\nu^2 + \frac{1}{2}\sigma^2\nu} + \frac{1}{2}\gamma\nu\right)^{-1}$ and $G = \left(\sqrt{\frac{1}{4}\gamma^2\nu^2 + \frac{1}{2}\sigma^2\nu} - \frac{1}{2}\gamma\nu\right)^{-1}$.

Lévy α-stable Process: Suppose $X_1 \sim S_\alpha(\beta, \sigma, \gamma)$, which reduces to Log-Stable process if $\beta = -1$ and $\gamma = 0$, then

$$\psi_J(u) = \sigma^\alpha |u|^\alpha (1 - i\beta \mathrm{sign}(u)\tan(\frac{\pi\alpha}{2}) + i\gamma u,\ \pi(x) = \begin{cases} c_1 \frac{1}{x^{1+\alpha}} & x > 0 \\ c_2 \frac{1}{|x|^{1+\alpha}} & x < 0 \end{cases},\ \bar{\mu} = \gamma - \int_{1_{|x|>1}} x\pi(dx),$$

where $c_1 = \frac{\sigma^\alpha(1+\beta)}{2}$ and $c_2 = \frac{\sigma^\alpha(1-\beta)}{2}$.

A.2 Three Lemmas

In this subsection, we prove three Lemmas, which will be used in later analysis.

Lemma 1. Suppose $f(x)$ and $g(x)$ are continuous functions,

(i) if $f(x) \sim g(x)$ when $x \to \infty$ (i.e. $\lim_{x\to\infty} \frac{f(x)}{g(x)} = 1$), then for any constant $a > 0$,

$$\int_a^\infty |f(x)|dx < \infty \Leftrightarrow \int_a^\infty |g(x)|dx < \infty;$$

(ii) if $f(x) \sim g(x)$ when $x \to 0+$ (i.e. $\lim_{x\to 0+} \frac{f(x)}{g(x)} = 1$), then for any constant $a > 0$,

$$\int_0^a |f(x)|dx < \infty \Leftrightarrow \int_0^a |g(x)|dx < \infty;$$

(iii) if $f(x) \sim g(x)$ when $x \to 0-$ (i.e. $\lim_{x\to 0-} \frac{f(x)}{g(x)} = 1$), then for any constant $a > 0$,

$$\int_{-a}^{0} |f(x)|dx < \infty \Leftrightarrow \int_{-a}^{0} |g(x)|dx < \infty;$$

(iv) if $f(x) \sim g(x)$ when $x \to -\infty$ (i.e. $\lim_{x\to -\infty} \frac{f(x)}{g(x)} = 1$), then for any constant $a > 0$,

$$\int_{-\infty}^{-a} |f(x)|dx < \infty \Leftrightarrow \int_{-\infty}^{-a} |g(x)|dx < \infty.$$

Proof. First, we prove ($\Leftarrow$) for (i). Since $\lim_{x\to\infty} \frac{f(x)}{g(x)} = 1$, then for $\epsilon = \frac{1}{2}$, $\exists\ M > a > 0$, such that $\forall\ x > M$, $\left|\frac{f(x)}{g(x)} - 1\right| \leq \frac{1}{2}$. This implies that $\forall\ x > M$,

$$\left|\frac{f(x)}{g(x)}\right| - 1 \leq \left|\frac{f(x)}{g(x)} - 1\right| \leq \frac{1}{2} \Longrightarrow |f(x)| \leq \frac{3}{2}|g(x)|.$$

If $\int_a^\infty |g(x)|dx < \infty$, then

$$\int_M^\infty |f(x)|dx \leq \frac{3}{2}\int_M^\infty |g(x)|dx < \infty.$$

By the continuity of $f(x)$, $\int_a^M |f(x)|dx$ has to be finite. Therefore,

$$\int_a^\infty |f(x)|dx = \int_a^M |f(x)|dx + \int_M^\infty |f(x)|dx < \infty.$$

Next, we prove ($\Rightarrow$) for (i). Since $\lim_{x\to\infty} \frac{f(x)}{g(x)} = 1$, then for $\epsilon = \frac{1}{2}$, $\exists\ M > a > 0$, such that $\forall$ $x > M$, $\left|\frac{f(x)}{g(x)} - 1\right| \leq \frac{1}{2}$. This implies that $\forall\ x > M$,

$$1 - \left|\frac{f(x)}{g(x)}\right| \leq \left|\frac{f(x)}{g(x)} - 1\right| \leq \frac{1}{2} \Longrightarrow |g(x)| \leq 2|f(x)|$$

If $\int_a^\infty |f(x)|dx < \infty$, then

$$\int_M^\infty |g(x)|dx \leq 2\int_M^\infty |f(x)|dx < \infty.$$

By the continuity of $g(x)$, $\int_a^M |g(x)|dx$ has to be finite. Therefore,

$$\int_a^\infty |g(x)|dx = \int_a^M |g(x)|dx + \int_M^\infty |g(x)|dx < \infty.$$

This completes the proof of (i). Since similar proof can be applied to the other three cases, we skip the proofs of (ii), (iii), and (iv) here.

Lemma 2. For any constants $M > 0$ and $a > 0$, we have (i) $\int_a^\infty e^{-Mx}\frac{1}{x}dx < \infty$; and (ii) $\int_{-\infty}^{-a} e^{Mx}\frac{1}{-x}dx < \infty$.

Proof. For (i), by integration by parts and the fact that $\frac{1}{M}\int_a^\infty \frac{e^{-Mx}}{x^2}dx \geq 0$,

$$\int_a^\infty e^{-Mx}\frac{1}{x}dx = \frac{1}{M}\frac{e^{-Ma}}{a} - \frac{1}{M}\int_a^\infty \frac{e^{-Mx}}{x^2}dx \leq \frac{1}{M}\frac{e^{-Ma}}{a} + \frac{1}{M}\int_a^\infty \frac{e^{-Mx}}{x^2}dx,$$

Since,

$$\int_a^\infty \frac{e^{-Mx}}{x^2}dx \le \int_a^\infty \frac{1}{x^2}dx = -\frac{1}{x}|_a^\infty = \frac{1}{a},$$

we have

$$0 < \int_a^\infty e^{-Mx}\frac{1}{x}dx \le \frac{e^{-Ma}}{aM} + \frac{1}{aM} < \infty.$$

For (ii), by the transform $-x = y$, case (ii) is reduced to case (i), and the proof is skipped.

Lemma 3. For any constants a, b, and c, the integral $\int_0^\infty e^{ax^2+bx+c}dx$ is finite if and only if the leading coefficient is negative (i.e., $a < 0$ if $a \neq 0$ or $b < 0$ if $a = 0$).

Proof. If $a = 0$,

$$\int_0^\infty e^{ax^2+bx+c}dx = \int_0^\infty e^{bx+c}dx = e^c\int_0^\infty e^{bx}dx.$$

It is easy to see that the integral is finite if and only if $b < 0$.

If $a \neq 0$,

$$\begin{aligned}\textstyle\int_0^\infty e^{ax^2+bx+c}dx &= \textstyle\int_0^\infty e^{a(x+\frac{b}{2a})^2-(\frac{b^2}{4a}-c)}dx \\ &= e^{-(\frac{b^2}{4a}-c)}\textstyle\int_0^\infty e^{a(x+\frac{b}{2a})^2}dx \\ &= e^{-(\frac{b^2}{4a}-c)}\textstyle\int_{\frac{b}{2a}}^\infty e^{ay^2}dy \text{ (after transforming } y = x + \frac{b}{2a}) \\ &= e^{-(\frac{b^2}{4a}-c)}(\textstyle\int_{\frac{b}{2a}}^1 e^{ay^2}dy + \int_1^\infty e^{ay^2}dy).\end{aligned}$$

The first term is always finite by the continuity of e^{ay^2}. Hence the integral $\int_0^\infty e^{ax^2+bx+c}dx$ is finite if and only if the second term if finite. If $a < 0$, $\int_1^\infty e^{ay^2}dy \le \int_1^\infty e^{ay}dy = -\frac{e^{ay}}{a} < \infty$. If $a > 0$, $\int_1^\infty e^{ay^2}dy \ge \int_1^\infty e^{ay}dy = \infty$. This completes the proof.

A.3 Proof of Proposition 1.

Since the Brownian parts under both $\mathbb{P}$ and $\mathbb{Q}$ are absent for all four models, condition (i) of Sato's theorem is automatically satisfied. It is easy to see that condition (iii) of Sato's theorem is satisfied for MJ, CMJ, and VG. Hence our analysis of these three models focuses on condition (ii) of Sato's theorem. We use $f(x)$ to denote the integrand in condition (ii) of Sato's theorem.

MJ. Suppose the parameters under $\mathbb{P}$ and $\mathbb{Q}$ are $(\lambda^{\mathbb{P}}, \mu_y^{\mathbb{P}}, \sigma_y^{\mathbb{P}})$ and $(\lambda^{\mathbb{Q}}, \mu_y^{\mathbb{Q}}, \sigma_y^{\mathbb{Q}})$, respectively. The integral in condition (ii) is

$$\begin{aligned}\textstyle\int_{-\infty}^\infty f(x)dx &= \textstyle\int_{-\infty}^\infty (e^{\frac{\phi(x)}{2}} - 1)^2\pi_{\mathbb{P}}(dx) \\ &= \textstyle\int_{-\infty}^\infty (\pi_{\mathbb{Q}} + \pi_{\mathbb{P}} - 2\sqrt{\pi_{\mathbb{Q}}\pi_{\mathbb{P}}})dx \\ &= \textstyle\int_{-\infty}^\infty \frac{\lambda^{\mathbb{Q}}}{\sqrt{2\pi}\sigma_y^{\mathbb{Q}}}\exp\left\{-\frac{(x-\mu_y^{\mathbb{Q}})^2}{2(\sigma_y^{\mathbb{Q}})^2}\right\}dx + \int_{-\infty}^\infty \frac{\lambda^{\mathbb{P}}}{\sqrt{2\pi}\sigma_y^{\mathbb{P}}}\exp\left\{-\frac{(x-\mu_y^{\mathbb{P}})^2}{2(\sigma_y^{\mathbb{P}})^2}\right\}dx \\ &\quad - \textstyle\int_{-\infty}^\infty 2\sqrt{\frac{\lambda^{\mathbb{Q}}\lambda^{\mathbb{P}}}{\sigma_Y^{\mathbb{Q}}\sigma_y^{\mathbb{P}}}\frac{1}{2\pi}}\exp\left\{-\frac{1}{4}\left[\frac{(x-\mu_y^{\mathbb{Q}})^2}{(\sigma_y^{\mathbb{Q}})^2} + \frac{(x-\mu_y^{\mathbb{P}})^2}{(\sigma_y^{\mathbb{P}})^2}\right]\right\}dx \\ &= \lambda^{\mathbb{Q}} + \lambda^{\mathbb{P}} - 2\sqrt{\frac{\lambda^{\mathbb{Q}}\lambda^{\mathbb{P}}}{\sigma_Y^{\mathbb{Q}}\sigma_y^{\mathbb{P}}}\frac{1}{2\pi}}\textstyle\int_{-\infty}^\infty \exp\left\{-\frac{1}{4}\left[\frac{(x-\mu_y^{\mathbb{Q}})^2}{(\sigma_y^{\mathbb{Q}})^2} + \frac{(x-\mu_y^{\mathbb{P}})^2}{(\sigma_y^{\mathbb{P}})^2}\right]\right\}dx,\end{aligned}$$

Note that

$$-\frac{1}{4}\left[\frac{(x-\mu_y^{\mathbb{Q}})^2}{(\sigma_y^{\mathbb{Q}})^2}+\frac{(x-\mu_y^{\mathbb{P}})^2}{(\sigma_y^{\mathbb{P}})^2}\right]=-\frac{1}{2}\left(W\left(x-\frac{S}{W}\right)^2-\frac{S^2}{W}+\frac{1}{2}\left[\left(\frac{\mu_y^{\mathbb{Q}}}{\sigma_y^{\mathbb{Q}}}\right)^2+\left(\frac{\mu_y^{\mathbb{P}}}{\sigma_y^{\mathbb{P}}}\right)^2\right]\right)$$

where $W=\frac{1}{2}(\frac{1}{(\sigma_y^{\mathbb{Q}})^2}+\frac{1}{(\sigma_y^{\mathbb{P}})^2})$ and $S=\frac{1}{2}(\frac{\mu_y^{\mathbb{Q}}}{(\sigma_y^{\mathbb{Q}})^2}+\frac{\mu_y^{\mathbb{P}}}{(\sigma_y^{\mathbb{P}})^2})$. As a result, the third term becomes

$$-2\sqrt{\frac{\lambda^{\mathbb{Q}}\lambda^{\mathbb{P}}}{\sigma_y^{\mathbb{Q}}\sigma_y^{\mathbb{P}}}\frac{1}{W}}\exp\left(\frac{S^2}{2W}-\frac{1}{4}\left[\left(\frac{\mu_y^{\mathbb{Q}}}{\sigma_y^{\mathbb{Q}}}\right)^2+\left(\frac{\mu_y^{\mathbb{P}}}{\sigma_y^{\mathbb{P}}}\right)^2\right]\right).$$

Therefore, the integral in condition (ii) is finite no matter how the three parameters differ between $\mathbb{P}$ and $\mathbb{Q}$.

CMJ. Suppose the parameters under $\mathbb{P}$ and $\mathbb{Q}$ are $(\lambda^{\mathbb{P}},\mu_y^{\mathbb{P}},\sigma_y^{\mathbb{P}},\mu_v^{\mathbb{P}},\rho_J^{\mathbb{P}})$ and $(\lambda^{\mathbb{Q}},\mu_y^{\mathbb{Q}},\sigma_y^{\mathbb{Q}},\mu_v^{\mathbb{Q}},\rho_J^{\mathbb{Q}})$, respectively. Since jumps in CMJ are two dimensional, the Lévy measure of CMJ is a function of two variables, x_1 and x_2. The integral in condition (ii) becomes

$$\begin{aligned}
&\textstyle\int_0^\infty\int_{-\infty}^\infty(e^{\frac{\phi(x)}{2}}-1)^2\pi_{\mathbb{P}}(dx_1dx_2)\\
&=\textstyle\int_0^\infty\frac{\lambda^{\mathbb{Q}}}{\mu_v^{\mathbb{Q}}}\exp\left(-\frac{x_2}{\mu_v^{\mathbb{Q}}}\right)\left(\int_{-\infty}^\infty\frac{1}{\sqrt{2\pi}\sigma_y^{\mathbb{Q}}}\exp\left(-\frac{(x_1-\omega_y^{\mathbb{Q}})^2}{2(\sigma_y^{\mathbb{Q}})^2}\right)dx_1\right)dx_2\\
&+\textstyle\int_0^\infty\frac{\lambda^{\mathbb{P}}}{\mu_v^{\mathbb{P}}}\exp\left(-\frac{x_2}{\mu_v^{\mathbb{P}}}\right)\left(\int_{-\infty}^\infty\frac{1}{\sqrt{2\pi}\sigma_y^{\mathbb{P}}}\exp\left(-\frac{(x_1-\omega_y^{\mathbb{P}})^2}{2(\sigma_y^{\mathbb{P}})^2}\right)dx_1\right)dx_2\\
&-2\textstyle\int_0^\infty\int_{-\infty}^\infty\sqrt{\frac{\lambda^{\mathbb{Q}}\lambda^{\mathbb{P}}}{\mu_v^{\mathbb{Q}}\mu_v^{\mathbb{P}}\sigma_y^{\mathbb{Q}}\sigma_y^{\mathbb{P}}}\frac{1}{2\pi}}\exp\left[-\frac{1}{2}\left(\frac{1}{\mu_v^{\mathbb{Q}}}+\frac{1}{\mu_v^{\mathbb{P}}}\right)x_2\right]\exp\left(-\frac{1}{4}\left[\left(\frac{x_1-\omega_y^{\mathbb{Q}}}{\sigma_y^{\mathbb{Q}}}\right)^2+\left(\frac{x_1-\omega_y^{\mathbb{P}}}{\sigma_y^{\mathbb{P}}}\right)^2\right]\right)dx_1dx_2,
\end{aligned}$$

where $\omega_y^{\mathbb{Q}}=\mu_y^{\mathbb{Q}}+\rho_J^{\mathbb{Q}}x_2$ and $\omega_y^{\mathbb{P}}=\mu_y^{\mathbb{P}}+\rho_J^{\mathbb{P}}x_2$.

One can easily see that the first and second terms equal $\lambda^{\mathbb{Q}}$ and $\lambda^{\mathbb{P}}$, respectively. What is left is to show that the third term is finite. After some algebra, the third term becomes

$$-2\int_0^\infty\sqrt{\frac{\lambda^{\mathbb{Q}}\lambda^{\mathbb{P}}}{\mu_v^{\mathbb{Q}}\mu_v^{\mathbb{P}}\sigma_y^{\mathbb{Q}}\sigma_y^{\mathbb{P}}}}\exp\left\{-\frac{1}{2}\left(\frac{1}{\mu_v^{\mathbb{Q}}}+\frac{1}{\mu_v^{\mathbb{P}}}\right)x_2+\frac{S^2}{2W}-\frac{1}{4}\left[\left(\frac{\omega_y^{\mathbb{Q}}}{\sigma_y^{\mathbb{Q}}}\right)^2+\left(\frac{\omega_y^{\mathbb{P}}}{\sigma_y^{\mathbb{P}}}\right)^2\right]\right\}\sqrt{\frac{1}{W}}dx_2,$$

where $W=\frac{1}{2}(\frac{1}{(\sigma_y^{\mathbb{Q}})^2}+\frac{1}{(\sigma_y^{\mathbb{P}})^2})$ and $S=\frac{1}{2}(\frac{\omega_y^{\mathbb{Q}}}{(\sigma_y^{\mathbb{Q}})^2}+\frac{\omega_y^{\mathbb{P}}}{(\sigma_y^{\mathbb{P}})^2})$. Note that

$$-\frac{1}{2}\left(\frac{1}{\mu_v^{\mathbb{Q}}}+\frac{1}{\mu_v^{\mathbb{P}}}\right)x_2+\frac{S^2}{2W}-\frac{1}{4}\left[\left(\frac{\omega_y^{\mathbb{Q}}}{\sigma_y^{\mathbb{Q}}}\right)^2+\left(\frac{\omega_y^{\mathbb{P}}}{\sigma_y^{\mathbb{P}}}\right)^2\right]$$

$$=-\frac{1}{2}\left(\frac{1}{\mu_v^{\mathbb{Q}}}+\frac{1}{\mu_v^{\mathbb{P}}}\right)x_2-\frac{1}{4}\frac{1}{(\sigma_y^{\mathbb{Q}})^2+(\sigma_y^{\mathbb{P}})^2}\left[\left(\mu_y^{\mathbb{Q}}+\rho_J^{\mathbb{Q}}x_2\right)^2+\left(\mu_y^{\mathbb{P}}+\rho_J^{\mathbb{P}}x_2\right)^2-2\left(\mu_y^{\mathbb{Q}}+\rho_J^{\mathbb{Q}}x_2\right)\left(\mu_y^{\mathbb{P}}+\rho_J^{\mathbb{P}}x_2\right)\right],$$

which is proportional to a function with the form $e^{\beta_2x_2^2+\beta_1x_2+\beta_0}$, and

$$\beta_2=-\frac{1}{4}\frac{1}{(\sigma_y^{\mathbb{Q}})^2+(\sigma_y^{\mathbb{P}})^2}(\rho_J^{\mathbb{Q}}-\rho_J^{\mathbb{P}})^2,$$

$$\beta_1 = -\frac{1}{2}\left(\frac{1}{\mu_v^{\mathbb{Q}}} + \frac{1}{\mu_v^{\mathbb{P}}}\right) x_2 - \frac{1}{2}\frac{1}{(\sigma_y^{\mathbb{Q}})^2 + (\sigma_y^{\mathbb{P}})^2}(\rho_J^{\mathbb{Q}} - \rho_J^{\mathbb{P}})(\mu_y^{\mathbb{Q}} - \mu_y^{\mathbb{P}}).$$

According to Lemma 3, the third term is finite if and only if the leading coefficient of $\beta_2 x_2^2 + \beta_1 x_2 + \beta_0$ is negative. If $\rho_J^{\mathbb{Q}} \neq \rho_J^{\mathbb{P}}$, then $\beta_2 < 0$ and the third term is finite. If $\rho_J^{\mathbb{Q}} = \rho_J^{\mathbb{P}}$, then $\beta_2 = 0$ and $\beta_1 = -\frac{1}{2}(\frac{1}{\mu_v^{\mathbb{Q}}} + \frac{1}{\mu_v^{\mathbb{P}}}) < 0$, and the third term is finite too.

Therefore, $(\lambda, \mu_y, \sigma_y, \rho_J, \mu_v)$ can change freely between $\mathbb{P}$ and $\mathbb{Q}$.

VG. Suppose the parameters under $\mathbb{P}$ and $\mathbb{Q}$ are $(\nu^{\mathbb{P}}, \gamma^{\mathbb{P}}, \sigma^{\mathbb{P}})$ and $(\nu^{\mathbb{Q}}, \gamma^{\mathbb{Q}}, \sigma^{\mathbb{Q}})$, respectively. Because $f(x) = (\sqrt{\pi_{\mathbb{Q}}} - \sqrt{\pi_{\mathbb{P}}})^2$ and is nonnegative, the integral $\int_{-\infty}^{\infty} f(x)dx = \int_{-\infty}^{0} f(x)dx + \int_0^{\infty} f(x)dx$ is finite if and only if both $\int_{-\infty}^{0} f(x)dx$ and $\int_0^{\infty} f(x)dx$ are finite.

Over the positive half line, the integrand is

$$f(x) = \frac{1}{x}\left[\frac{1}{\nu^{\mathbb{Q}}}\exp\left(-M^{\mathbb{Q}}x\right) + \frac{1}{\nu^{\mathbb{P}}}\exp(-M^{\mathbb{P}}x) - 2\sqrt{\frac{1}{\nu^{\mathbb{Q}}\nu^{\mathbb{P}}}}\ \exp\left(-\frac{1}{2}(M^{\mathbb{Q}} + M^{\mathbb{P}})x\right)\right].$$

Remember that $\pi_{VG}(x) = \frac{1}{\nu}\frac{\exp(-Mx)}{x}$, where $M = \left(\sqrt{\frac{1}{4}\gamma^2\nu^2 + \frac{1}{2}\sigma^2\nu} + \frac{1}{2}\gamma\nu\right)^{-1}$ for $x > 0$.

For any constant $a > 0$, $\int_0^{\infty} f(x)dx = \int_0^{a} f(x)dx + \int_a^{\infty} f(x)dx$. A direct application of Lemma 2 shows that $\int_a^{\infty} f(x)dx$ is finite because each of the three components of $f(x)$ has the same functional form as in case (i) of Lemma 2. For $\int_0^a f(x)dx$, we need to examine the behavior of $f(x)$ around zero.

If $\nu^{\mathbb{Q}} \neq \nu^{\mathbb{P}}$, when $x \to 0+$,

$$\frac{1}{x}\left[\frac{1}{\nu^{\mathbb{Q}}}\exp\left(-M^{\mathbb{Q}}x\right) + \frac{1}{\nu^{\mathbb{P}}}\exp(-M^{\mathbb{P}}x) - 2\sqrt{\frac{1}{\nu^{\mathbb{Q}}\nu^{\mathbb{P}}}}\ \exp\left(-\frac{1}{2}(M^{\mathbb{Q}} + M^{\mathbb{P}})x\right)\right] \sim \frac{C}{x},$$

where

$$C = \frac{1}{\nu^{\mathbb{Q}}} + \frac{1}{\nu^{\mathbb{P}}} - 2\sqrt{\frac{1}{\nu^{\mathbb{Q}}\nu^{\mathbb{P}}}} > 0.$$

According to case (ii) of Lemma 1, because $\int_0^a \frac{C}{x}dx = \infty$, we have $\int_0^a f(x) = \infty$.

If $\nu^{\mathbb{Q}} = \nu^{\mathbb{P}} = \nu$, then

$$\begin{aligned} &\lim_{x\to 0+}\frac{1}{x}\left[\frac{1}{\nu^{\mathbb{Q}}}\exp\left(-M^{\mathbb{Q}}x\right) + \frac{1}{\nu^{\mathbb{P}}}\exp(-M^{\mathbb{P}}x) - 2\sqrt{\frac{1}{\nu^{\mathbb{Q}}\nu^{\mathbb{P}}}}\ \exp\left(-\frac{1}{2}(M^{\mathbb{Q}} + M^{\mathbb{P}})x\right)\right] \\ &= \frac{1}{\nu}[-M^{\mathbb{Q}} - M^{\mathbb{P}} - 2(-\tfrac{1}{2})(M^{\mathbb{Q}} + M^{\mathbb{P}})] = 0. \end{aligned}$$

So for $\epsilon = 1$, there exists $M > 0$ such that $\forall\ 0 < x < M < a$,

$$\left|\frac{1}{x}\left[\frac{1}{\nu^{\mathbb{Q}}}\exp\left(-M^{\mathbb{Q}}x\right) + \frac{1}{\nu^{\mathbb{P}}}\exp(-M^{\mathbb{P}}x) - 2\sqrt{\frac{1}{\nu^{\mathbb{Q}}\nu^{\mathbb{P}}}}\ \exp\left(-\frac{1}{2}(M^{\mathbb{Q}} + M^{\mathbb{P}})x\right)\right]\right| \leq 1.$$

Therefore,

$$\begin{aligned} \int_0^a |f(x)|dx &= \int_0^M |f(x)|dx + \int_M^a |f(x)|dx \\ &\leq M + \int_M^a |f(x)|dx < \infty. \end{aligned}$$

The second integral is finite by the continuity of $f(x)$. This proves $\int_0^\infty f(x)dx < \infty$. By the transform $y = -x$, the exact proof can be applied to the integral over the negative half line, which is finite too. Therefore, condition (ii) is satisfied if and only if $\nu^{\mathbb{Q}} = \nu^{\mathbb{P}}$ and the other two parameters, γ and σ, can change freely between $\mathbb{P}$ and $\mathbb{Q}$.

LS. Suppose the parameters of a Lévy α-stable process are $(\alpha^{\mathbb{P}}, \beta^{\mathbb{P}}, \sigma^{\mathbb{P}}, \gamma^{\mathbb{P}})$ and $(\alpha^{\mathbb{Q}}, \beta^{\mathbb{Q}}, \sigma^{\mathbb{Q}}, \gamma^{\mathbb{Q}})$ under $\mathbb{P}$ and $\mathbb{Q}$, respectively. The integral in condition (ii) of Sato's theorem is finite when both $\int_{-\infty}^0 f(x)dx$ and $\int_0^\infty f(x)dx$ are finite.

First, we focus on $\int_0^\infty f(x)dx$. For $x > 0$, the integrand is

$$f(x) = c_1^{\mathbb{Q}}|x|^{-\alpha^{\mathbb{Q}}-1} + c_1^{\mathbb{P}}|x|^{-\alpha^{\mathbb{P}}-1} - 2\sqrt{c_1^{\mathbb{Q}}c_1^{\mathbb{P}}}|x|^{\frac{-\alpha^{\mathbb{Q}}-\alpha^{\mathbb{P}}}{2}-1}$$

where $c_1^{\mathbb{Q}} = \frac{(\sigma^{\mathbb{Q}})^\alpha(1+\beta^{\mathbb{Q}})}{2}$ and $c_1^{\mathbb{P}} = \frac{(\sigma^{\mathbb{P}})^\alpha(1+\beta^{\mathbb{P}})}{2}$. For any constant $a > 0$, $\int_0^\infty f(x)dx = \int_0^a f(x)dx + \int_a^\infty f(x)dx$. And for the second term,

$$\begin{aligned} \int_a^\infty f(x)dx &= \frac{c_1^{\mathbb{Q}}}{-\alpha^{\mathbb{Q}}}x^{-\alpha^{\mathbb{Q}}}|_a^\infty + \frac{c_1^{\mathbb{P}}}{-\alpha^{\mathbb{P}}}x^{-\alpha^{\mathbb{P}}}|_a^\infty + \frac{4\sqrt{c_1^{\mathbb{Q}}c_1^{\mathbb{P}}}}{\alpha^{\mathbb{Q}}+\alpha^{\mathbb{P}}}x^{\frac{-\alpha^{\mathbb{Q}}-\alpha^{\mathbb{P}}}{2}}|_a^\infty \\ &= \frac{c_1^{\mathbb{Q}}}{\alpha^{\mathbb{Q}}a^{\alpha^{\mathbb{Q}}}} + \frac{c_1^{\mathbb{P}}}{\alpha^{\mathbb{P}}a^{\alpha^{\mathbb{P}}}} - \frac{4\sqrt{c_1^{\mathbb{Q}}c_1^{\mathbb{P}}}}{\alpha^{\mathbb{Q}}+\alpha^{\mathbb{P}}}a^{\frac{-\alpha^{\mathbb{Q}}-\alpha^{\mathbb{P}}}{2}} < \infty. \end{aligned}$$

So what is left is to check the finiteness of $\int_0^a f(x)dx$.

If $\alpha^{\mathbb{P}} < \alpha^{\mathbb{Q}}$, then

$$\begin{aligned} f(x) &= \frac{1}{x^{\alpha^{\mathbb{Q}}+1}}(c_1^{\mathbb{Q}} + c_1^{\mathbb{P}}x^{\alpha^{\mathbb{P}}-\alpha^{\mathbb{Q}}} - 2\sqrt{c_1^{\mathbb{Q}}c_1^{\mathbb{P}}}x^{\frac{\alpha^{\mathbb{Q}}-\alpha^{\mathbb{P}}}{2}}) \\ &\sim \frac{c_1^{\mathbb{Q}}}{x^{\alpha^{\mathbb{Q}}+1}} \quad \text{when} \quad x \to 0+. \end{aligned}$$

Since

$$\int_0^a \frac{c^{\mathbb{Q}}}{x^{\alpha^{\mathbb{Q}}+1}}dx = \frac{c^{\mathbb{Q}}}{-\alpha^{\mathbb{Q}}}x^{-\alpha^{\mathbb{Q}}}|_0^a = \infty,$$

according to Lemma 1 (ii), $\int_0^a f(x)dx$ is infinite.

If $\alpha^{\mathbb{P}} = \alpha^{\mathbb{Q}} = \alpha$, but $c_1^{\mathbb{Q}} \neq c_1^{\mathbb{P}}$, then

$$\int_0^a f(x)dx = \frac{c_1^{\mathbb{Q}} + c_1^{\mathbb{P}} - 2\sqrt{c_1^{\mathbb{Q}}c_1^{\mathbb{P}}}}{-\alpha}x^{-\alpha}|_0^a = \infty.$$

If $\alpha^{\mathbb{P}} > \alpha^{\mathbb{Q}}$, we have $\int_0^a f(x)dx = \infty$ and the proof is symmetric to the one for $\alpha^{\mathbb{P}} < \alpha^{\mathbb{Q}}$.

If $\alpha^{\mathbb{P}} = \alpha^{\mathbb{Q}}$ and $c_1^{\mathbb{Q}} = c_1^{\mathbb{P}}$, then $f(x)$ is identically zero and its integral over $[0, a]$ is finite.

So only when $\alpha^{\mathbb{P}} = \alpha^{\mathbb{Q}}$ and $c_1^{\mathbb{Q}} = c_1^{\mathbb{P}}$, $\int_0^\infty f(x)dx$ is finite. For $\int_{-\infty}^0 f(x)dx$, by the simple transform $y = -x$, the same proof applies and we conclude again that $\int_{-\infty}^0 f(x)dx$ is finite only when $\alpha^{\mathbb{P}} = \alpha^{\mathbb{Q}}$ and $c_2^{\mathbb{Q}} = c_2^{\mathbb{P}}$.

Therefore, in terms of jump parameters, the following two equations must be satisfied

$$(\sigma^{\mathbb{P}})^\alpha(1 + \beta^{\mathbb{P}}) = (\sigma^{\mathbb{Q}})^\alpha(1 + \beta^{\mathbb{Q}}),$$

$$(\sigma^{\mathbb{P}})^{\alpha}(1-\beta^{\mathbb{P}}) = (\sigma^{\mathbb{Q}})^{\alpha}(1-\beta^{\mathbb{Q}}),$$

and from which we conclude that

$$\beta^{\mathbb{P}} = \beta^{\mathbb{Q}} \text{ and } \sigma^{\mathbb{P}} = \sigma^{\mathbb{Q}}.$$

In general, this means that to maintain the equivalence between the two Lévy α-stable processes, (α, β, σ) have to be the same under $\mathbb{P}$ and $\mathbb{Q}$, which implies that $\pi_{\mathbb{P}}(x) = \pi_{\mathbb{Q}}(x)$.

Unlike the previous three models, we need to check condition (iii) of Sato's theorem for LS. The difference between the two Lévy drifts under $\mathbb{P}$ and $\mathbb{Q}$ is

$$\bar{\mu}_{\mathbb{Q}} - \bar{\mu}_{\mathbb{P}} = \left(\gamma^{\mathbb{Q}} - \int_{1_{|x|>1}} x\pi_{\mathbb{Q}}(dx)\right) - \left(\gamma^{\mathbb{P}} - \int_{1_{|x|>1}} x\pi_{\mathbb{P}}(dx)\right).$$

Because the Lévy measures under $\mathbb{P}$ and $\mathbb{Q}$ are the same, the left-hand side of condition (iii) of Sato's theorem becomes

$$\bar{\mu}_{\mathbb{Q}} - \bar{\mu}_{\mathbb{P}} = \gamma^{\mathbb{Q}} - \gamma^{\mathbb{P}},$$

and the right-hand side of condition (iii) becomes zero. This implies that condition (iii) is satisfied only when $\gamma^{\mathbb{Q}} = \gamma^{\mathbb{P}}$.

Therefore, we further conclude that to maintain the equivalence between the two Lévy α-stable processes, $(\alpha, \beta, \sigma, \gamma)$ must be the same under $\mathbb{P}$ and $\mathbb{Q}$.

APPENDIX B. Descriptions of MCMC Methods

B.1 Priors for Model Parameters

In this section, we discuss the priors for parameters of all four models. For most parameters that have been considered in LWY (2006), we choose the same priors and hyperparameter values. And for most new parameters that only appear in this joint study, we choose standard conjugate priors whenever possible to simplify numerical simulations.

- **Priors for parameters common to four models**. We consider the following prior distributions: $\kappa \sim N(0,1)$ (truncated at zero), $\theta \sim N(0,1)$ (truncated at zero), $\rho \sim Uniform(0,1)$, $\sigma_v \sim \frac{1}{\sigma_v}$, $\eta^s \sim N(0,1)$, $\eta^v \sim N(0,1)$, $\rho_c \sim N(0,1)$, and $\sigma_c \sim \frac{1}{\sigma_c}$.

- **Priors for parameters common to SVMJ and SVCMJ.** For $\mu_y^{\mathbb{P}}$ and $\mu_y^{\mathbb{Q}}$, we choose standard conjugate priors: $\mu_y^{\mathbb{P}} \sim N(0,1)$ and $\mu_y^{\mathbb{Q}} \sim N(0,1)$. We choose flat priors for σ_y and λ: $\sigma_y \sim \frac{1}{\sigma_y}$ and $\lambda \sim Uniform(0,1)$.

- **Priors for parameters unique to SVCMJ**. For μ_v and ρ_J, we choose the following priors: $\mu_v \sim \frac{1}{\mu_v}$ and $\rho_J \sim N(0,1)$.

- **Priors for parameters unique to SVVG**. We choose the following priors for the five parameters that are unique to SVVG: $\gamma^{\mathbb{P}} \sim N(0,1), \gamma^{\mathbb{Q}} \sim N(0,1), \nu \sim \frac{1}{\nu}, \sigma^{\mathbb{P}} \sim \frac{1}{\sigma^{\mathbb{P}}}$, and $\sigma^{\mathbb{Q}} \sim \frac{1}{\sigma^{\mathbb{Q}}}$.

- **Priors for parameters unique to SVLS**. For α and σ, we choose the following joint priors: $\alpha \sim Uniform(1,2)$ and $\sigma \sim \frac{1}{\sigma}$.

Although we choose flat priors for the variance parameters, the priors of most other parameters are proper priors, pretty uninformative, and have been used in previous studies. In general, as the sample size becomes large, the information contained in the likelihood function dominates that in the priors. As a result, we find the results computed later seem to be relatively invariant to the choice of priors.

B.2 MCMC Methods for SVMJ

In this section, we discuss the updating algorithms and the posterior distributions of model parameters and latent variables for SVMJ. Compared to LWY (2006), the posterior likelihood here always has an additional component, which is the likelihood of option pricing errors. Since the computation of option price involves numerical integration, the parameters that appear in the option pricing formula usually do not have known posterior distributions. To overcome this difficulty, we adopt the method of Damine, Wakefield, and Walker (1999) (hereafter DWW) to update these parameters. Parameters that are not involved in the option pricing formula we usually have standard known posterior distributions, from which we draw posterior samples. In this and the following sections, we discuss the updating methods, first for parameters that appear in the option pricing formula, then for the rest.

- **Posterior for** κ. The posterior of κ is proportional to

$$\propto \underbrace{\prod_{t=0}^{T-1} \exp\left(-\frac{[(C_{t+1}-F_{t+1})-\rho_c(C_t-F_t)]^2}{2\sigma_c^2}\right)}_{:=l(\kappa)} \times N(\frac{\mathcal{S}}{\mathcal{W}}, \sqrt{\frac{1}{\mathcal{W}}})\ 1_{\kappa>0}$$

where $\mathcal{W} = \frac{\Delta}{(1-\rho^2)\sigma_v^2}\sum_{t=0}^{T-1}\frac{(\theta-v_t)^2}{v_t}+1$, $\mathcal{S} = \frac{1}{\sigma_v(1-\rho^2)}\sum_{t=0}^{T-1}\frac{(\theta-v_t)(\frac{B_{t+1}}{\sigma_v}-\rho A_{t+1})}{v_t}$, $A_{t+1} = Y_{t+1} - Y_t - (r_t - \frac{1}{2}v_t + \psi_J(-i) + \eta^s v_t)\Delta - N_{t+1}^y \xi_{t+1}^y$, and $B_{t+1} = v_{t+1} - v_t$. We denote the first term as $l(\kappa)$, omitting dependence on other parameters to simplify notation. Its calculation involves numerical integration because of the option pricing formula involved. The second term in the posterior is a truncated normal distribution and is the same as the corresponding posterior distribution of κ in LWY (2006), except for the different definition of the drift term in A_{t+1}. This combination motivates us to use the DWW method. Specifically, for a given previous draw, $\kappa^{(g)}$, the algorithm for $(g+1)$-th iteration is:

  1. Draw $\kappa^{(g+1)}$ from $N(\frac{\mathcal{S}}{\mathcal{W}}, \sqrt{\frac{1}{\mathcal{W}}})\ 1_{\kappa>0}$;
  2. Draw an auxiliary variable u from $Uniform(0, l(\kappa^{(g)}))$;
  3. Accept $\kappa^{(g+1)}$ if $l(\kappa^{(g+1)}) > u$; otherwise, keep $\kappa^{(g)}$.

- **Posterior for** θ. Similarly, the posterior of θ is proportional to

$$\propto \underbrace{\prod_{t=0}^{T-1} \exp\left(-\frac{[(C_{t+1}-F_{t+1})-\rho_c(C_t-F_t)]^2}{2\sigma_c^2}\right)}_{:=l(\theta)} \times N(\frac{\mathcal{S}}{\mathcal{W}}, \sqrt{\frac{1}{\mathcal{W}}})\ 1_{\theta>0}$$

where $\mathcal{W} = \frac{\kappa^2\Delta}{\sigma_v^2(1-\rho^2)}\sum_{t=0}^{T-1}\frac{1}{v_t}+1, \mathcal{S} = \frac{\kappa}{(1-\rho^2)\sigma_v}\sum_{t=0}^{T-1}(\frac{B_{t+1}/\sigma_v-\rho A_{t+1}}{v_t}), A_{t+1} = Y_{t+1} - Y_t - (r_t - \frac{1}{2}v_t + \psi_J(-i) + \eta^s v_t)\Delta - N_{t+1}^y\xi_{t+1}^y$, and $B_{t+1} = v_{t+1} + (\kappa\Delta - 1)v_t$. Again we use the DWW method and the updating algorithm is the same as that for κ.

- **Posterior for** σ_v. The posterior of σ_v is proportional to

$$\propto \underbrace{\prod_{t=0}^{T-1} \exp\left(-\frac{[(C_{t+1}-F_{t+1})-\rho_c(C_t-F_t)]^2}{2\sigma_c^2}\right) \times \exp(\frac{\rho}{1-\rho^2}(\sum_{t=0}^{T-1}A_{t+1}B_{t+1})\frac{1}{\sigma_v})}_{:=l(\sigma_v)}$$

$$\times(\frac{1}{\sigma_v^2})^{\frac{T}{2}+\frac{1}{2}}\exp(-\frac{\sum_{t=0}^{T-1}B_{t+1}^2}{2(1-\rho^2)}\frac{1}{\sigma_v^2})$$

where $A_{t+1} = \frac{Y_{t+1}-Y_t-(r_t-\frac{1}{2}v_t+\psi_J(-i)+\eta^s v_t)\Delta-N_{t+1}^y\xi_{t+1}^y}{\sqrt{v_t\Delta}}$ and $B_{t+1} = \frac{v_{t+1}-v_t-\kappa(\theta-v_t)\Delta}{\sqrt{v_t\Delta}}$. The algorithm is similar to that for κ:

1. Draw $\frac{1}{(\sigma_v^{(g+1)})^2}$ from $\Gamma(\frac{T}{2}+\frac{3}{2},(\frac{\sum_{t=0}^{T-1}B_{t+1}^2}{2(1-\rho^2)})^{-1})$;
2. Draw an auxiliary variable u from $Uniform(0,l(\sigma_v^{(g)}))$;
3. Accept $\sigma_v^{(g+1)}$ if $l(\sigma_v^{(g+1)})>u$; otherwise, keep $\sigma_v^{(g)}$.

- **Posterior for** ρ. The posterior of ρ is proportional to the function $\pi(\rho)$

$$\propto \pi(\rho) := \prod_{t=0}^{T-1}\exp\left(-\frac{[(C_{t+1}-F_{t+1})-\rho_c(C_t-F_t)]^2}{2\sigma_c^2}\right)\times$$

$$(1-\rho^2)^{-\frac{T}{2}}\exp\left(-12(1-\rho^2)\sum_{t=0}^{T-1}(A_{t+1}^2+B_{t+1}^2)+\frac{\rho}{(1-\rho^2)}\sum_{t=0}^{T-1}A_{t+1}B_{t+1}\right)$$

where $A_{t+1} = \frac{Y_{t+1}-Y_t-(r_t-\frac{1}{2}v_t+\psi_J(-i)+\eta^s v_t)\Delta-N_{t+1}^y\xi_{t+1}^y}{\sqrt{v_t\Delta}}$ and $B_{t+1} = \frac{v_{t+1}-v_t-\kappa(\theta-v_t)\Delta}{\sigma_v\sqrt{v_t\Delta}}$. It is well known that the sampling distribution of Pearson's correlation is negatively skewed and the so-called "Fisher's Z transformation" converts Pearson's correlation to a normally distributed variable. Motivated by Fisher's idea, we develop the following algorithm:

1. Draw $\frac{1}{2}\log\frac{1+\rho^{(g+1)}}{1-\rho^{(g+1)}}$ from $N(\frac{1}{2}\log\frac{1+\rho_r}{1-\rho_r},\frac{1}{T-3})$, where $\rho_r = Corr(\mathbf{A},\mathbf{B})$, $\mathbf{A} = \{A_{t+1}\}_{t=0}^{T-1}$, $\mathbf{B} = \{B_{t+1}\}_{t=0}^{T-1}$, and $g(\rho_r) = \frac{1}{2}\log\frac{1+\rho_r}{1-\rho_r}$ is the formula of Fisher's Z transformation.
2. Accept $\rho^{(g+1)}$ with probability

$$\min\left(\frac{\pi(\rho^{(g+1)}}{\pi(\rho^{(g)}}\times\frac{\exp(-\frac{(g(\rho^{(g)}-g(\rho_r))^2}{\frac{2}{T-3}})}{\exp(-\frac{(g(\rho^{(g+1)}-g(\rho_r))^2}{\frac{2}{T-3}})},1\right).$$

By removing the skewness of the distribution for the candidate draw, our algorithm converges more quickly than the one without the transformation.

- **Posteriors for** η^v and $\mu_y^{\mathbb{Q}}$. Since the updating methods and the posteriors of η^v and $\mu_y^{\mathbb{Q}}$ are the same, we focus our discussion on η^v. The posterior of η^v is proportional to

$$\propto \pi(\eta^v) := \prod_{t=0}^{T-1}\exp\left(-\frac{[(C_{t+1}-F_{t+1})-\rho_c(C_t-F_t)]^2}{2\sigma_c^2}\right)\times\exp(-\frac{(\eta^v)^2}{2}).$$

We update the parameter using the Metropolis-Hasting algorithm. A normal distribution centered at the previous draw with constant variance 1 is used as the proposal distribution for the candidate draw, which is accepted with the probability $\min\left(\frac{\pi(\eta^{v(g+1)})}{\pi(\eta^{v(g)})},1\right)$.

- **Posterior for σ_y.** The posterior of σ_y is proportional to

$$\propto \underbrace{\prod_{t=0}^{T-1} \exp\left(-\frac{[(C_{t+1}-F_{t+1})-\rho_c(C_t-F_t)]^2}{2\sigma_c^2}\right)}_{:=l(\sigma_y)} \times (\frac{1}{\sigma_y^2})^{\frac{T}{2}+\frac{1}{2}} \exp(-\frac{1}{2}\sum_{t=0}^{t-1}(\xi_{t+1}^y-\mu_y^{\mathbb{P}})^2 \frac{1}{\sigma_y^2}).$$

  We use the DWW method to update the parameter:

  1. Draw $\frac{1}{(\sigma_y^{(g+1)})^2}$ from $\Gamma(\frac{T}{2}+\frac{3}{2}, \frac{1}{\frac{1}{2}\sum_{t=0}^{T-1}(\xi_{t+1}^y-\mu_y^{\mathbb{P}})^2})$;
  2. Draw an auxiliary variable u from $Uniform(0, l(\sigma_y^{(g)}))$;
  3. Accept $\sigma_y^{(g+1)}$ if $l(\sigma_y^{(g+1)}) > u$; otherwise, keep $\sigma_y^{(g)}$.

- **Posterior for λ.** The posterior of λ is proportional to

$$\propto \underbrace{\prod_{t=0}^{T-1} \exp\left(-\frac{[(C_{t+1}-F_{t+1})-\rho_c(C_t-F_t)]^2}{2\sigma_c^2}\right)}_{:=l(\lambda)} \times \lambda^{\sum_{t=0}^{T-1} N_{t+1}}(1-\lambda)^{T-\sum_{t=0}^{T-1} N_{t+1}}.$$

  The DWW method is used and the proposal distribution for the candidate draw is $Beta(\sum_{t=0}^{T-1} N_{t+1} + 1, T-\sum_{t=0}^{T-1} N_{t+1}+1)$. The algorithm is skipped.

For parameters that do not appear in the option pricing formula, i.e., $(\eta^s, \mu_y^{\mathbb{P}}, \rho_c, \sigma_c)$, we obtain known posterior distributions.

- **Posterior for η^s.** The posterior of η^s follows a normal distribution $\eta^s \sim N(\frac{\mathcal{S}}{\mathcal{W}}, \frac{1}{\mathcal{W}})$, where $\mathcal{W} = \frac{\Delta}{(1-\rho^2)}\sum_{t=0}^{T-1} v_t + 1$, $\mathcal{S} = \frac{1}{(1-\rho^2)}\sum_{t=0}^{T-1}(A_{t+1} - \frac{\rho}{\sigma_v}B_{t+1})$, $A_{t+1} = Y_{t+1} - Y_t - (r_t - \frac{1}{2}v_t + \psi_J(-i) + \eta^s v_t)\Delta - N_{t+1}^y \xi_{t+1}^y$, and $B_{t+1} = v_{t+1} - v_t - \kappa(\theta - v_t)\Delta$.

- **Posterior for $\mu_y^{\mathbb{P}}$.** The posterior of $\mu_y^{\mathbb{P}}$ follows a normal distribution $\mu_y^{\mathbb{P}} \sim N(\frac{\mathcal{S}}{\mathcal{W}}, \frac{1}{\mathcal{W}})$, where $\mathcal{W} = \frac{T}{\sigma_y^2} + 1$, and $\mathcal{S} = \frac{\xi_{t=0}^{T-1}\xi_{t+1}}{\sigma_y^2}$.

- **Posterior for ρ_c.** The posterior of ρ_c follows a normal distribution $\rho_c \sim N(\frac{\mathcal{S}}{\mathcal{W}}, \frac{1}{\mathcal{W}})$, where $\mathcal{W} = \frac{\sum_{t=0}^{T-1} A_t^2}{\sigma_c^2} + 1, \mathcal{S} = \frac{\sum_{t=0}^{T-1} A_t A_{t+1}}{\sigma_c^2}$, and $A_{t+1} = C_{t+1} - F_{t+1}$.

- **Posterior for σ_c.** The posterior of σ_c follows a gamma distribution $\frac{1}{\sigma_c^2} \sim \Gamma(\frac{T}{2}+\frac{3}{2}, \frac{1}{\frac{1}{2}\sum_{t=0}^{T-1}(A_{t+1}-\rho_c A_t)^2})$, where $A_{t+1} = C_{t+1} - F_{t+1}$.

Next we consider the posteriors of latent jump and volatility variables.

- **Posterior for ξ_{t+1}^y.** The posterior of ξ_{t+1}^y is $\xi_{t+1}^y \sim N(\frac{\mathcal{S}}{\mathcal{W}}, \frac{1}{\mathcal{W}})$, where $\mathcal{W} = \frac{N_{t+1}^2}{(1-\rho^2)v_t\Delta} + \frac{1}{\sigma_y^2}, \mathcal{S} = \frac{N_{t+1}}{(1-\rho^2)v_t\Delta}(A_{t+1} - \rho B_{t+1}/\sigma_v) + \frac{\mu_y}{\sigma_y^2}$, $A_{t+1} = Y_{t+1} - Y_t - (r_t - \frac{1}{2}v_t + \psi_J(-i) + \eta^s v_t)\Delta$, and $B_{t+1} = v_{t+1} - v_t - \kappa(\theta - v_t)\Delta$.

- **Posterior for** N_{t+1}. The posterior of N_{t+1} is $N_{t+1} \sim Bernoulli(\frac{\alpha_1}{\alpha_1+\alpha_2})$, where $\alpha_1 = e^{-\frac{1}{2(1-\rho^2)}[A_1^2-2\rho A_1 B]}\lambda$, $\alpha_2 = e^{-\frac{1}{2(1-\rho^2)}[A_2^2-2\rho A_2 B]}(1-\lambda)$, $A_1 = \left(Y_{t+1} - Y_t - (r_t - \frac{1}{2}v_t + \psi_J(-i) + \eta^s v_t)\Delta - \xi^y_{t+1}\right)/\sqrt{v_t\Delta}$, $A_2 = \left(Y_{t+1} - Y_t - (r_t - \frac{1}{2}v_t + \psi_J(-i) + \eta^s v_t)\Delta\right)/\sqrt{v_t\Delta}$, and $B = (v_{t+1} - v_t - \kappa(\theta - v_t)\Delta)/(\sigma_v\sqrt{v_t\Delta})$.

- **Posterior for** v_{t+1}. For $0 < t+1 < T$, the posterior of v_{t+1} is proportional to

$$\propto \exp(-\frac{1}{2\sigma_c^2}[(C_{t+1} - F_{t+1})^2 - 2\rho_c(C_{t+1} - F_{t+1})(C_t - F_t)])\times$$

$$\exp(-\frac{1}{2\sigma_c^2}[\rho_c^2(C_{t+1} - F_{t+1})^2 - 2\rho_c(C_{t+2} - F_{t+2})(C_{t+1} - F_{t+1})])\times$$

$$\exp\left\{-\frac{\left[-2\rho\epsilon^y_{t+1}\epsilon^v_{t+1} + \left(\epsilon^v_{t+1}\right)^2\right]}{2(1-\rho^2)}\right\} \times \frac{1}{v_{t+1}} \times \exp\left\{-\frac{\left[(\epsilon^y_{t+2})^2 - 2\rho\epsilon^y_{t+2}\epsilon^v_{t+2} + (\epsilon^v_{t+2})^2\right]}{2(1-\rho^2)}\right\},$$

where $\epsilon^y_{t+1} = \left(Y_{t+1} - Y_t - (r_t - \frac{1}{2}v_t + \psi_J(-i) + \eta^s v_t)\Delta - N^y_{t+1}\xi^y_{t+1}\right)/\sqrt{v_t\Delta}$, and $\epsilon^v_{t+1} = (v_{t+1} - v_t - \kappa(\theta - v_t)\Delta)/(\sigma_v\sqrt{v_t\Delta})$. And the posterior for v_t when $t = 0$ and $t = T$ can be derived in the similar way.

While LWY (2006) use ARMS to update v_t and obtain very good results, the implementation of ARMS here is difficult because it requires intensive numerical integrations for each adaptive rejection Metropolis iteration. As a result, we use the traditional Metropolis-Hasting method to update v_t, and use the Student-t distribution with a degree of freedom of 6 as the proposal distribution.

B.3 MCMC Methods for SVCMJ

The common parameters and latent variables between SVMJ and SVCMJ have similar posterior distributions. So in this section, we focus on the posterior distributions of the parameters and latent variables that are unique to SVCMJ.

- **Posterior for** μ_v. The posterior of μ_v is proportional to

$$\propto \underbrace{\prod_{t=0}^{T-1} \exp\left(-\frac{[(C_{t+1} - F_{t+1}) - \rho_c(C_t - F_t)]^2}{2\sigma_c^2}\right)}_{:=l(\mu_v)} \times (\frac{1}{\mu_v})^{T+1} \exp(-\frac{1}{\mu_v}\sum_{t=0}^{T-1}\xi^v_{t+1}).$$

The DWW method is used and the proposal distribution for the candidate draw is $IG(T+2, \frac{1}{\sum_{t=0}^{T-1}\xi^v_{t+1})})$.

- **Posterior for** ρ_J. The posterior of ρ_J is proportional to

$$\propto \underbrace{\prod_{t=0}^{T-1} \exp\left(-\frac{[(C_{t+1}-F_{t+1})-\rho_c(C_t-F_t)]^2}{2\sigma_c^2}\right)}_{:=l(\rho_J)} \times N(\frac{\mathcal{S}}{\mathcal{W}}, \sqrt{\frac{1}{\mathcal{W}}}),$$

where $\mathcal{W} = \frac{\sum_{t=0}^{T-1}(\xi_{t+1}^v)^2}{\sigma_y^2} + 1$, $\mathcal{S} = \frac{\sum_{t=0}^{T-1}\xi_{t+1}^v A_{t+1}}{\sigma_y^2}$, and $A_{t+1} = \xi_{t+1}^y - \mu_y^{\mathbb{P}}$. The DWW method is used and the proposal distribution for the candidate draw is $N(\frac{\mathcal{S}}{\mathcal{W}}, \sqrt{\frac{1}{\mathcal{W}}})$.

- **Posterior for** ξ_{t+1}^v. The posterior of ξ_{t+1}^v follows a normal distribution $\xi_{t+1}^v \sim N(\frac{\mathcal{S}}{\mathcal{W}}, \frac{1}{\mathcal{W}})\ 1_{\xi_{t+1}^v>0}$, where $\mathcal{W} = \frac{N_{t+1}^2}{(1-\rho^2)v_t\Delta} + \frac{\rho_J^2}{\sigma_y^2}, \mathcal{S} = \frac{N_{t+1}}{(1-\rho^2)v_t\Delta}(-\rho A_{t+1} + \frac{B_{t+1}\sigma_v}{+}\frac{\xi_{t+1}^y-\mu_y^{\mathbb{P}})\rho_J}{\sigma_y^2} - \frac{1}{\mu_v}$, $A_{t+1} = Y_{t+1} - Y_t - (r_t - \frac{1}{2}v_t + \psi_J(-i) + \eta^s v_t)\Delta$, and $B_{t+1} = v_{t+1} - v_t - \kappa(\theta - v_t)\Delta - N_{t+1}\xi_{t+1}^v$.

B.4 MCMC Methods for SVVG

The common parameters and latent variables between SVMJ and SVVG have similar posterior distributions. So in this section we focus on the posterior distributions of the parameters and latent variables that are unique to SVVG.

- **Posterior for** ν. The posterior of ν is proportional to

$$\propto \underbrace{\prod_{t=0}^{T-1} \exp\left(-\frac{[(C_{t+1}-F_{t+1})-\rho_c(C_t-F_t)]^2}{2\sigma_c^2}\right)\left(\frac{1}{\nu^{\frac{\Delta}{\nu}}\Gamma(\frac{\Delta}{\nu})}\right)^T \left(\prod_{t=0}^{T-1} G_t\right)^{\frac{\Delta}{\nu}-1}}_{:=l(\nu)} \times \exp\left\{-\frac{1}{\nu}(\sum_{t=0}^{T-1} G_t)\right\}\frac{1}{\nu}.$$

The DWW method is used and the proposal distribution for the candidate draw is $IG(2, \frac{1}{\sum_{t=0}^{T-1} G_{t+1})})$.

- **Posteriors for** $\gamma^{\mathbb{Q}}$ and $\sigma^{\mathbb{Q}}$. The algorithms for updating $\gamma^{\mathbb{Q}}$ and $\sigma^{\mathbb{Q}}$ are the same as that for η^v in SVMJ, except that the candidate draw for $\sigma^{\mathbb{Q}}$ needs to be truncated at zero since it has to be a positive number.

- **Posterior for** $\gamma^{\mathbb{P}}$. The posterior of $\gamma^{\mathbb{P}}$ is $\gamma^{\mathbb{P}} \sim N(\frac{\mathcal{S}}{\mathcal{W}}, \frac{1}{\mathcal{W}})$, where $\mathcal{W} = \frac{1}{(\sigma^{\mathbb{P}})^2}\sum_{t=0}^{T-1} G_{t+1} + 1$, and $\mathcal{S} = \frac{1}{(\sigma^{\mathbb{P}})^2}\sum_{t=0}^{T-1} J_{t+1}$.

- **Posterior for** $\sigma^{\mathbb{P}}$. The posterior of $\sigma^{\mathbb{P}}$ is $(\sigma^{\mathbb{P}})^2 \sim IG(\frac{T}{2} + \frac{3}{2}, \frac{1}{\frac{1}{2}\sum_{t=0}^{T-1}\frac{(J_{t+1}-\gamma^{\mathbb{P}}G_{t+1})^2}{G_{t+1}}})$.

- **Posterior for** J_{t+1}. The posterior of J_{t+1} follows a normal distribution $J_{t+1} \sim N(\frac{\mathcal{S}}{\mathcal{W}}, \frac{1}{\mathcal{W}})$, where $\mathcal{W} = \frac{1}{(1-\rho^2)v_t\Delta} + \frac{1}{(\sigma^{\mathbb{P}})^2 G_{t+1}}$, $\mathcal{S} = \frac{1}{(1-\rho^2)v_t\Delta}(A_{t+1} - \frac{\rho B_{t+1}}{\sigma_v}) + \frac{\gamma^{\mathbb{P}}}{(\sigma^{\mathbb{P}})^2}$, $A_{t+1} = Y_{t+1} - Y_t - (r_t - \frac{1}{2}v_t + \psi_J(-i) + \eta^s v_t)\Delta$, and $B_{t+1} = v_{t+1} - v_t - \kappa(\theta - v_t)\Delta$.

- **Posterior for** G_{t+1}. The posterior of G_{t+1} is proportional to

$$\propto G_{t+1}^{\frac{\Delta}{\nu}-\frac{3}{2}} \exp\left\{-\frac{J_t^2}{2\sigma^2}\frac{1}{G_{t+1}}\right\} \exp\left\{-\left(\frac{(\gamma^{\mathbb{P}})^2}{2(\sigma^{\mathbb{P}})^2}+\frac{1}{\nu}\right) G_{t+1}\right\}.$$

  This is exactly the same as the posterior of G_{t+1} in LYW (2006) who use ARMS to update G_{t+1}. Since the iterations do not involve numerical integration, we still use ARMS here.

B.5 MCMC Methods for SVLS

The common parameters and latent variables between SVMJ and SVLS have similar posterior distributions. So in this section we focus on the posterior distributions of the parameters and latent variables that are unique to SVLS.

- **Posterior for** α. The posterior of α is proportional to

$$\begin{aligned}\pi(\alpha) \quad \propto \quad & \prod_{t=0}^{T-1} \exp\left(-\frac{[(C_{t+1}-F_{t+1})-\rho_c(C_t-F_t)]^2}{2\sigma_c^2}\right) \times \left(\frac{\alpha}{\alpha-1}\right)^T \exp\left\{-\sum_{t=0}^{T-1} \left|\frac{S_{t+1}}{\sigma\Delta^{\frac{1}{\alpha}} t_\alpha(U_{t+1})}\right|^{\frac{\alpha}{\alpha-1}}\right\} \\ & \times \prod_{t=0}^{T-1} \left|\frac{S_{t+1}}{\sigma\Delta^{\frac{1}{\alpha}} t_\alpha(U_{t+1})}\right|^{\frac{\alpha}{\alpha-1}} \times \left[\left(\frac{1}{\sigma}\right)^{\frac{\alpha}{\alpha-1}}\right]^{m+1} \exp\left\{-\left(\frac{1}{\sigma}\right)^{\frac{\alpha}{\alpha-1}}\frac{1}{M}\right\} \times \mathbf{1}(\alpha)_{\alpha\in[1.01,2]}.\end{aligned}$$

  We use the same algorithm as in LWY (2006) to update α, and see LWY (2006) for details.

- **Posterior for** σ. The posterior of σ is proportional to

$$\propto \underbrace{\prod_{t=0}^{T-1} \exp\left(-\frac{[(C_{t+1}-F_{t+1})-\rho_c(C_t-F_t)]^2}{2\sigma_c^2}\right)}_{:=l(\sigma)} \times$$

$$\left[\left(\frac{1}{\sigma}\right)^{\frac{\alpha}{\alpha-1}} T+1\right] \exp\left\{-\left(\frac{1}{\sigma}\right)^{\frac{\alpha}{\alpha-1}}\left(\sum_{t=0}^{T-1}\left|\frac{S_{t+1}}{\Delta^{\frac{1}{\alpha}} t_\alpha(U_{t+1})}\right|^{\frac{\alpha}{\alpha-1}}\right)\right\}$$

  The DWW method is used with the following proposal distribution $(\frac{1}{\sigma})^{\frac{\alpha}{\alpha-1}} \sim \Gamma(T+\frac{\alpha-1}{\alpha}+1, \frac{1}{\sum_{t=0}^{T-1}|\frac{S_{t+1}}{\Delta^{\frac{1}{\alpha}} t_\alpha(U_{t+1})}|^{\frac{\alpha}{\alpha-1}}+\frac{1}{M}})$.

- **Posteriors for** S_{t+1} **and** U_{t+1}. The posteriors for S_{t+1} and U_{t+1} are the same as those in LWY (2006), and we follow the same updating algorithms. See LWY (2006) for details.

Table 1. Summary Statistics of Spot and Option Prices of the S&P 500 Index

This table provides summary statistics of spot and option prices of the S&P 500 index between January 4, 1993 and December 31, 1993. Panel A reports summary statistics of continuously compounded daily returns of the S&P 500 index during the sample period. Panel B reports summary statistics on time-to-maturity, price, implied volatility, strike price, spot price, and moneyness (strike/spot) of the short-term ATM SPX option used in model estimation. We restrict the time-to-maturity of the option to be between 20 and 50 days. On a few days without such options, we use an option whose time-to-maturity is closest to 20 days. Because the time-to-maturity of an option changes daily, in general we have to use different options on different dates.

Panel A. Summary statistics of continuously compounded daily returns of the S&P 500 index between January 4, 1993 and December 31, 1993.

	Mean	Variance	Skewness	Kurtosis	Min	Max
S&P 500	0.000292	0.0000316	-0.0332	5.5602	-0.0256	0.0223

Panel B. Summary statistics for the short-term ATM SPX option used in model estimation between January 4, 1993 and December 31, 1993.

	Mean	Median	Std. Dev.	Min	Max
Time-to-maturity	34	35	9.24	16	50
Option price	7.14	7.25	1.61	3.44	10.72
Implied volatility	0.092	0.0914	0.0095	0.0679	0.1223
Strike price	449.8207	450	10.3086	425	450
Spot price	450.0755	448.394	10.1711	427.0155	470.0928
Moneyness (Strike/Spot)	0.9994	0.9994	0.003	0.9946	1.0055

Table 2. Parameter Estimates of AJD and Lévy Jump Models

This table reports posterior estimates of model parameters of AJD and Lévy jump models using daily returns on the S&P 500 index and daily prices of a short-term ATM SPX option between January 4, 1993 and December 31, 1993. We discard the first 10,000 runs as "burn-in" period and use the last 90,000 iterations in MCMC simulations to estimate model parameters. Specifically, we take the mean of the posterior distribution as parameter estimate and the standard deviation of the posterior as standard error.

	SVMJ	SVCMJ	SVVG	SVLS
κ	2.6387	3.3627	15.778	6.2792
	(0.544)	(0.6452)	(1.3706)	(0.467)
θ	0.0049	0.0076	0.0060	0.0055
	(0.0030)	(0.0022)	(0.0011)	(0.0017)
σ_v	0.1198	0.1676	0.3043	0.1852
	(0.0116)	(0.0179)	(0.0315)	(0.0268)
ρ	-0.7014	-0.7786	-0.8167	-0.5619
	(0.0163)	(0.0324)	(0.0511)	(0.0746)
η^v	3.0526	1.1074	4.7128	2.9419
	(0.8005)	(0.5933)	(2.2753)	(1.336)
η^s	3.7020	4.3586	4.328	3.5962
	(2.7850)	(2.499)	(3.046)	(1.784)
ρ_c	0.8952	0.8665	0.895	0.9023
	(0.0557)	(0.0495)	(0.0584)	(0.0660)
σ_c	0.2039	0.2257	0.1869	0.2666
	(0.0275)	(0.0216)	(0.0189)	(0.0256)
λ	0.0103	0.0048	--	--
	(0.0216)	(0.0040)		
μ_y^P	0.0150	-0.03376	--	--
	(0.0108)	(0.0108)		
μ_y^Q	-0.3091	-0.3414	--	--
	(0.1294)	(0.0892)		
σ_y	0.0107	0.0103	--	--
	(0.0064)	(0.0063)		
μ_v	--	0.00849	--	--
		(0.0075)		
ρ_J	--	-0.0038	--	--
		(0.00492)		
ν	--	--	0.0142	--
			(0.0017)	
γ^P	--	--	0.0256	--
			(0.0315)	
σ^P	--	--	0.0462	--
			(0.0070)	
γ^Q	--	--	0.0030	--
			(0.0056)	
σ^Q	--	--	0.0412	--
			(0.0150)	
α	--	--	--	1.846
				(0.0012)
σ	--	--	--	0.0352
				(0.0014)

Table 3. Kolmogorov-Smirnov Goodness-of-Fit Test of Model Residuals

This table provides Kolmogorov-Smirnov (KS) tests of the hypotheses that the standardized model residuals of returns and volatility of each of the four models follow N(0,1). We report the KS statistics and their corresponding p-values for both residuals of all four models.

	Return Residuals				Volatility Residuals			
	SVMJ	SVCMJ	SVVG	SVLS	SVMJ	SVCMJ	SVVG	SVLS
KS Statistics	0.096	0.0934	0.0619	0.0695	0.0950	0.0893	0.0642	0.0592
p-values	0.0317	0.041	0.3246	0.2531	0.0305	0.0537	0.2902	0.3797

Table 4. In-Sample Performances in Option Pricing

This table provides summary information on the in-sample performances of the four models in pricing the short-term ATM options used in model estimation. Absolute pricing error is defined as the absolute value of the difference between model and market prices of an option. Percentage pricing error is defined as the absolute pricing error of an option divided by the market price of the option.

Panel A. Time series mean and standard deviation (in parentheses) of the absolute and percentage pricing errors of the short-term ATM options used in model estimation.

	SVMJ	SVCMJ	SVVG	SVLS
Absolute	0.44	0.44	0.16	0.24
(in dollar)	(0.2913)	(0.3268)	(0.1189)	(0.1890)
Percentage	0.0629	0.0634	0.024	0.0361
	(0.0419)	(0.0467)	(0.0186)	(0.0329)

Panel B. Diebold-Mariano (DM) statistics for in-sample option pricing errors. The DM statistics measure whether the first model has significantly smaller absolute and percentage pricing errors than the second model in each of the six pairs of models in the first row. Bold entries mean that the difference is significant at the 5% level for one-sided test. To save space, we omit “SV” in the names of all four models.

	VG-MJ	LS-MJ	VG-LS	VG-CMJ	LS-CMJ	MJ-CMJ
Absolute	**-2.3192**	**-2.0840**	**-2.1356**	**-2.2950**	**-1.9849**	0.0165
Percentage	**-2.3254**	**-1.9715**	**-1.9908**	**-2.2970**	**-1.8967**	-0.0842

Panel C. Kolmogorov-Smirnov test of the hypotheses that the standardized option pricing errors of each of the four models follow N(0,1). We report the KS statistics and their corresponding p-values for each model.

	SVMJ	SVCMJ	SVVG	SVLS
KS Statistics	0.0846	0.0794	0.0800	0.0765
P-values	0.0525	0.0812	0.0771	0.1022

Table 5. Out-of-Sample Performances in Option Pricing

This table reports the out-of-sample performances of the four models in option pricing. Based on the estimates of model parameters and latent volatility variables using the spot and option prices of the S&P 500 index, we obtain the theoretical price of each option that is not used in model estimation (12,725 in total) under each of the four models. We divide these options into six moneyness (defined as the ratio between strike and spot prices) and five maturity groups. The numbers of options belonging to each moneyness/maturity group during the entire sample also are reported. Based on options that are available on each day, we obtain daily arithmetic weighted average of absolute and percentage pricing errors of options within each moneyness/maturity group. Then we obtain the time series means of the daily pricing errors over the sample period for each option group. Absolute pricing error is defined as the absolute value of the difference between model and market prices of an option. Percentage pricing error is defined as the absolute value of the difference between model and market prices of an option divided by the market price of the option.

Panel A. Time series mean of daily weighted average of absolute pricing errors (in dollar) of out-of-sample options in each moneyness/maturity group.

		<0.93	0.93-0.97	0.97-1.0	1.0-1.03	1.03-1.07	>1.07	All
<1m	#	410	731	650	387	9	0	2187
	SVMJ	0.2265	0.3663	0.4277	0.3347	0.6449	N/A	0.3410
	SVCMJ	0.2148	0.3518	0.3867	0.3025	0.3220	N/A	0.3172
	SVVG	0.2319	0.3061	0.2399	0.2234	0.2404	N/A	0.2553
	SVLS	0.1779	0.2817	0.2760	0.2580	0.2277	N/A	0.2524
1-2m	#	694	896	679	676	306	0	3251
	SVMJ	0.5133	0.8113	0.7902	0.5226	0.3700	N/A	0.6371
	SVCMJ	0.4575	0.6893	0.6252	0.4697	0.3393	N/A	0.5400
	SVVG	0.4667	0.5653	0.3045	0.2467	0.2835	N/A	0.3915
	SVLS	0.3996	0.5682	0.3721	0.3444	0.4344	N/A	0.4297
2-3m	#	605	693	611	612	613	16	3150
	SVMJ	0.7937	1.3026	1.2660	0.8602	0.4593	0.4491	0.9452
	SVCMJ	0.6335	0.9732	0.9043	0.7091	0.4726	0.3407	0.7250
	SVVG	0.6639	0.8261	0.4889	0.3119	0.4252	0.1543	0.5286
	SVLS	0.5467	0.7267	0.4215	0.4468	0.6531	0.5792	0.5527
3-6m	#	941	415	334	328	370	170	2558
	SVMJ	1.1953	1.8914	1.9260	1.5650	0.8238	0.4239	1.3352
	SVCMJ	0.8150	1.2498	1.3257	1.2193	0.8240	0.5618	0.9805
	SVVG	0.9454	1.1721	0.8257	0.4151	0.4524	0.5474	0.7876
	SVLS	0.6982	0.8231	0.4669	0.3818	0.8369	0.9546	0.6700
>6m	#	696	170	128	120	154	311	1579
	SVMJ	1.8625	3.2767	3.0434	3.2549	2.4035	1.0897	2.1051
	SVCMJ	0.9751	1.7010	1.7761	1.8833	1.6684	1.0344	1.2712
	SVVG	1.4383	2.1033	1.4651	1.4414	0.6432	0.4837	1.2285
	SVLS	0.8029	0.9653	0.4122	0.4376	0.8658	1.3964	0.8610
All	#	3346	2905	2402	2123	1452	497	12725
	SVMJ	0.8482	1.0786	1.0641	0.8752	0.6895	0.7868	0.9296
	SVCMJ	0.5997	0.7877	0.7595	0.6776	0.6109	0.7943	0.6832
	SVVG	0.6953	0.7172	0.4541	0.3392	0.3832	0.4422	0.5444
	SVLS	0.5095	0.5792	0.3702	0.3768	0.6378	1.1006	0.5093

Panel B. Time series mean of daily weighted average of percentage pricing errors of out-of-sample options in each moneyness/maturity group.

		<0.93	0.93-0.97	0.97-1.0	1.0-1.03	1.03-1.07	>1.07	All
<1m	#	410	731	650	387	9	0	2187
	SVMJ	0.0058	0.0165	0.0512	0.1486	0.4547	N/A	0.0492
	SVCMJ	0.0055	0.0159	0.0467	0.1361	0.2269	N/A	0.0455
	SVVG	0.0059	0.0136	0.0299	0.1079	0.1822	N/A	0.0358
	SVLS	0.0046	0.0127	0.0345	0.1251	0.1754	N/A	0.0391
1-2m	#	694	896	679	676	306	0	3251
	SVMJ	0.0123	0.0318	0.0601	0.1091	0.2230	N/A	0.0675
	SVCMJ	0.0109	0.0269	0.0480	0.1060	0.2098	N/A	0.0600
	SVVG	0.0111	0.0217	0.0223	0.0637	0.1813	N/A	0.0413
	SVLS	0.0096	0.0220	0.0280	0.0860	0.2698	N/A	0.0565
2-3m	#	605	693	611	612	613	16	3150
	SVMJ	0.0171	0.0466	0.0778	0.1086	0.1836	0.4048	0.0929
	SVCMJ	0.0135	0.0346	0.0557	0.0944	0.2011	0.3132	0.0800
	SVVG	0.0140	0.0290	0.0289	0.0453	0.1974	0.1445	0.0608
	SVLS	0.0116	0.0255	0.0256	0.0651	0.2977	0.5322	0.0858
3-6m	#	941	415	334	328	370	170	2558
	SVMJ	0.0223	0.0570	0.0905	0.1220	0.1562	0.2099	0.0840
	SVCMJ	0.0152	0.0379	0.0632	0.0989	0.1845	0.2801	0.0793
	SVVG	0.0173	0.0349	0.0377	0.0315	0.1260	0.2680	0.0552
	SVLS	0.0129	0.0244	0.0215	0.0350	0.2222	0.4668	0.0770
>6m	#	696	170	128	120	154	311	1579
	SVMJ	0.0279	0.0739	0.1064	0.1369	0.1759	0.2232	0.1013
	SVCMJ	0.0146	0.0386	0.0624	0.0824	0.1262	0.2383	0.0821
	SVVG	0.0212	0.0472	0.0507	0.0580	0.0453	0.1524	0.0552
	SVLS	0.0118	0.0216	0.0141	0.0194	0.0726	0.3948	0.0902
All	#	3346	2905	2402	2123	1452	497	12725
	SVMJ	0.0169	0.0368	0.0686	0.1206	0.1983	0.2558	0.0799
	SVCMJ	0.0124	0.0277	0.0513	0.1044	0.1965	0.2761	0.0682
	SVVG	0.0138	0.0244	0.0294	0.0601	0.1497	0.1810	0.0478
	SVLS	0.0105	0.0205	0.0273	0.0774	0.2484	0.4202	0.0678

Panel C. Diebold-Mariano statistics for out-of-sample absolute option pricing errors. The DM statistics provide pair-wise comparison of the four models by testing whether one model has significantly smaller average absolute pricing errors for all options in a moneyness/maturity group than another model. Bold entries mean that the difference is significant at the 5% level for one-sided test. To save space, we omit "SV" in the names of all four models.

		<0.93	0.93-0.97	0.97-1.0	1.0-1.03	1.03-1.07	>1.07	All
<1m	CMJ-MJ	**-1.7668**	-0.8338	-0.9281	-0.8031	-1.1932	N/A	-1.0157
	VG-MJ	1.4395	**-1.9841**	**-2.1976**	**-1.8955**	-1.1874	N/A	**-2.1534**
	LS-MJ	**-1.9624**	**-2.1164**	**-2.0520**	**-1.8198**	-1.1521	N/A	**-2.1822**
	VG-CMJ	**1.8063**	**-1.9994**	**-2.1509**	**-1.9837**	-1.0054	N/A	**-2.2147**
	LS-CMJ	**-1.9434**	**-2.0074**	**-1.8812**	-1.3121	-0.7914	N/A	**-2.1042**
	VG-LS	1.9787	1.7326	1.7082	-1.2879	0.2645	N/A	0.5039
1-2m	CMJ-MJ	**-1.7604**	-1.5251	-1.2552	-0.5710	-0.4336	N/A	-1.1861
	VG-MJ	**-1.8993**	**-2.2908**	**-2.2814**	**-2.0180**	-0.8580	N/A	**-2.1810**
	LS-MJ	**-2.1464**	**-2.2012**	**-2.2132**	**-1.9686**	0.8279	N/A	**-2.1971**
	VG-CMJ	1.1031	**-1.9680**	**-2.1355**	**-2.2564**	-0.8512	N/A	**-2.2246**
	LS-CMJ	**-2.0388**	**-1.7929**	**-1.9642**	-1.5753	1.1398	N/A	**-1.9545**
	VG-LS	2.1589	-0.1343	**-1.7099**	-1.5248	**-1.7043**	N/A	**-1.9527**
2-3m	CMJ-MJ	**-1.7324**	**-1.7959**	-1.6328	-0.9777	0.1582	-1.0337	-1.5235
	VG-MJ	**-1.8912**	**-2.2737**	**-2.3052**	**-2.1745**	-0.2667	-1.1509	**-2.2117**
	LS-MJ	**-1.9515**	**-2.2209**	**-2.2649**	**-2.0783**	1.3863	1.2100	**-2.1834**
	VG-CMJ	1.2902	**-1.6519**	**-2.0447**	**-2.2686**	-0.6865	-1.2063	**-2.1223**
	LS-CMJ	**-1.7439**	**-1.9372**	**-2.1862**	**-2.0230**	1.6082	1.2561	**-2.1516**
	VG-LS	1.9874	1.6638	1.2299	**-1.6618**	**-1.9679**	-1.2501	-1.5180
3-6m	CMJ-MJ	**-1.6966**	-1.5935	-1.5966	-1.3984	0.0017	1.4403	-1.6223
	VG-MJ	**-1.9068**	**-1.8075**	**-1.8741**	**-1.8678**	**-1.7757**	0.6340	**-1.9135**
	LS-MJ	**-1.8979**	**-1.8001**	**-1.8703**	**-1.8696**	0.1379	1.3620	**-1.9118**
	VG-CMJ	1.5495	-1.0360	**-1.7960**	**-1.8395**	**-1.7288**	-0.0786	**-1.7093**
	LS-CMJ	**-1.8516**	**-1.8211**	**-1.8706**	**-1.8459**	0.0975	1.1861	**-1.8510**
	VG-LS	1.8822	1.7771	1.8449	0.5368	**-1.7159**	-1.6189	1.8466
>6m	CMJ-MJ	-1.5920	-1.4692	-1.2808	-1.3175	-1.2192	-0.5187	-1.5557
	VG-MJ	**-1.7633**	**-1.6492**	-1.4216	-1.5072	-1.5206	-1.5965	**-1.7735**
	LS-MJ	**-1.7636**	-1.6375	-1.4247	-1.4948	-1.4752	1.2163	**-1.7800**
	VG-CMJ	1.5676	1.4175	-1.4570	-1.3412	-1.6055	-1.6312	-0.5975
	LS-CMJ	**-1.7604**	**-1.6774**	-1.4605	-1.5514	-1.4854	1.1355	**-1.7806**
	VG-LS	1.7607	1.6244	1.4291	1.4431	-1.1041	-1.5995	1.7905
All	CMJ-MJ	**-1.9016**	**-1.9638**	**-1.8676**	-0.8352	-0.8352	0.1097	**-1.9099**
	VG-MJ	**-2.2597**	**-2.3311**	**-2.3773**	**-2.3265**	**-2.1020**	**-1.7403**	**-2.3763**
	LS-MJ	**-2.1899**	**-2.2645**	**-2.3387**	**-2.2224**	-0.6282	1.3636	**-2.3450**
	VG-CMJ	1.6180	**-1.6520**	**-2.1540**	**-2.2960**	**-2.3739**	**-1.7134**	**-2.1240**
	LS-CMJ	**-2.1576**	**-2.0566**	**-2.1546**	**-2.0084**	0.4012	1.2432	**-2.1495**
	VG-LS	2.1226	2.0109	1.7971	-0.6805	**-2.1395**	**-1.7513**	1.2602

Panel D. Diebold-Mariano statistics for out-of-sample percentage option pricing errors. The DM statistics provide pair-wise comparison of the four models by testing whether one model has significantly smaller average percentage pricing errors for all options in a moneyness/maturity group than another model. Bold entries mean that the difference is significant at the 5% level for one-sided test. To save space, we omit “SV” in the names of all four models.

		<0.93	0.93-0.97	0.97-1.0	1.0-1.03	1.03-1.07	>1.07	All
<1m	CMJ-MJ	**-1.8850**	-0.8150	-0.9270	-0.7585	-1.1818	N/A	-0.9228
	VG-MJ	1.3796	**-1.9967**	**-2.2112**	**-1.7763**	-1.1784	N/A	**-2.0898**
	LS-MJ	**-1.9569**	**-2.1059**	**-2.0019**	**-1.6502**	-1.1426	N/A	**-2.0485**
	VG-CMJ	1.6496	**-2.0335**	**-2.1848**	**-1.9168**	-0.9024	N/A	**-2.2132**
	LS-CMJ	**-1.9396**	**-1.9917**	**-1.8855**	-0.7639	-0.6630	N/A	**-1.7508**
	VG-LS	1.9797	1.5824	**-1.8616**	-1.3085	0.1974	N/A	-1.5654
1-2m	CMJ-MJ	**-1.8195**	-1.6080	-1.2548	-0.1624	-0.3166	N/A	-0.6672
	VG-MJ	**-1.8943**	**-2.2905**	**-2.2800**	**-1.7687**	-0.6587	N/A	**-1.7678**
	LS-MJ	**-2.0938**	**-2.1898**	**-2.2169**	**-1.6601**	0.9121	N/A	**-1.6579**
	VG-CMJ	0.6688	**-1.9888**	**-2.1456**	**-2.1737**	-0.6489	N/A	**-2.1122**
	LS-CMJ	**-2.0024**	**-1.7760**	**-1.9752**	-1.2314	1.1470	N/A	-0.5227
	VG-LS	2.1212	-0.3528	**-1.8068**	-1.3359	**-1.6689**	N/A	**-1.7763**
2-3m	CMJ-MJ	**-1.7939**	-1.6333	**-1.7332**	-0.7565	0.5252	-1.0135	-0.8370
	VG-MJ	**-1.8533**	**-2.2729**	**-2.3072**	**-2.1214**	0.2460	-1.1503	**-1.6702**
	LS-MJ	**-1.8715**	**-2.2149**	**-2.2678**	**-1.9509**	1.6306	1.2039	-0.5083
	VG-CMJ	0.9732	**-1.6578**	**-2.0610**	**-2.2676**	-0.1112	-1.2093	**-1.9506**
	LS-CMJ	**-1.6515**	**-1.9207**	**-2.1928**	**-1.8926**	1.6314	1.2546	0.8804
	VG-LS	1.8733	1.6264	1.0487	**-1.6689**	**-2.0008**	-1.2514	**-2.0436**
3-6m	CMJ-MJ	**-1.7666**	-1.6382	**-1.7258**	-1.3049	0.8921	1.4194	-0.5147
	VG-MJ	**-1.9032**	**-1.8226**	**-1.8840**	**-1.8833**	-1.0246	0.5775	**-1.6532**
	LS-MJ	**-1.8998**	**-1.8149**	**-1.8809**	**-1.8905**	1.3086	1.3656	-0.6250
	VG-CMJ	1.5456	-1.2034	**-1.7934**	**-1.8315**	**-1.6591**	-0.1326	**-1.6502**
	LS-CMJ	**-1.8284**	**-1.8263**	**-1.8662**	**-1.8367**	1.0389	1.2126	-0.2382
	VG-LS	1.8905	1.7901	1.8580	-0.7960	**-1.7273**	**-1.6573**	**-1.8472**
>6m	CMJ-MJ	**-1.7460**	**-1.8248**	-1.3664	-1.4648	-1.2954	0.5983	-1.4166
	VG-MJ	**-1.7535**	**-1.6633**	-1.4153	-1.5224	-1.5534	-1.3260	**-1.7210**
	LS-MJ	**-1.7589**	**-1.6538**	-1.4177	-1.5331	-1.4787	1.4281	-0.8345
	VG-CMJ	1.5641	**-1.6546**	**-1.4598**	-1.3693	**-1.6536**	-1.5141	**-1.7206**
	LS-CMJ	**-1.7444**	**-1.6794**	**-1.6537**	**-1.6524**	-1.4851	1.3563	0.5618
	VG-LS	1.7606	1.6426	1.4211	1.5088	1.2626	-1.5859	-1.6403
All	CMJ-MJ	**-1.7702**	-1.6413	-1.6381	-0.9811	-0.0556	0.6563	-1.0911
	VG-MJ	**-2.3261**	**-2.3804**	**-2.3958**	**-2.2341**	-1.1596	-1.0329	**-2.0320**
	LS-MJ	**-2.2811**	**-2.3280**	**-2.3671**	**-2.2381**	1.3526	1.4279	**-1.6567**
	VG-CMJ	1.6203	**-1.7274**	**-2.2020**	**-2.3510**	**-1.7514**	-1.3495	**-2.2100**
	LS-CMJ	**-2.1184**	**-2.0353**	**-2.1701**	**-1.6855**	1.5986	1.4341	-0.0787
	VG-LS	2.2243	2.0025	1.1281	-1.4085	**-2.0515**	**-1.8444**	**-2.1713**

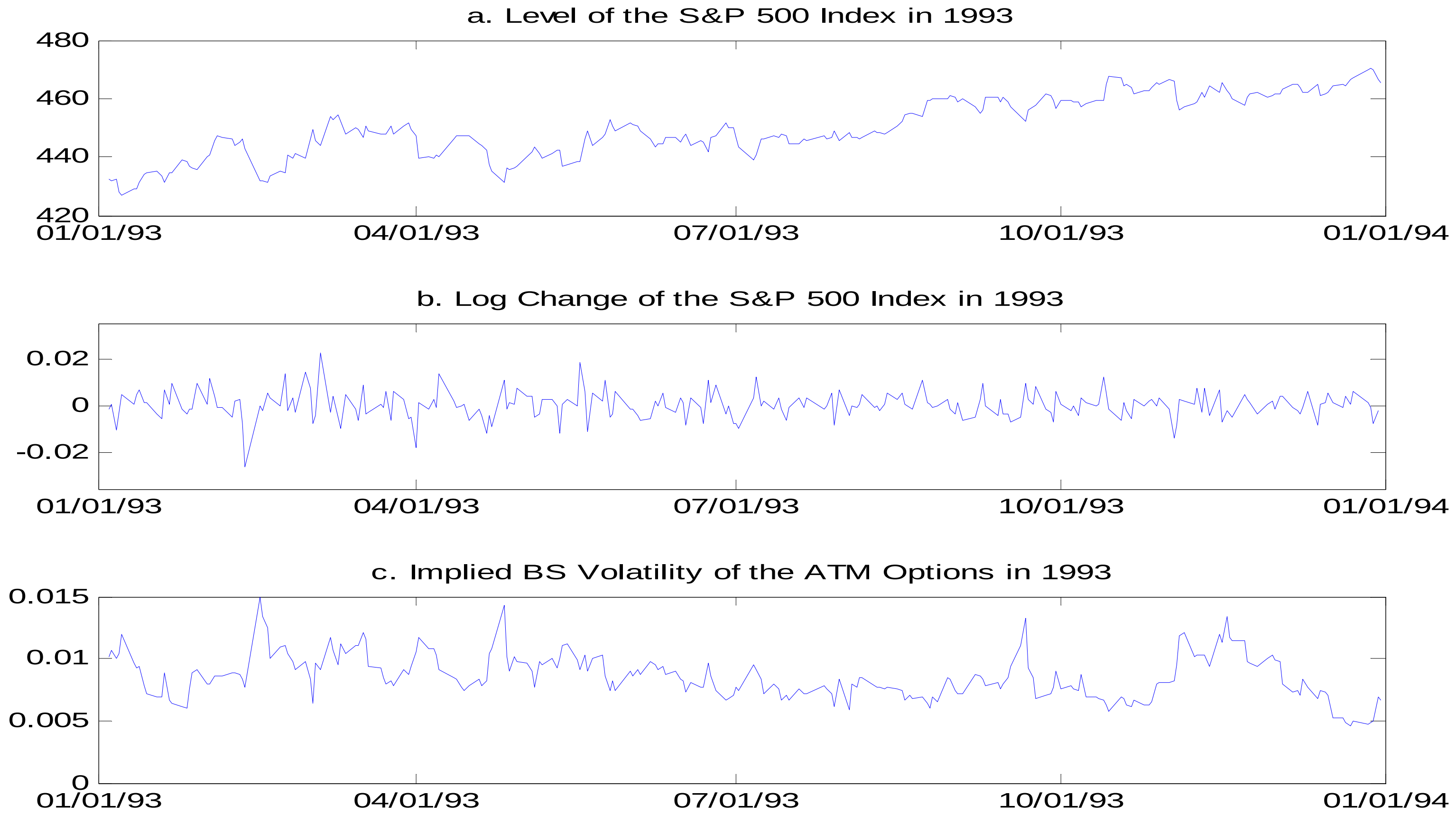

Figure 1. Level and log change of the S&P 500 index, and implied volatility of the short-term ATM SPX options used in model estimation between January 4, 1993 and December 31, 1993.

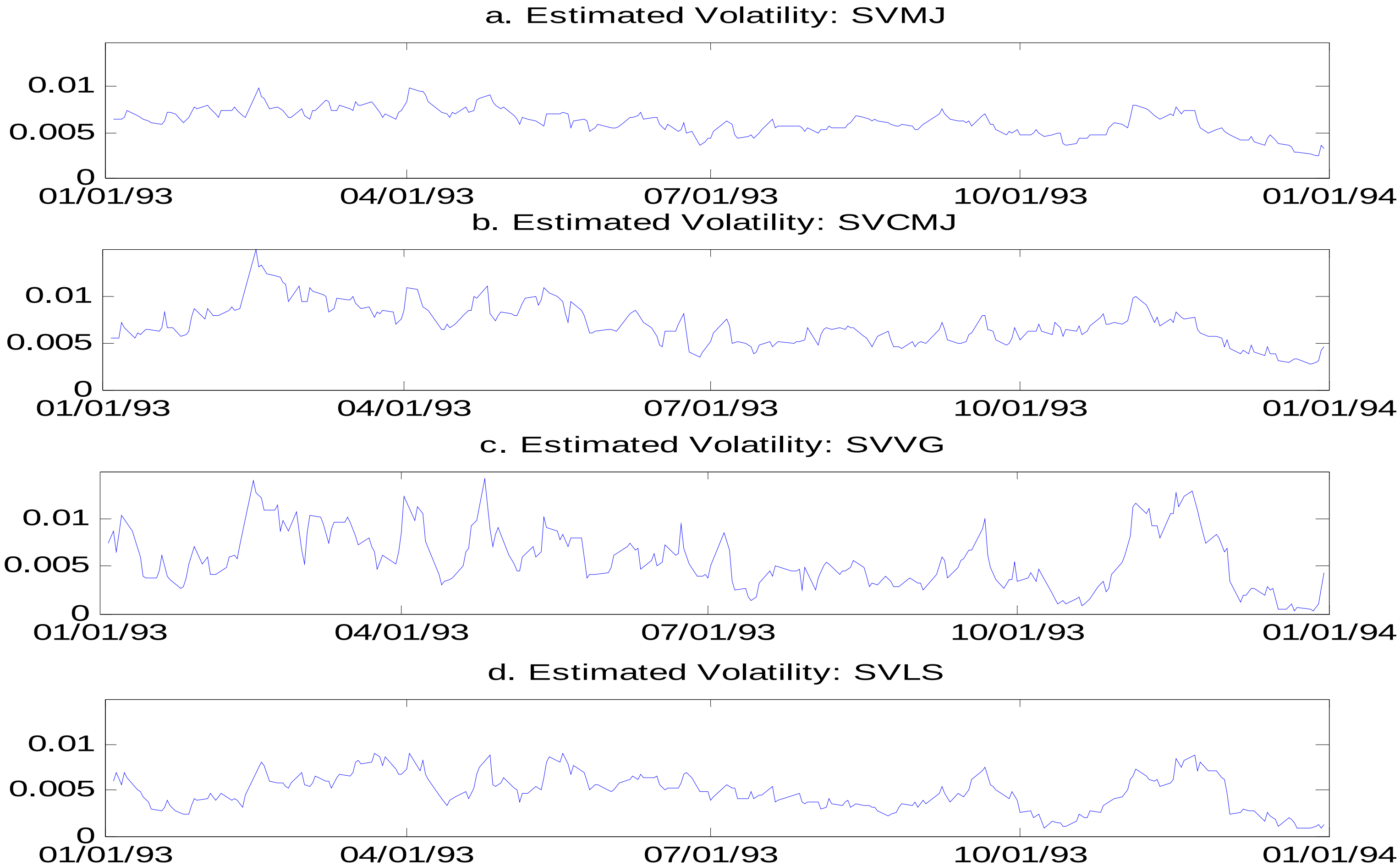

Figure 2. Estimated volatility variables of SVMJ, SVCMJ, SVVG, and SVLS using daily returns of the S&P 500 index and daily prices of the short-term ATM SPX options between January 4, 1993 and December 31, 1993.

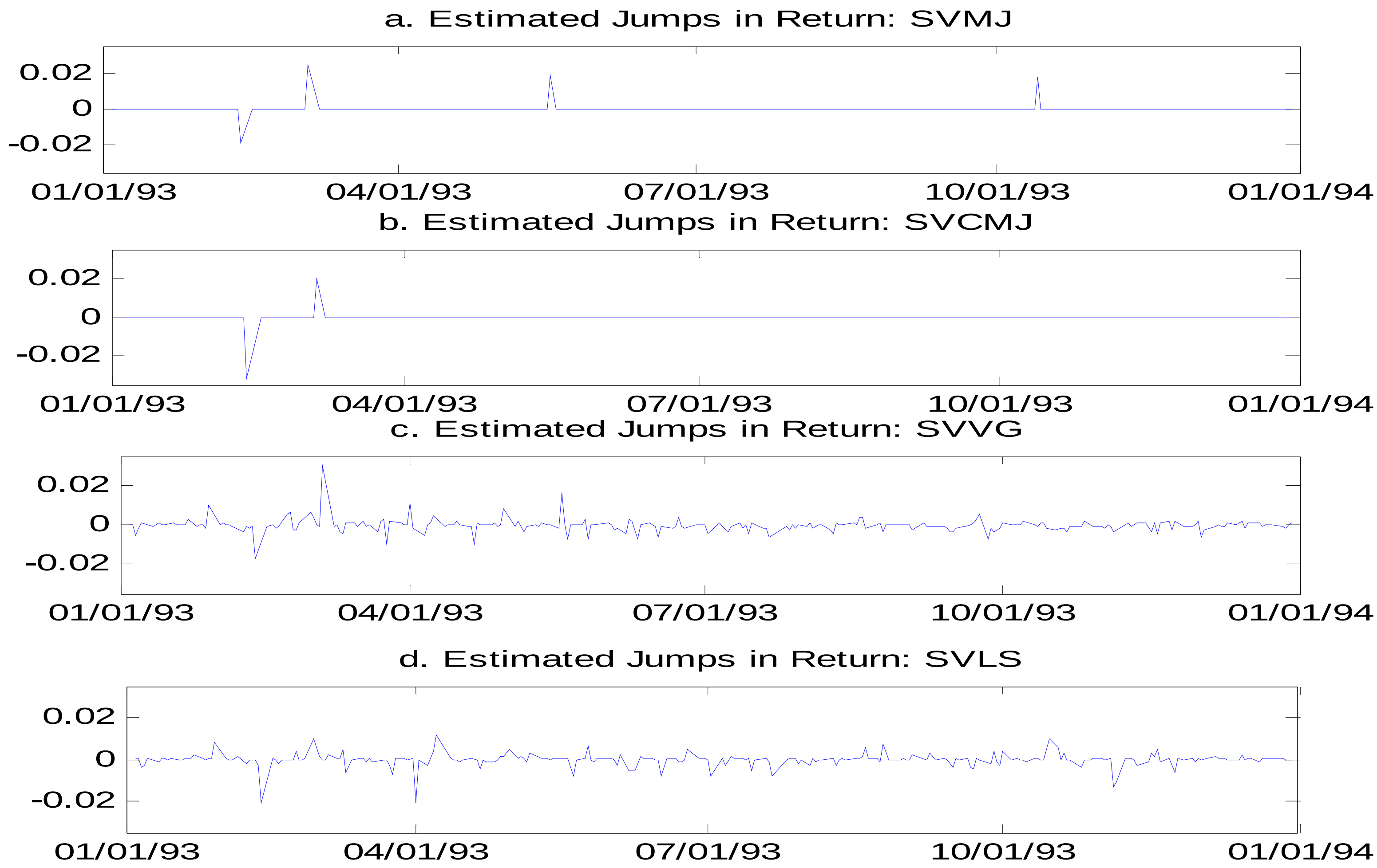

Figure 3. Estimated jumps in returns of SVMJ, SVCMJ, SVVG, and SVLS using daily returns of the S&P 500 index and daily prices of the short-term ATM SPX options between January 4, 1993 and December 31, 1993.

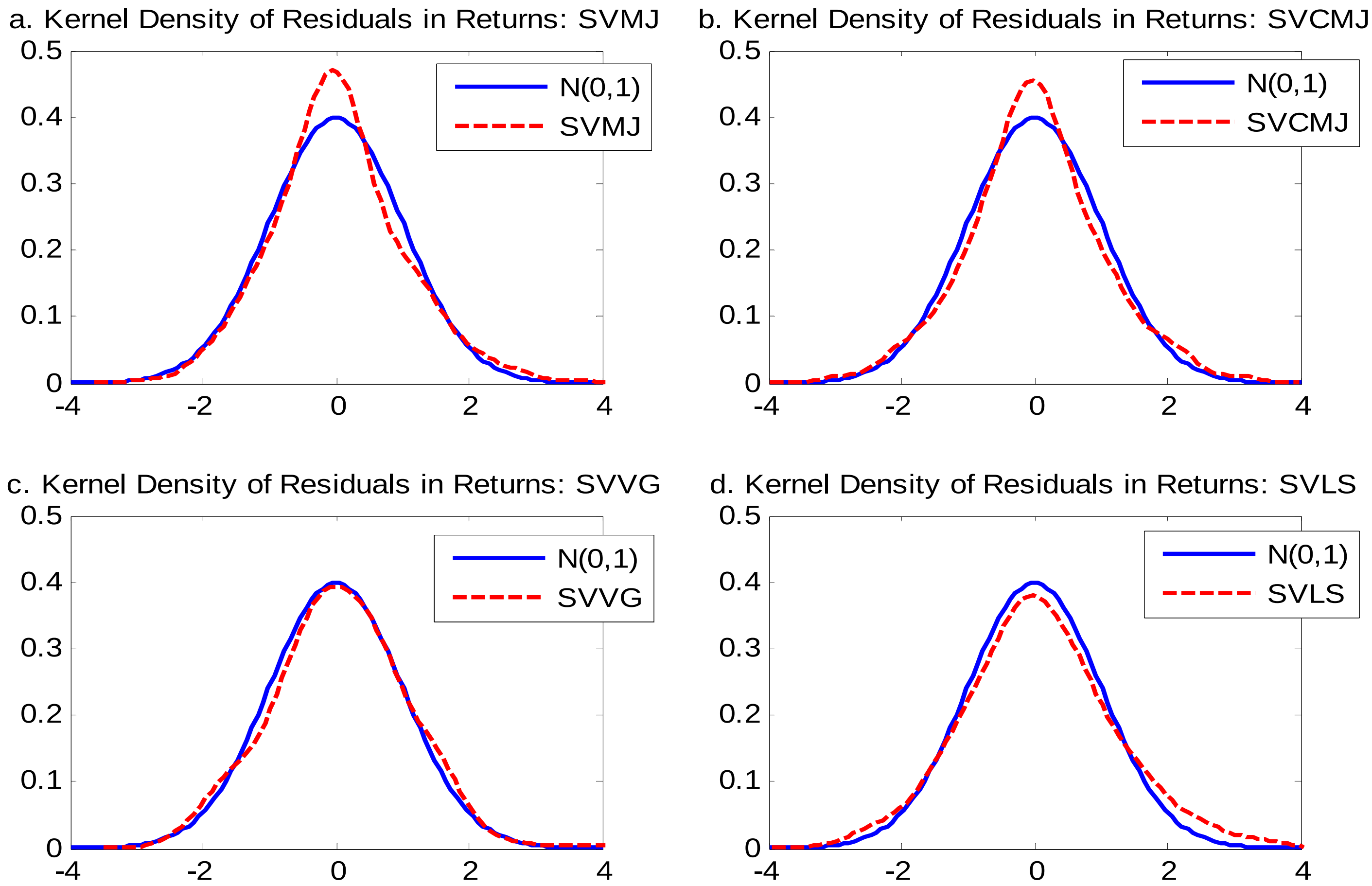

Figure 4. Kernel densities of standardized model residuals of returns of SVMJ, SVCMJ, SVVG, and SVLS, which are estimated using daily returns of the S&P 500 index and daily prices of the short-term ATM SPX options between January 4, 1993 and December 31, 1993.

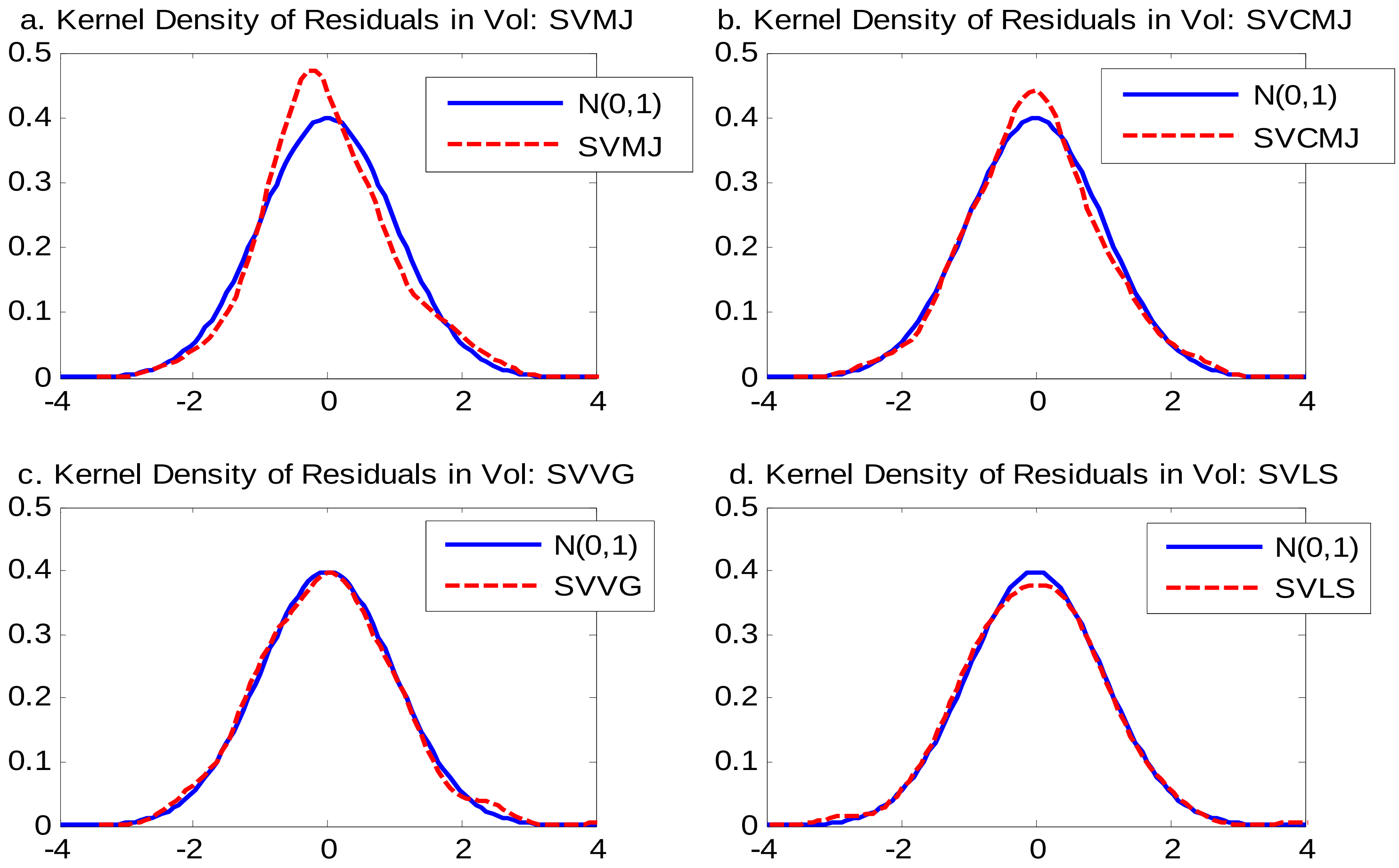

Figure 5. Kernel densities of standardized model residuals of volatility of SVMJ, SVCMJ, SVVG, and SVLS, which are estimated using daily returns of the S&P 500 index and daily prices of the short-term ATM SPX options between January 4, 1993 and December 31, 1993.

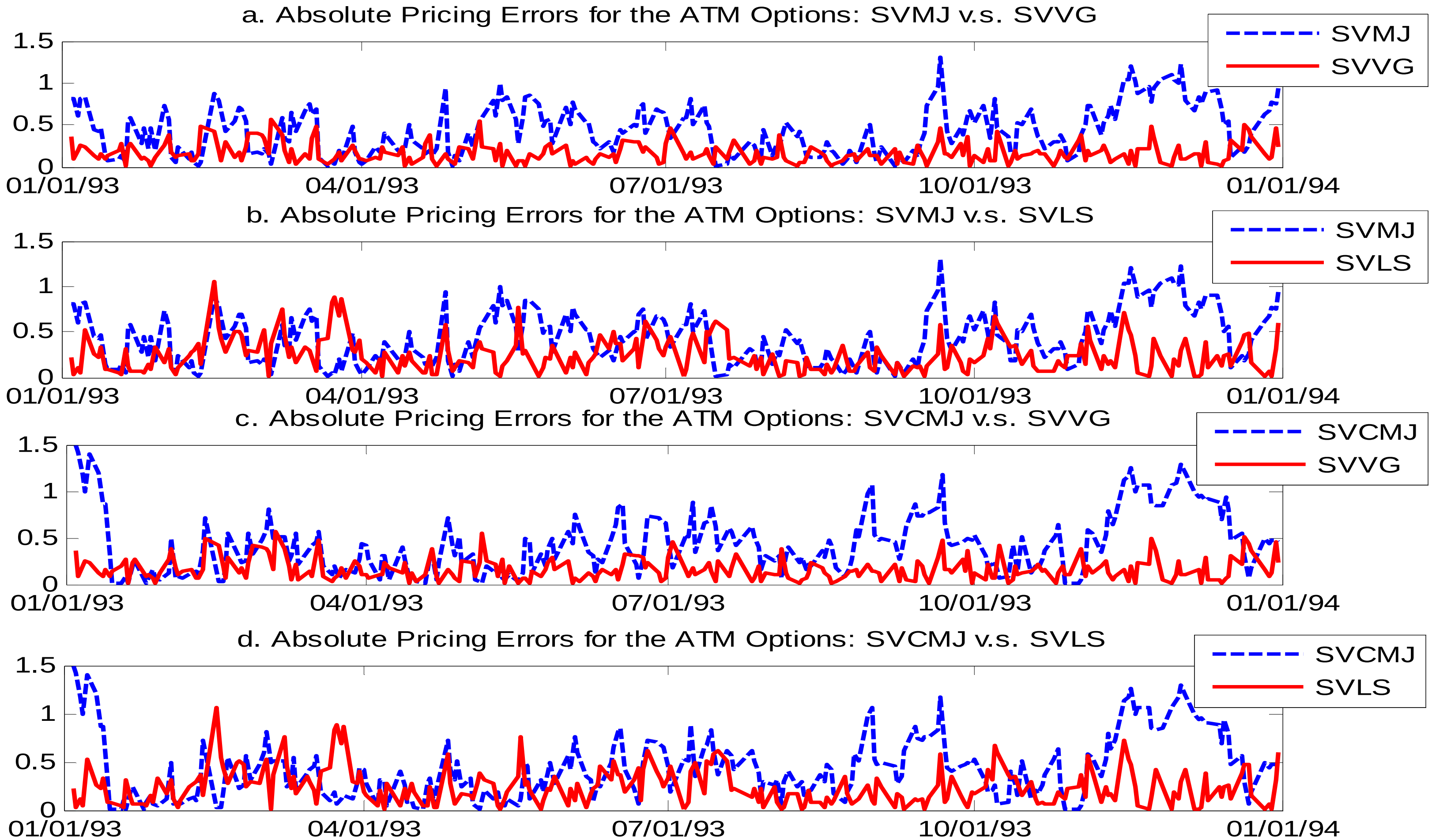

Figure 6. In-sample absolute option pricing errors of SVMJ, SVCMJ, SVVG, and SVLS, which are estimated using daily returns of the S&P 500 index and daily prices of the short-term ATM SPX options between January 4, 1993 and December 31, 1993.

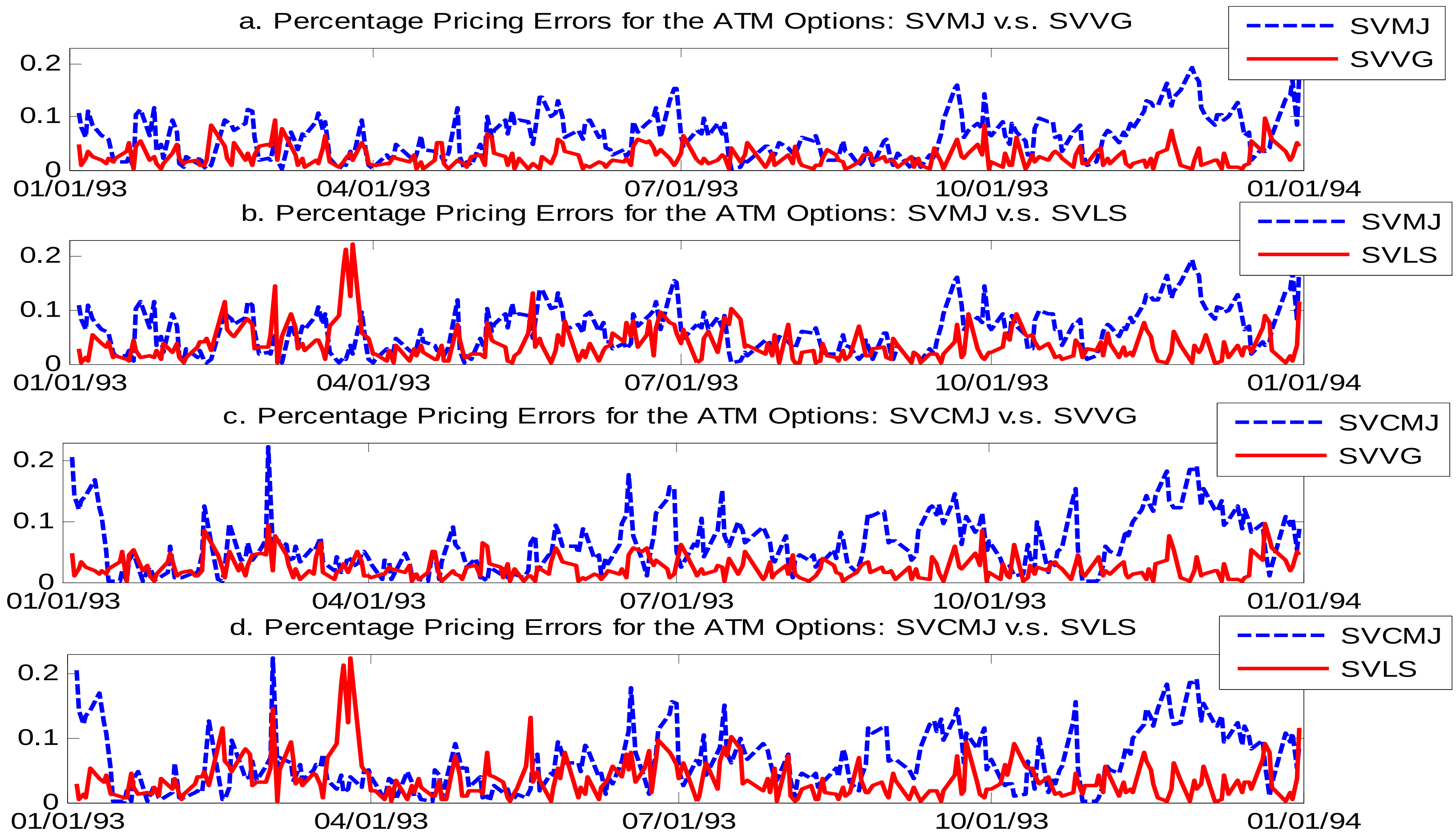

Figure 7. In-sample percentage option pricing errors of SVMJ, SVCMJ, SVVG, and SVLS, which are estimated using daily returns of the S&P 500 index and daily prices of the short-term ATM SPX options between January 4, 1993 and December 31, 1993.

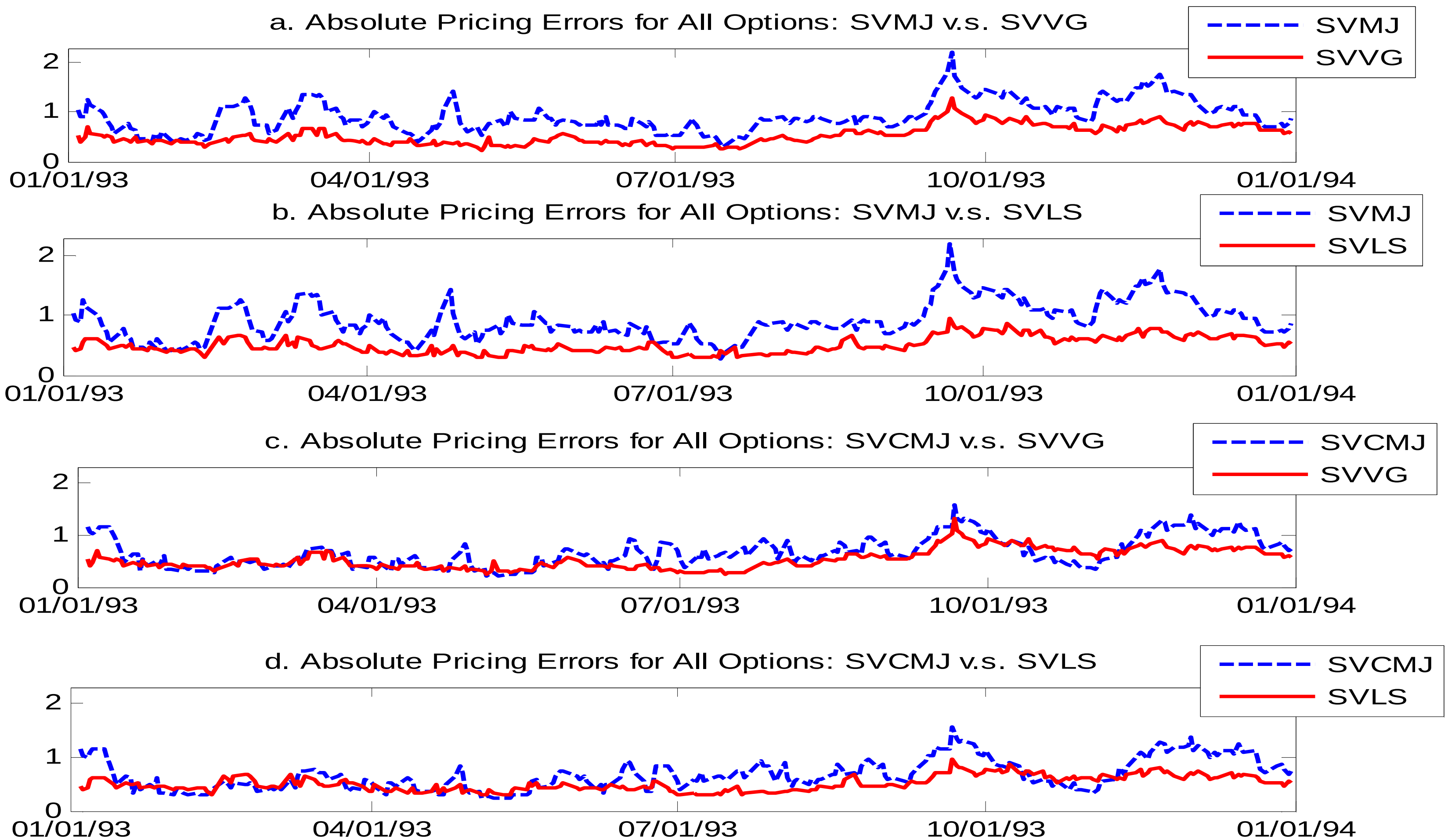

Figure 8. Average absolute pricing errors for all out-of-sample options of SVMJ, SVCMJ, SVVG, and SVLS, which are estimated using daily returns of the S&P 500 index and daily prices of the short-term ATM SPX options between January 4, 1993 and December 31, 1993.

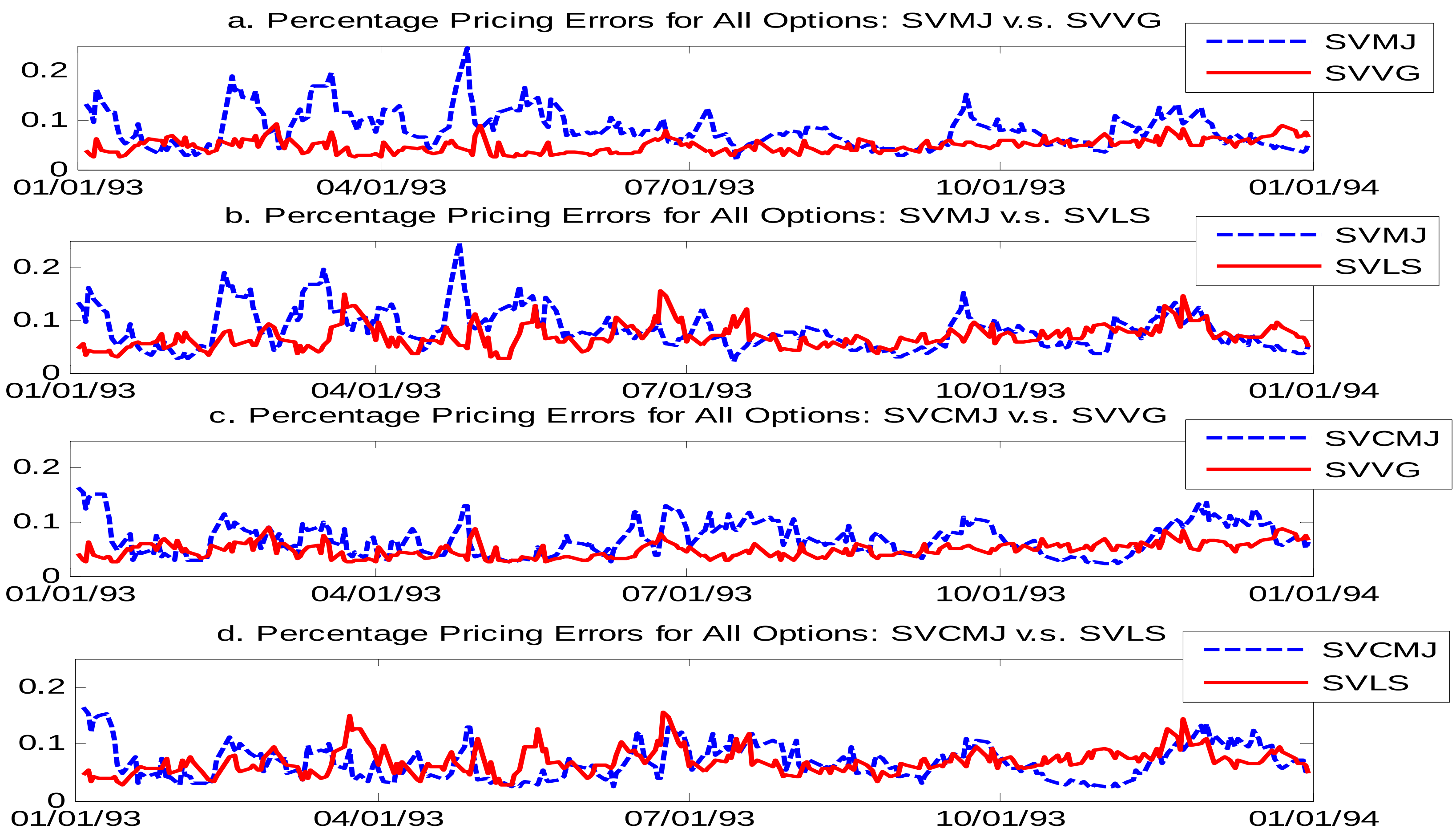

Figure 9. Average percentage pricing errors for all out-of-sample options of SVMJ, SVCMJ, SVVG, and SVLS, which are estimated using daily returns of the S&P 500 index and daily prices of the short-term ATM SPX options between January 4, 1993 and December 31, 1993.